Development of selenium- and tellurium containing surfactants and their biological activity against cancer cells

Dissertation
zur Erlangung des Grades
des Doktors der Naturwissenschaften
der Naturwissenschaftlich-Technischen Fakultät III
Chemie, Pharmazie, Bio- und Werkstoffwissenschaften
der Universität des Saarlandes

von

Diplom Apotheker Peng Du

Saarbrücken

2014

Tag des Kolloquiums: 28. Oktober. 2014

Dekan:	Prof. Dr. Volkhard Helms
Berichterstatter:	Prof. Dr. Claus Jacob
	Prof. Dr. Ingolf Bernhardt
Vorsitz:	Prof. Dr. Christian Ducho
Akad. Mitarbeiterin:	Dr. Sonja Keßler

Diese Dissertation entstand unter der Anleitung von Prof. Dr. Claus Jacob in der Arbeitsgruppe für Bioorganische Chemie, Fachrichtung 8.2 Pharmazie der Naturwissenschaftlich-Technischen Fakultät III der Universität des Saarlandes im Zeitraum von August 2010 bis Juni 2013.

Dedicated to my parents and my family

Acknowledgement/Danksagung

Ich bedanke mich herzlich bei Herrn **Prof. Dr. Claus Jacob** für die Möglichkeit, diese Dissertation mit den sehr interessanten Themen im Fachbereich Pharmazie, Fachrichtung Bioorganische Chemie anzufertigen.

Ebenso bedanke ich mich herzlich bei Herrn **Prof. Dr. Ingolf Bernhardt** für die Übernahme des Koreferates sowie Herrn **Prof. Dr. Christian Ducho** für die Übernahme des Prüfungsvorsitzes.

Ich bedanke mich herzlich bei Frau **Dr. Sonja Keßler** für die Teilnahme am Prüfungsausschuss als akademische Mitarbeiterin.

Ein weiterer großer Dank gilt **Herrn Prof. Dr. Gilbert Kirsch** und dem **gesamten Team** für die schöne Zeit im Labor und die hilfreiche Unterstützung bei Fragen jeder Art.

Desweiteren bedanke ich mich herzlich bei Herrn **Prof. Dr. Mathias Montenarh** sowie dem **gesamten Team** für die ausgezeichnete Betreuung und jedes hilfreiche Gespräch bei Fragen.

Ferner bekanke ich mich bei Herrn **Dr. Torsten Burkholz**, Herrn **Dr. Zhanjie Xu**, Herrn **Dr. Nathaniel Saidu**, Herrn **Hadi Ebrahimnejad**, Herrn **Benjamin Hanf**, Herrn **Dr. Khairan Khairan** und Frau **Uma M. Viswanathan** für die gute Zusammenarbeit im Labor.

Ein weiterer Dank gilt allen **internen und externen Kooperationspartnern** im Rahmen meiner Veröffentlichungen.

Ein besonderer Dank gilt meinen **Eltern,** die mich bei meinem Pharmazie-Studium sowie der Promotion in jeder Hinsicht unterstützt haben.

Zum Schluss bedanke ich mich bei meiner Ehefrau **Taotao Kuang** für ihr aufgebrachtes Verständnis und ihre große Unterstützung in den letzten Jahren.

The publications attached to this thesis

Pulication 1

Synthesis of amphiphilic, chalcogen-based redox modulators with in vitro cytotoxic activity against cancer cells, macrophages and microbes

Peng Du, Uma M. Viswanathan, Khairan Khairan, Tomislav Buric, Nathaniel E. B. Saidu, Zhanjie Xu, Benjamin Hanf, Inga Bazukyan, Armen Trchounian, Frank Hannemann, Ingolf Bernhardt, Torsten Burkholz, Britta Diesel, Alexandra K. Kiemer, Karl-Herbert Schäfer, Mathias Montenarh, Gilbert Kirsch and Claus Jacob

This manuscript was published as an article in the following journal:

Medicinal Chemistry Communications, 2014, 5, 25-31

Publication 2

A new tellurium-containing amphiphilic molecule induces apoptosis in HCT116 colon cancer cells

Peng Du, Nathaniel Edward Bennett Saidu, Johanna Intemann, Claus Jacob, Mathias Montenarh

This manuscript was published as an article in the following journal:

Biochimica et Biophysica Acta 1840 (2014) 1808–1816

Publication 3

Synthesis of amphiphilic seleninic acid derivatives with considerable activity against cellular membranes and certain pathogenic microbes

Peng Du, Uma M. Viswanathan, Zhanjie Xu, Hadi Ebrahimnejad, Benjamin Hanf, Torsten Burkholz, Marc Schneider, Ingolf Bernhardt, Gilbert Kirsch, Claus Jacob

This manuscript was published as an article in the following journal:

Journal of Hazardous Materials 269 (2014) 74–82

Declaration of author contributions for publications 1-3

Publication 1

The first author, Peng Du (Division of Bioorganic Chemistry, Saarland University, Saarbruecken, Germany), hereby declares that under the guidance of Prof. Dr. Gilbert Kirsch (Laboratoire d'Ing´enierie Mol´eculaire et Biochimie Pharmacologique, SRSMC UMR, Universit´e de Lorraine, Metz, France) and Prof. Dr. Claus Jacob (Division of Bioorganic Chemistry, Saarland University,Saarbruecken, Germany), Peng Du designed, synthesized, purified and chemically characterized the amphiphilic selenium- and tellurium-containing compounds mentioned in this paper with some technical assistance from Dr. Zhanjie Xu (Laboratoire d'Ing´enierie Mol´eculaire et Biochimie Pharmacologique, SRSMC UMR, Universit´e de Lorraine, Metz, France).

With the essential guidance from Prof. Dr. Claus Jacob, I personally characterized the biological activities of the compounds with the haemolysis assay, circular dichroism measurements, REM and EDX measurements, MTT assay, ROS assay and mitochondria potential measurements. The biological investigations were supervised by the following collaborators as listed below:

1. Prof. Dr. Ingolf Bernhardt and Mr. Benjamin Hanf (Division of Biophysics, Saarland University, Saarbruecken, Germany) provided necessary technical assistance with the haemolysis assay used for the compounds synthesized.

2. Dr. Frank Hannemann (Division of Biochemistry, Saarland University, Saarbruecken, Germany) provided necessary technical assistance in the circular dichroism measurements with the compounds.

3. Prof. Dr. Karl-Herbert Schäfer (Department of Biotechnology, University of Applied Sciences Kaiserslautern, Zweibruecken, Germany) and Dr. Khairan Khairan (Division of Bioorganic Chemistry, Saarland University, Saarbruecken, Germany) provided necessary technical assistance with the REM and EDX measurements.

4. Prof. Dr. Alexandra K. Kiemer and Dr. Britta Diesel (Department of Pharmacy, Saarland University, Saarbruecken, Germany) supervised the MTT assay on RAW 264.7 cells.

5. Prof. Dr. Mathias Montenarh and Dr. Nathaniel E. B. Saidu (Division of Medical Biochemistry and Molecular Biology, Saarland University, Homburg, Germany) provided necessary technical assistance with the MTT assay with HCT116 and ARPE-19 cells, and the ROS measurements and the mitochondria potential assay with HCT116 cells.

Ms. Uma M. Viswanathan (Division of Bioorganic Chemistry, Saarland University, Saarbruecken, Germany) carried out the CMC determination and Cyclic Voltammetry studies. Ms. Uma M. Viswanathan also performed the bacterium-inhibition assay under the supervision of Dr. Inga Bazukyan and Prof. Dr. Armen Trchounian (Division of Microbiology, Plants and Microbes Biotechnology, Yerevan State University, Yerevan, Armenia). Dr. Khairan Khairan performed the nematode assay.

Prof. Dr. Claus Jacob wrote and submitted the manuscript, Mr. Tomislav Buric (Division of Bioorganic Chemistry, Saarland University, Saarbruecken, Germany) and Dr. Torsten Burkholz (Division of Bioorganic Chemistry, Saarland University, Saarbruecken, Germany) kindly reviewed the manuscript and provided necessary supervision during the laboratory based studies and as a part of the submission of the manuscript.

Publication 2

The first author, Peng Du (Division of Bioorganic Chemistry, Saarland University, Saarbruecken, Germany), declares that under the principle guidance of Prof. Dr. Claus Jacob (Division of Bioorganic Chemistry, Saarland University, Saarbruecken, Germany), Peng Du designed, synthesized, purified and chemically characterized the new amphiphilic selenium- and tellurium-containing compounds for all the biological tests mentioned in this paper.

With appropriate guidance from Prof. Dr. Mathias Montenarh (Division of Medical Biochemistry and Molecular Biology, Saarland University, Homburg, Germany), Peng Du performed the ROS assay, tubulin immunofluorescence analysis, cell cycle analysis and analysis of apoptosis.

Dr. Nathaniel Edward Bennett Saidu (Division of Medical Biochemistry and Molecular Biology, Saarland University, Homburg, Germany) carried out the Western Blot analysis involving HCT 116 cells. Ms Johanna Intemann (Division of Medical Biochemistry and Molecular Biology, Saarland University, Homburg, Germany) carried out Western Blot analysis involving ARPE-19 cells.

Prof. Dr. Mathias Montenarh wrote and submitted the manuscript; Prof. Dr. Claus Jacob and Dr. Nathaniel Edward Bennett Saidu revised the manuscript and provided necessary assistance during the submission

Publication 3

The first author, Peng Du (Division of Bioorganic Chemistry, Saarland University, Saarbruecken, Germany), hereby declares that under the principle guidance of Prof. Dr. Gilbert Kirsch (Laboratoire d'Ing´enierie Mol´eculaire et Biochimie Pharmacologique, SRSMC UMR, Universit ´e de Lorraine, Metz, France) and Prof. Dr. Claus Jacob (Division of Bioorganic Chemistry, Saarland University, Saarbruecken, Germany), Peng Du designed, synthesized, purified and chemically characterized novel amphiphilic seleninic acid derivatives mentioned in this publication with some technical assistance from Dr. Zhanjie Xu (Laboratoire d'Ing´enierie Mol´eculaire et Biochimie Pharmacologique, SRSMC UMR, Universit ´e de Lorraine, Metz, France).

With the essential guidance from Prof. Dr. Claus Jacob, Peng Du characterized the synthesized compounds biologically with the haemolysis assay and Ca^{2+}-uptake assay with technical assistance of Mr. Benjamin Hanf under supervision of Prof. Dr. Ingolf Bernhardt (Division of Biophysics, Saarland University, Saarbruecken, Germany).

Under the supervision of Prof. Dr. Marc Schneider (Division of Pharmaceutics and Biopharmacy, Philipps University, Marburg, Germany), Ms. Uma M. Viswanathan

(Division of Bioorganic Chemistry, Saarland University, Saarbruecken, Germany) performed the CMC determination for the compounds.

Under the supervision of Prof. Dr. Claus Jacob, Dr. Hadi Ebrahimnejad (Department of Food Hygiene, Shahid Bahonar University, Kerman, Irand) performed the antifungal activity assays for the compounds.

Prof. Dr. Claus Jacob wrote and submitted the manuscript; Dr. Torsten Burkholz (Division of Bioorganic Chemistry, Saarland University, Saarbruecken, Germany) kindly reviewed the manuscript and provided necessary assistance during the laboratory based research work and during the submission of this manuscript.

List of other publications which are not attached to this thesis

- **Synthesis of chromenoindole derivatives from *Robinia pseudoacacia***

  L. Dejon, H. Mohammed, **P. Du**, C. Jacob, A. Speicher, *Med. Chem. Commun.*, *(2013,) 4, 1580-1583*

- **Emerging Biological Applications of Chalcogens: Amphiphilic Selenic Acids with Multiple Impact on Living Cells**

  P. Du, U.M. Viswanathan, Z. Xu, H. Ebrahimnejad, B. Hanf, T. Burkholz, M. Schneider, I. Bernhardt, G. Kirsch, M. Montenarh, C. Jacob,. *in E.R. Rene, P. Kijjanapanich, P.N.L. Lens (eds.), Proceedings of the 3rd International Conference on Research Frontiers in Chalcogen Cycle Science & Technology, Delft, The Netherlands, May 27-28, 59-68 (2013).*

Reviews:

- **Control of oxidative posttranslational cysteine modifications: from intricate chemistry to widespread biological and medical applications**

  C. Jacob, E. Battaglia, T. Burkholz, **D. Peng**, D. Bagrel, M. Montenarh, *Chemical Research in Toxicology, 25, 588-604 (2012).*

- **Proanthocyanidins: Oligomeric Structures with Unique Biochemical Properties and Great Therapeutic Promise**

  Z. Xu, **P. Du**, P. Meiser and C. Jacob, *Natural Product Communications, 7(3), 381-388 (2012).*

Contents

1. Introduction

The human organism is composed of trillions of living cells. In an adult body, the total amount of cells is kept steadily. Progenitor cells undergo mitosis and divide into two daughter cells, such that the damaged or worn-out cells that need to be cleared via necrosis or programmed cell death can be replaced. The new cells grow, differentiate to specialized cells, perform special cellular functions during their life span and undergo apoptosis at the end of their "lifetime". If the proliferation of new cells is out of control or the damaged cells carrying modified genotypes escape from apoptosis, cancer could emerge [1].

In the last few decades, cancer has become more and more serious as a dominate cause of death [2]. According to the record of "Cancer Report in Europe", prostate cancer, lung cancer and intestine cancer are the top three kinds of cancer that result in human death in men, while breast cancer, intestine cancer and lung cancer are the top three cancers in women [3].

1.1. Oxidative stress

Cells in aerobic organisms need energy to survive and to maintain their house-keeping functions for the body. In human cells, adenosine triphosphate (ATP) is the most important source of energy [4]. During the ATP generation process, the oxidative phosphorylation of glucose, reactive species and primarily pro-oxidants are produced, and immediately detoxified by the cellular anti-oxidant defence systems. As a result of the detoxification, the concentration of reactive species in healthy mammalian cells is precisely regulated in a specifically dynamic range to maintain the cell's various functions [5, 6].

In general, cancer cells need more cellular energy supply because they proliferate much faster than the healthy cells in organs [1]. In order to survive and adapt to such a "tough" microenvironment like hypoxia and nutrient deprivation, cancer cells need to maintain their energy supply differently, which usually leads to their suffering from oxidative stress (OS) [7]. OS is a phenomenon where the balance between the pro-oxidants and the anti-oxidants has been broken, and the pro-oxidants dominate in this case [8]. OS usually leads to increased intracellular concentrations of reactive species, mostly the reactive oxygen species (ROS), as well as the reactive nitrogen species (RNS), the reactive nitrogen oxygen species (RNOS) and free metal ions [5, 8-10]. In fact, increased ROS levels have been observed in many types of cancer cells [5] and OS is now considered as a hallmark in many cancer cells, as shown in Fig 1. [5, 7, 8, 11-13]. Interestingly, besides cancers, OS is also involved in many other diseases, such as inflammation and arthritis [11]. Increased ROS levers in cancer cells can increase glycolysis and promote the pentose phosphate cycle to such extent that more biological energy can be provided for the uncontrolled cell growth and cell immortalization [6, 14, 15].

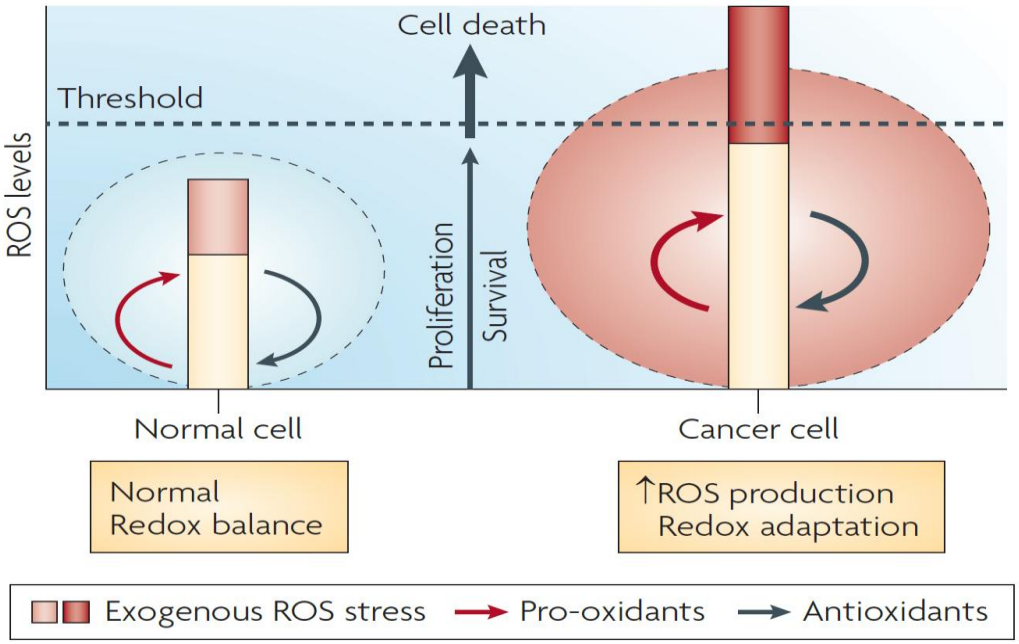

Fig 1. *Different levels of ROS are found in healthy cells and cancer cells and elevated ROS levels are a hallmark of many cancer cells. Because of this fairly specific tumour redox microenvironment, exogenous ROS stress increases ROS levels in cancer cells over a critical threshold leading to cell death. Alternatively, inhibition of antioxidant enzymes, conversion of existing ROS to more aggressive ROS and catalytic oxidation of thiol proteins/enzymes can also be employed to kill such cancer cells rather selectively. The picture has been adapted from* [5].

1.1.1. Reactive species

In chemistry, ROS, RNS and RNOS are considered to be very active substances. The reactive species exist in two forms, the free radical form carrying unpaired valence electrons (*e.g.* the hydroxyl radical $^{\cdot}OH$, the superoxide radical $O_2^{\cdot-}$ and the nitric oxide $^{\cdot}NO$), and the non-radical form carrying paired valence electrons like H_2O_2 and peroxynitrite $ONOO^-$. Both forms are very highly reactive and tend to oxidize many biomolecules they encounter. [8].

Biologically, the reactive species have "two faces". On one hand, an increased concentration of reactive species results in damage in and to cells. For example, DNA damage (shown in Fig 2) induced by the ROS contributes to tumour formation, which is now widely accepted in cancer research. Among all the reactive species, ROS are the main triggers of carcinogenesis. On the other hand, the reactive oxidizing species can also contribute to cell growth, proliferation or apoptosis in healthy cells [8, 9, 15-17].

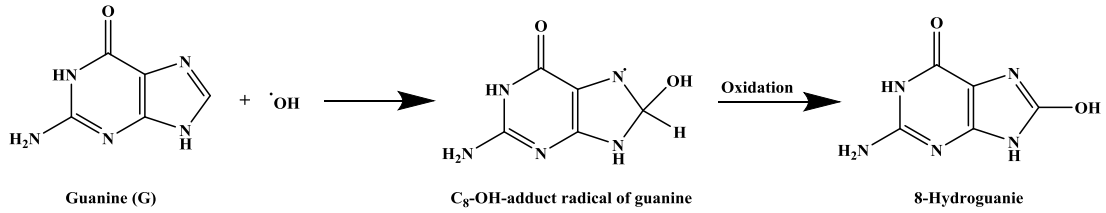

Fig 2. *An example reaction of DNA (guanine) damage with the hydroxyl radical causing damage. The modified guanine, 8-hydroguanine, is mutagenic and carcinogenic, which leads to gene instability and tumour formation. This picture has been adapted from* [10].

1.1.2. Anti-oxidant defence systems

Natural anti-oxidant defence systems detoxify ROS or diminish the harmful effects of ROS by cleaning ROS rapidly and keeping ROS concentrations at a low steady level to maintain ROS homeostasis in cells. Such antioxidant action can protect cells from oxidative damages to lipids, proteins and DNA [8].

Natural anti-oxidant defence systems against OS can be separated into two types, namely the anti-oxidant enzymatic system and the non-enzymatic system [8]. The anti-oxidant enzymatic system is composed of enzymes such as catalase (CAT), superoxide dismutase (SOD), glutathione peroxidase (GPx), peroxiredoxin (Prx) and a range of other peroxidases. SOD catalyzes the reaction of $O_2^{\cdot}$ to H_2O_2 and O_2 [18, 19]. After that, H_2O_2 is decomposed by CAT into H_2O and O_2 [20]. GPx reduces H_2O_2 to H_2O by simultaneously oxidizing glutathione (L-γ-glutamyl-L-cysteinylglycine, GSH) to glutathione disulfide (GSSG) [20]. Prx catalyzes the same reaction as GPx does, yet primarly by oxidizing thiols of cytosolic proteins such as thioredoxin (Trx) [21]. The oxidation of protein-SH (thiol-form, P-SH) to either S-glutathiolated proteins (PSSG) or protein disulfide (P-S-S-P) is a

trigger for the activation of signal transduction pathways such as the activation or arrest of cell cycle. This process is reversible: the oxidized form (disulfide) can be reduced to thiol form by disulfide reductases, often in the presence of nicotinamide adenine dinucleotide phosphate (NADPH). The reduced thiol groups can therefore be recycled in subsequent enzymatic oxidative reactions [8, 9, 14]. The main processes are shown in Fig 3.

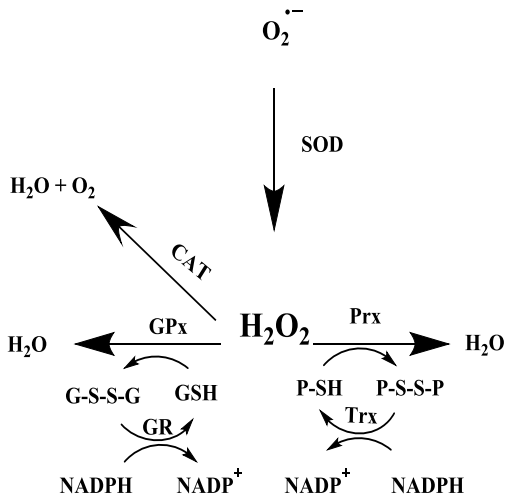

Fig 3. *Schematic representation of the homeostasis of the cellular redox balance in cells. As the main initial free radical species, the superoxide radical anion can be converted to H_2O_2 by SOD. The resulting H_2O_2 can be converted to H_2O and O_2 by Catalase (CAT), or detoxified to H_2O by GPx (with concomitant consumption of GSH) or Prx (using thiol residues in proteins, P-SH as "reducing equivalent"). In the presence of NADPH, the oxidized products (GSSG or P-S-S-P) can be reduced by glutathione reductase (GR) and thioredoxin (Trx), respectively. The recycled GSH and P-SH can be reused in the next oxidative reaction. The picture has been adapted from* [5, 12].

In contrast to the enzymatic antioxidant system, the non-enzymatic antioxidant system consists of small hydrophilic molecules like ascorbic acid (vitamin C, Fig 4) and hydrophobic molecules like tocopherols and tocotrienols (*i.e.* vitamin E group, Fig 4). Biologically, these substances can originate either endogenously (*e.g.* glutathione, GSH, see Fig 4) or exogenously (*e.g.* ascorbic acid). Actually, the two systems are working in a cooperative manner. For example, GSH detoxifies H_2O_2 to H_2O in the presence of GPx, as mentioned above.

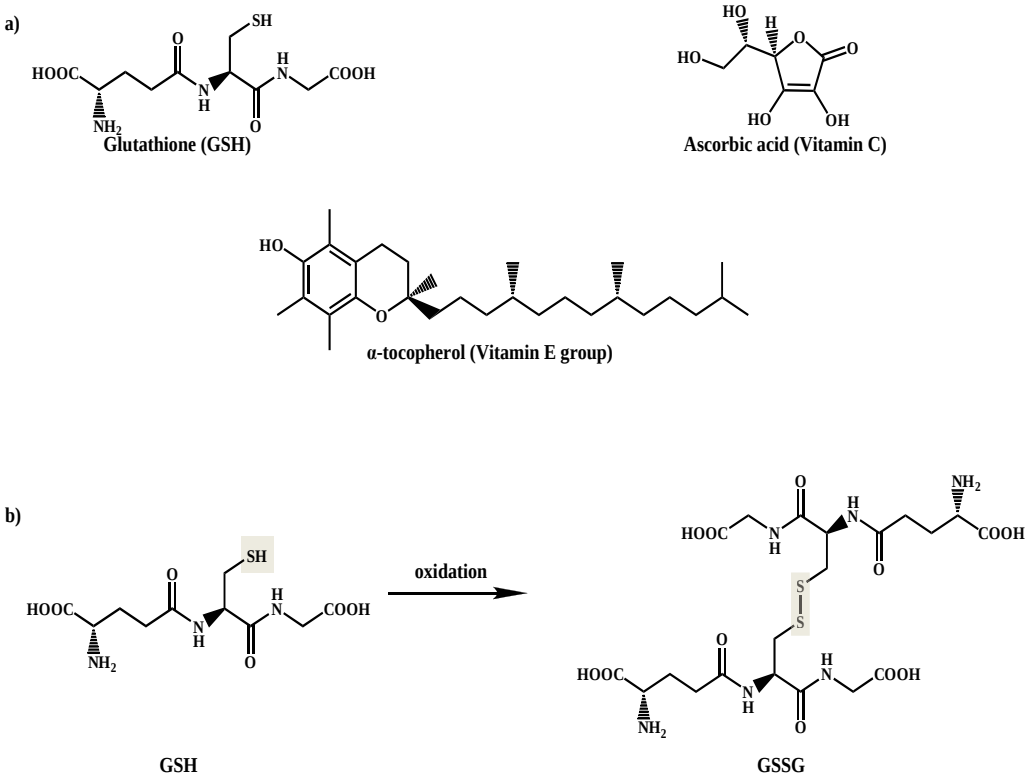

Fig 4. *Schematic overview of a non enzymatic antioxidant system. a) selected examples for anti-oxidants. b) Oxidation of GSH to GSSG. The oxidative reaction takes place at the thiol moiety of GSH.*

1.2. Apoptosis

Apoptosis is a form of programmed cell death which takes place during the development and aging of normal cells, by which cells can be "replaced" yet the overall cell population of tissues can be maintained without affecting biological functions of such tissues [22]. Generally, the apoptotic signaling pathways can be classified into intrinsic and extrinsic pathways [23], as shown in Fig 5. Extrinsic apoptosis pathways can be triggered by so-called death receptors on the plasma membrane, which is usually followed by the activation of caspase 8 and its down-stream caspase cascades. Intrinsic apoptosis pathways can be activated by cellular stresses and involved proteins such as Bcl-2-associated X protein (Bax), which can increase the permeability of the mitochondrial membrane. As a consequence, cytochrome *c* could be released into the cytoplasma. Once in the cytosol, cytochrome *c* can further activate caspase 9 and its down-stream caspase cascades. Both the extrinsic and intrinsic pathways ultimately lead to the activation of caspase 3 in the late stage of such signaling cascades [24]. Tumour cells may escape from programmed apoptosis by increasing intracellular anti-apoptotic molecules like B-cell lymphoma 2 protein (Bcl-2) or by decreasing pro-apoptotic proteins such as Bax protein [25]. Overexpressed Bcl-2 can prevent the increase of mitochondrial membrane permeability hence keeping cytochrome *c* inside the mitochondria [26]. Furthermore, Bcl-2 protein can inhibit directly the activation of caspase 9 to stop the death signaling cascades [26].

ROS can activate intrinsic pathways to "push" the cancer cells to undergo apoptosis. For instance, it can increase the permeability of the mitochondrial membrane and lead to the loss of mitochondrial membrane potential, which causes the increase of the mitochondrial ROS and cytochrome *c* release into the cytosol. Interestingly, the released mitochondrial ROS could act as a "second messenger" to trigger further ROS

release in neighbouring mitochondria. Thus, a positive feedback loop forms from mitochondrion to mitochondrion to release mitochondrial ROS into the cytosol, which often leads to severe injury to the mitochondria. This whole process is called “ROS induced ROS release” and is likely to play an important role in apoptosis [27], as is shown in Fig 5.

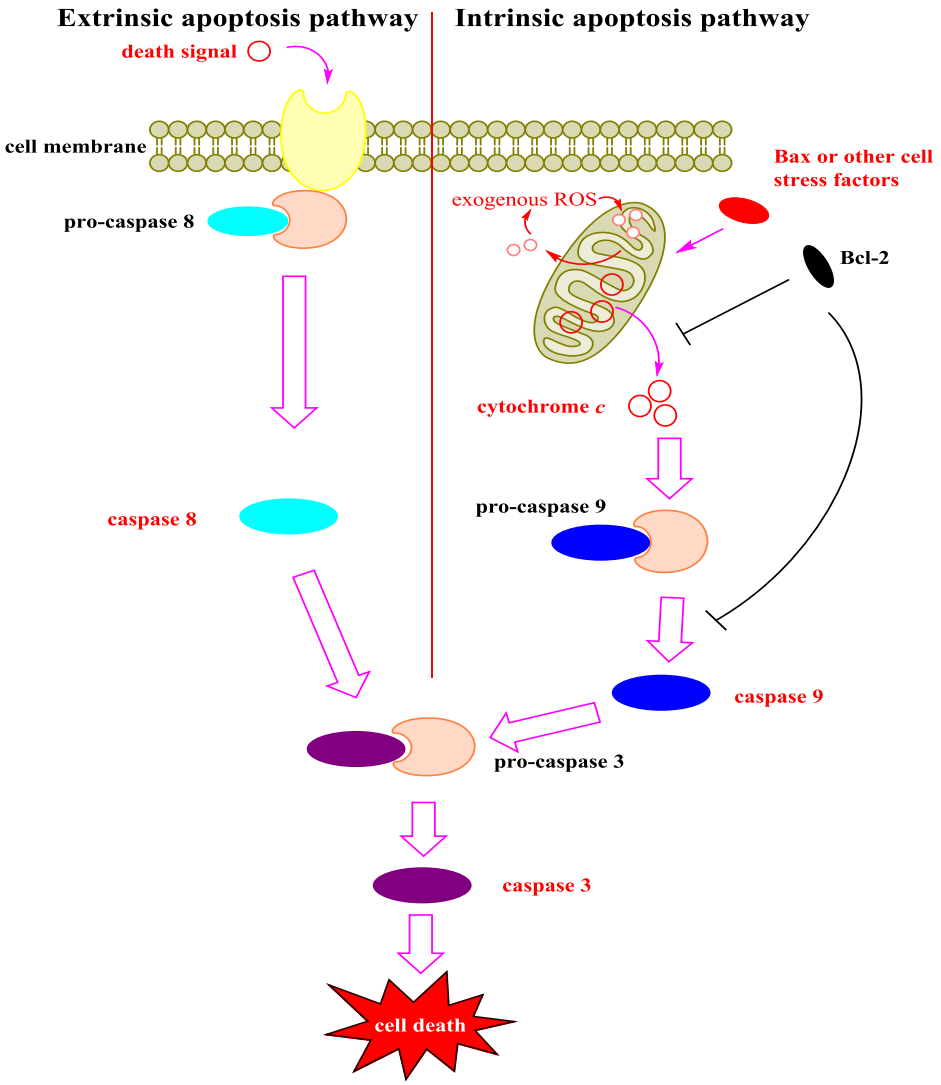

Fig 5. *Extrinsic and intrinsic apoptotic pathways. Extrinsic signaling begins with the activation of caspase 8 by activation of death receptor. Intrinsic signaling begins with modification of mitochondrial functions by the Bax protein or other*

cellular stress factors. Both pathways lead to the activation of caspase 3 as the last step to induce apoptosis. Exogenous ROS triggers mitochondrial ROS release. The released mitochondrial ROS then in itself acts as "induced exogenous ROS" in the cytoplasm to trigger ROS release in the neighbouring mitochondrion which leads to apoptosis. The picture has been adapted from [23, 27].

1.3. Endoplasmic reticulum stress

In eukaryotic cells, the endoplasmic reticulum (ER) represents the key organelle responsible for protein synthesis processes such as protein translation, protein folding and protein transportation. Interestingly, ROS are also involved in protein folding processes [28]. Under OS condition in certain cancer cells, the elevated ROS levels can result in corrupted ER function in the form of the accumulation of misfolded proteins, which is now called endoplasmic reticulum stress (ER stress) [29]. The most important response under ER stress, however, is the unfolded protein response (UPR). In healthy mammalian cells, UPR activates signaling pathways such as the increasing translation of chaperons involved in the protein folding process in order to compensate for the accumulation of misfolded proteins in ER. In this way, ER stress can be relieved and the normal cellular functions are recovered so that the cell can survive [30]. If UPR fails to compensate the corrupted ER function, ER stress signaling pathways will be triggered to activate apoptosis in the last step [31]. As shown in Fig 6, three pathways are involved in this kind of signaling: 1) the PERK/eIF2α/ATF4 pathway [32], 2) the IRE1α/ XBP1 pathway [33], and 3) the ATF6 pathway [34]. Among these three pathways, protein kinase RNA-like endoplasmic reticulum kinase (PERK), inositol-requiring enzyme 1α (IRE1α) and transcription factor 6 (ATF6) will be activated as initial events, respectively. Under normal conditions, PERK, IRE1α and ATF6 exist in inactive forms by binding to ER stress senor binding immunoglobulin protein (BiP). In the presence of UPR,

misfolded proteins competitively bind to BiP to release and hence also to trigger the respective activities of PERK, IRE1α and ATF6 [35]. The PERK pathway plays an important role in cancer cells, because this signaling pathway is involved in the cellular protein synthesis. In order to overcome the moderate to extreme hypoxia conditions, which exist in many tumour cells, cancer cells will adapt to the inhibition of global protein synthesis. Hence the activation of the PERK signaling pathway in cancer cells provides the necessary adaption to the hypoxia condition [32]. Therefore, PERK/eIF2α/ATF4-pathways will be discussed in more detail later on.

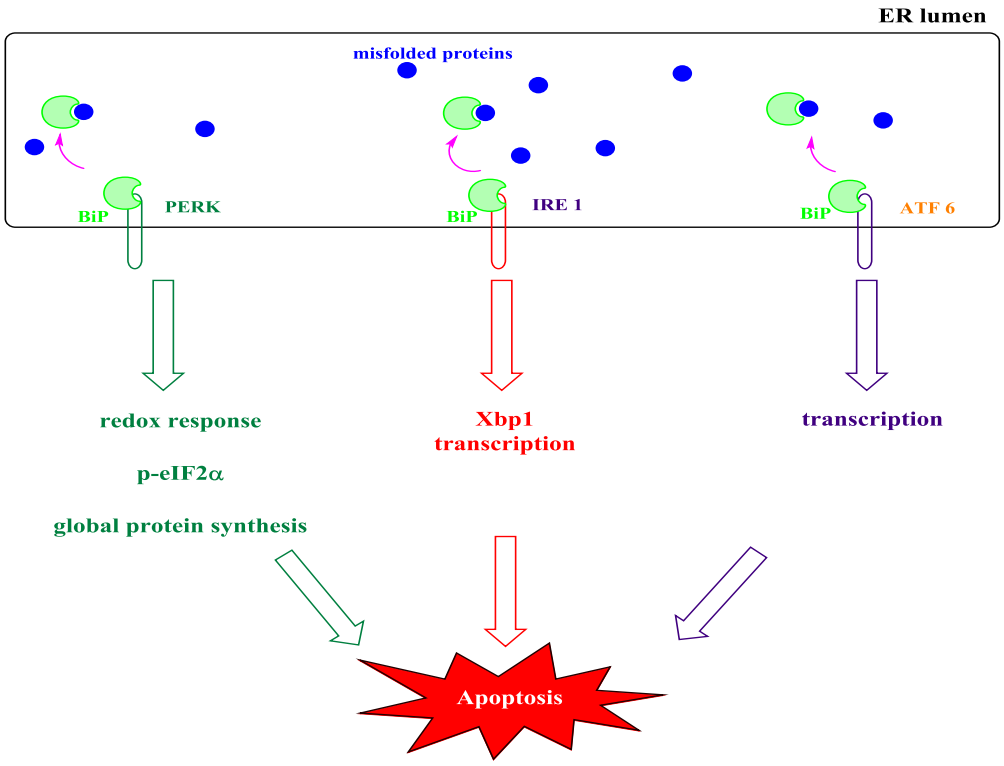

Fig 6. *Schematic representation of the 3 signaling pathways involved in the unfolded protein response (UPR). Upon the removal of BiP by binding of misfolded protein, PERK, IRE1 or ATF6 are activated as early events in these 3 pathways, respectively. The activation of PERK, IRE1 or ATF6 induces further downstream signaling. The picture has been adapted from* [36, 37].

1.3.1. The PERK/eIF2α/ATF4 pathway

Upon the removal of the inhibitory factor BiP from the complex of BiP and PERK under UPR, PERK will be released and hence activated as an early event to its downstream signaling pathway via its oligomerization and autophosphorylation [35]. Activated PERK inhibits the eukaryotic initiation factor 2α (eIF2α) by phosphorylation which is involved in the initiation phase of protein translation. Then the whole protein synthesis is turned off except the selective expression of anti-stress factors such as activating transcription factor 4 (ATF4) [38]. ATF4 is a transcription factor in turn regulating the expression of various pro-survival genes involved in the oxidative stress response, amino acid synthesis and differentiation. Interestingly, under prolonged ER-stress, ATF4 also upregulates the expression of pro-apoptosis proteins like C/EBP homologous protein (CHOP) [39]. It still remains elusive, however, how exactly CHOP activates apoptotic signaling [40]. It is already known that CHOP interacts with the Bcl-2 protein family to activate the intrinsic apoptotic signaling [41]. Overexpressed CHOP may, for instance, result in a decrease in Bcl-2 protein and could trigger the translocation of Bax protein from the cytosol to the mitochondria in order to transmit the death signal. Hence, both CHOP-knockout ($CHOP^{-/-}$) mice and Bax-knockout ($Bax^{-/-}$) mice are resistant to the apoptotic ER stress responses [41-43]. The entire signaling of PERK/eIF2α/ATF4 pathway is summarized in Fig 7.

Furthermore, the activation of PERK triggers not only the phosphorylation of eIF2α, but also the phosphorylation of nuclear factor (erythroid-derived 2)-like 2 (NFE2L2 or Nrf2) [37], as shown in Fig 7. Nrf2 is involved in antioxidant response pathways, which are described as "the primary cellular defence against the cytotoxic effects of oxidative stress" [44-46]. These pathways contribute to the survival of the cells under OS. Under normal conditions, Nrf2 exists in an inactive form by binding to kelch

like-ECH-associated protein 1 (Keap1) and cullin 3 proteins. Activated PERK phosphorylates Nrf2, which leads to its dissociation from the protein complex of Keap 1 and cullin 3. Activated Nrf2 upregulates the expression of antioxidant enzymes like heme oxygenase 1 (HO-1) to detoxify the cytotoxic effects of ROS [37, 47].

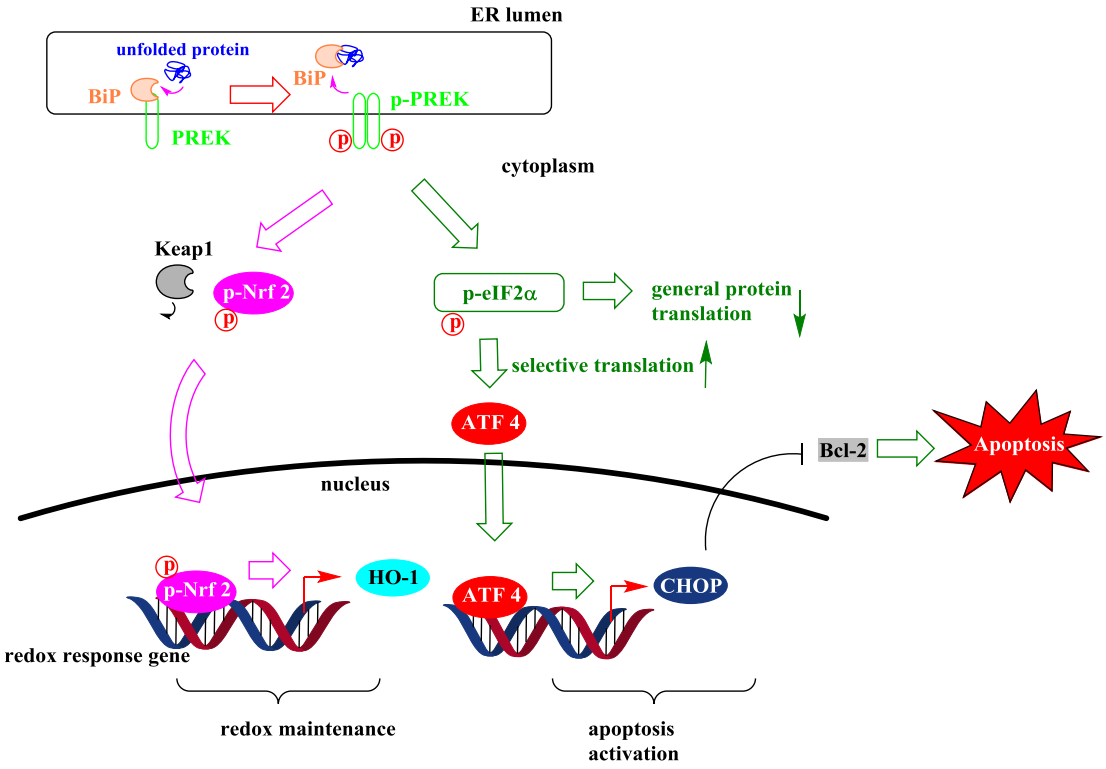

Fig 7. *Schematic representation of PERK mediated signaling pathways. Under ER stress, unfolded proteins bind to BiP competitively, which releases PERK from BiP. Then, PERK is activated by its oligomerization and autophosphorylation. Activated PERK phosphorylates Nrf2 as well as eIF2α. Phosphorylation of Nrf2 leads to its dissociation from Keap1. The activated Nrf2 proteins translocate into cell nucleus to promote the transcription of redox response genes like HO-1. Phosphorylation of eIF2α attenuates the translation of general proteins. Interestingly, phosphorylated eIF2α selectively promotes the translation of ATF4. ATF4 targets both anti-apoptotic and pro-apoptotic genes. If*

the ER stress exceeds its critical threshold, ATF4 will contribute to the transcription of the CHOP proteins. CHOP inhibits the transcription and hence activity of Bcl-2 proteins and hence triggers pro-apoptotic signaling cascades. The picture has been adapted from [36, 37, 40, 47].

Interestingly, cancer cells can survive PERK/eIF2α/ATF4 pathway-induced apoptosis. Therefore, one rationale in the development of anti-cancer durgs involves an increase of ER stress in cancer cells which subsequently activates the apoptotic pathway [36, 48].

1.4. Cell cycle

Cells proliferate via cell cycle. This process can be divided into three subphases: quiescent, interphase and cell division. Quiescent (G0) is a resting phase. Cells in the G0 phase can be activated by cytokines to enter the interphase that in itself contains 3 subphases, Gap 1 (G1), the synthesis period (S phase) and Gap 2 (G2). In G1, proteins are synthesized and the amount of cellular organelles is increased. The S phase starts with the synthesis of DNA and stops when all of the chromosomes have been duplicated. The G2 phase is a gap phase between S phase and the cell division phase. After further preparation in the G2 subphase, the progenitor cell finally undergoes mitosis, *e.g.* the pro-, prometa-, meta-, ana-, and telophase, and divides into two daughter cells [49].

Three key events are involved in the whole cell division process to ensure a high integrity of DNA in the two daughter cells: DNA replication in S phase, spindle formation and segregation of chromosomes during cell division. A defect in each of those three events could lead to genetic instability and tumour formation [50, 51].

The spindle apparatus is based on the fundamental machinery of microtubules and ensures the correct segregation of chromosomes between the two daughter cells during cell division. The highly dynamic cytoskeletal structures of microtubules are crucial for cell division in the prophase, prometaphase, and metaphase during mitosis. Tubulins are the basic components of microtubules and exist in 6 forms, of which α- and β-tubulin are the most common members of the tubulin protein family. Anti-cancer drugs like paclitaxel interfere with the microtubule dynamics by binding to the tubulins and therefore exhibit powerful anti-mitotic properties. These drugs lead to cell cycle arrest and apoptosis, and even to changes of microtubule mass under applied high doses [52-54].

1.5. Red blood cells

Before all the molecules that contain selenium and tellurium designed (described below in chemical considerations) can take effects inside the cell cytosol, they must cross the cell membrane before they can interact with their target proteins. Hence these compounds need specific ways to enter the cells, but this kind of facilitation should keep the integrity of the cell membrane. In contrast, certain compounds may also disrupt the membrane and hence the cell membrane can be considered as their prime target. Therefore, the interaction of the compounds with the cell membrane was investigated prior to all the anti-cancer experiments.

Mature red blood cells (RBCs) in mammals lack a cellular nucleus and the organelles such as mitochondria and do not possess complex signaling pathways. Therefore, RBCs are considered as an ideal model for investigating the interactions of chemical compounds with the cell membrane and the embedded proteins [55].

1.5.1. Cell membrane of red blood cells

The cell membrane of RBCs with a typical thickness of 7.5 nm is composed of lipids (41%), proteins (52%) and carbohydrates (7%) [56]. Lipids constitute the infrastructure of the cell membrane. They can be classified into three types: phospholipids (62.7%), neutral lipids (25.2%) and glyco-sphingophospholipids (ca. 12%) [57]. The most common phospholipids of human RBCs are sphingomyeline (Sph 26%), phosphatidylcholine (PC, 30%), phosphatidylethanolamine (PE, 27%) and phosphatidylserine (PS, 13%) [58, 59]. Phospholipids are asymmetrically distributed in the plasma membrane of the RBCs due to the presence of lipid transporters such as flippase, floppase and scramblase: normally, Sph and PC are located in the outer leaflet of the plasma membrane predominantly, while PE and PS are found in the inner leaflet of human RBCs. [60].

1.5.2. Performance of the interaction with cell membrane of red blood cells

The interaction of the compounds tested with the cell membrane or with the embedded proteins on the cell membrane can be presented in two forms: haemolysis and eryptosis. Due to the fact that the newly designed compounds are amphiphilic as surfactants, the interaction of surfactants with the cell membrane of RBCs will be discussed in detail.

The surfactants such as sodium dodecyl sulfate (SDS), which interact strongly with the cell membrane of RBCs, can cause haemolysis, while others such as benzethonium, which interact “softly” with the cell membrane, cause RBC to undergo eryptosis [61]. Eryptosis is the specific form of apoptosis of worn-out RBCs which is mediated by phosphatidylserine (PS) exposure from the inner to the outer leaflet of the membrane [62]. PS on the outside of the cell membrane can be detected by

macrophages. As a result, the worn out RBCs will be degraded by macrophages via phagocytosis. Therefore, PS exposure can be described as a biomarker for eryptosis. [63]. Elevated intracellular Ca^{2+} level in RBCs activate the scramblase and inhibit the flippase. These two processes will result in PS exposure on the cell surface [63, 64].

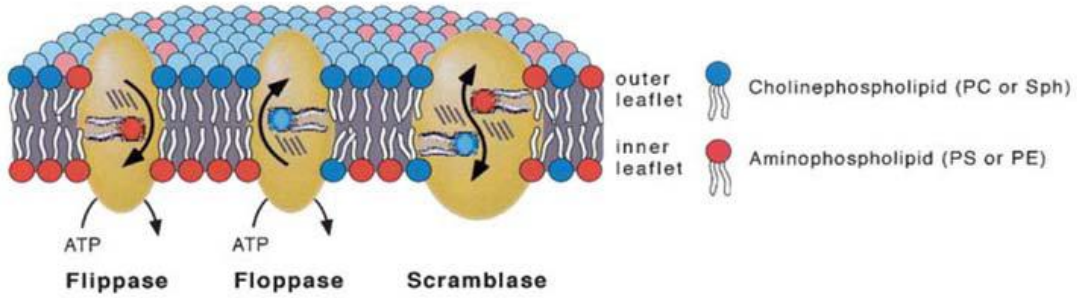

Fig 8. *Schematic representation of the different lipid transporters. Phosphatidylserine (PS) and phosphatidylethanolamine (PE) are translocated by flippase from the outer to the inner leaflet of the plasma membrane with ATP consumption. Floppase transports PC in the opposite direction. Scramblase exchanges PC with PS in an ATP-independent manner. The picture has been adapted from* [60].

1.6. Chemical considerations of the "chemistry" of redox modulation

It is already known that OS is present in many kinds of cancer cells due to hypoxia and energy deficiency. In such cases, the ROS levels have almost reached the critical redox threshold to trigger apoptosis in such cancer cells. The process does not take place in healthy cells. In the last few years, the effects of ROS in cancer cells and their modulation with small molecule compounds have drawn more and more attention. These compounds effectively work on the cancer cells and selectively inhibit the growth of these cells [65]. Such agents may, for instance, induce ROS

production in cancer cells to overwhelm the critical redox threshold, which would subsequently trigger the apoptosis signaling cascades. In contrast, although the ROS level could also be raised to a higher level with these compounds in healthy cells, these cells will not undergo apoptosis, because their energy metabolism and natural defence systems are still kept intact, *i.e.* these cells are "naturally" far away from the critical redox threshold. Based on the specific roles of ROS in cancer cells, there are three general strategies to design and develop new anti-cancer drugs as redox modulators [13], as is shown in Fig 9.:

A. Compounds are designed to raise the ROS level.

B. Compounds are designed to inhibit the antioxidant systems.

C. Compounds are designed to act as redox catalysts [13].

a)

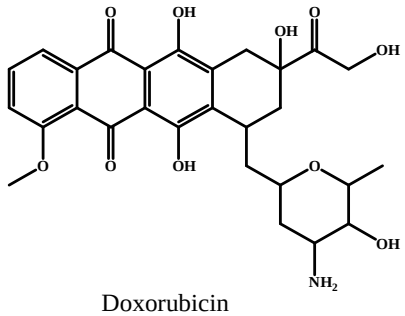

Doxorubicin

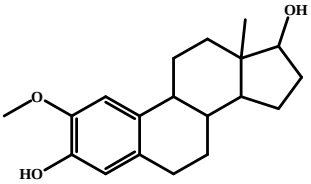

2-methoxyestradiol

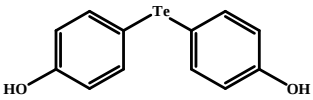

4,4'-tellurodiphenol

b)

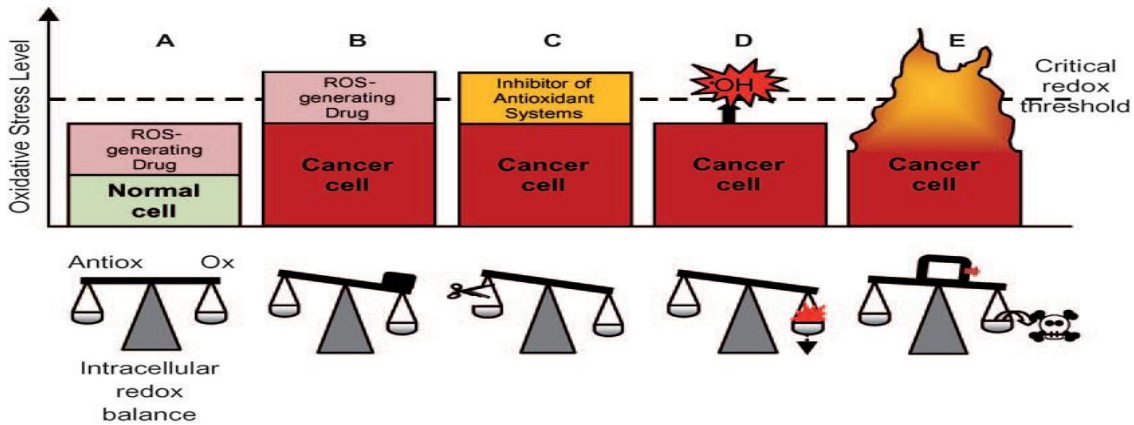

Fig 9. *Overview of the rational design for different types of redox modulators. a) Doxorubicin is shown as an example of a drug used for the generation of ROS, 2-methoxyestradiol represents an example of a drug used for inhibition of antioxidant systems and 4,4'-tellurodiphenol is an example of a drug which cause the catalytic oxidation of cellular thiols with the presence of ROS. b) In healthy cells, the redox balance is kept intact. In contrast, ROS generating drugs elevate the ROS level in the cells but still keep below the critical redox threshold. Due to the intact natural defence system in non cancerous cells, the effect of the ˙OH radical or minor oxidation of proteins can be compensated, therefore, the healthy cells can survive (A). In cancer cells, the elevated ROS level "naturally" reaches almost the threshold to trigger apoptosis. ROS generating drugs like doxorubicin or drugs that inhibit antioxidant systems, like SOD-inhibitor 2-methoxyestradiol, raise the ROS levels over this threshold. In this case, the cancer cells undergo apoptosis (B and C). Some SOD-mimics convert the existing ROS to more aggressive and toxic radicals (˙OH) (C). GPx-mimics like 4,4'-tellurodiphenol catalyze the oxidation of thiol groups (in proteins and enzymes) by* H_2O_2*, which leads to possible oxidation of proteins (and/or GSH) to induce the apoptosis in cancer cells (E). The picture has been adapted from* [13].

Based on the fact that the redox modulators have shown effective anti-cancer properties in many cell-based assays, this thesis is focused on the design and the development of selenium (Se)- and tellurium (Te)-containing compounds as promising anti-cancer drugs. It should be noted that such selenium and tellurium compounds are believed to work as catalysts rather than simple antioxidants.

Se and Te belong to the chalcogens in Group 16 of the Periodic Table, which is also known as the "oxygen family". Chemically, the oxidation states of Se and Te vary from -2 to +6.

Se is an essential trace element in the human body. It forms a component of proteins, for example, the glutathione peroxidase enzymes which are maintaining a low level of H_2O_2 in the cell. Lack of Se can lead to general fatigue, mental fatigue, hypothyroidism and even to more serious ailments such as reproductive disorders and miscarriage. Synthetic organo-selenide derivatives (with oxidation state -2) have been considered as antioxidants for a long time [66], other physiological activities have also been emerging. Ebselen (2-Phenyl-1,2-benzoselenazol-3-one), for instance, can induce apoptosis in various cancer cells [67-71]. The pro-apoptotic effect of ebselen has been investigated in multiple myeloma and human hepatoma cancer cells and seems to be related to enhance ROS levels in both cancer cell lines. *N*-acetyl cysteine, which is a precursor of intracellular GSH synthesis, can alleviate ebselen-induced apoptosis. These results suggested that ebselen can accelerate the oxidation of thiol moieties by H_2O_2, *e.g.* in GSH [67, 71]. The underlying mechanisms explaining the action of ebselen are depicted in Fig 10 [72]. The thiol moiety in GSH is not the only SH moiety that is involved in this scenario, but also the cysteine residues in proteins (P-SH). Once thiol groups in proteins have become oxidized to P-S-S-P, the structures and functional activities of these proteins will be altered, ultimately trigging various signaling pathways. This process may also induce apoptosis [13, 65, 73, 74].

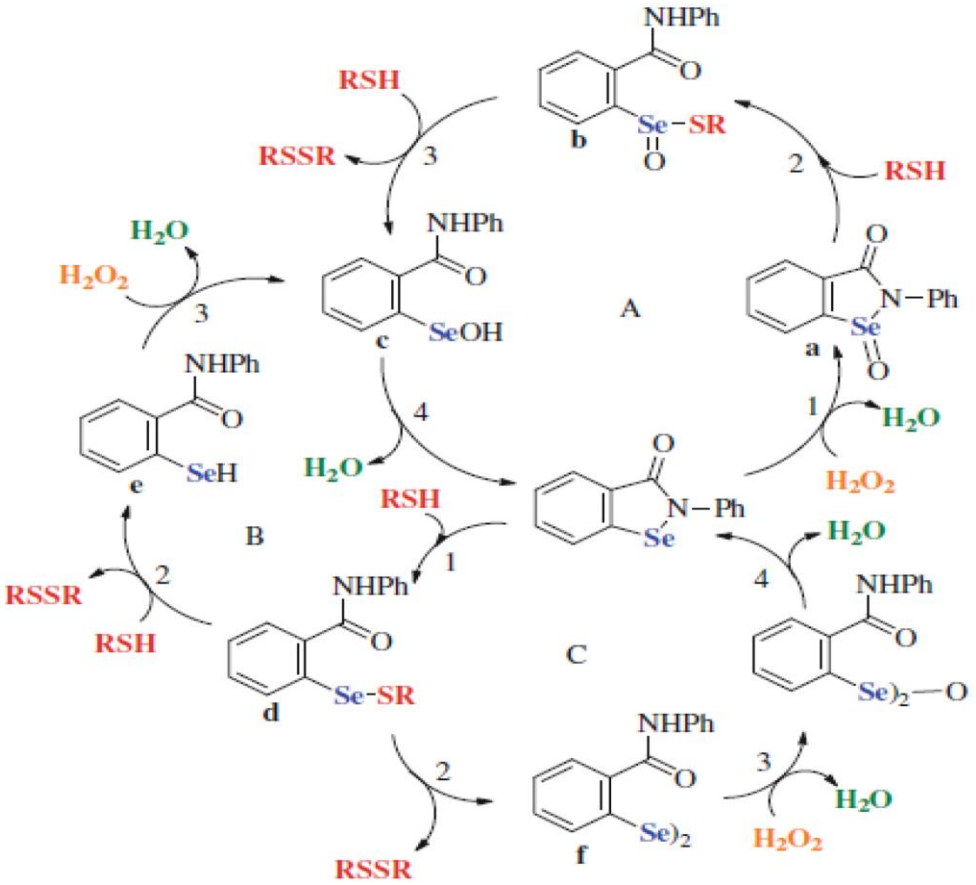

Fig 10. *The redox mechanisms of GPx-mimics using ebselen as an example. There are three possible catalytic redox cycles. Cycle A: Ebselen could be oxidized by* H_2O_2 *to the selenoxide derivative a. The selenoxide a could be converted to the thiolseleninate b by reduction with one thiol group, then, the latter could be reduced again by anther thiol group to seleninic acid c. Ebselen may be recycled via elimination of* H_2O*. Cycle B: Ebselen could be reduced directly by a thiol group to form selenyl sulfide d. Subsequently, compound d is able to react with another thiol group to form selenol e, which may be reoxidized by* H_2O_2*. Cycle C: The selenyl sulfide d could also be reduced by a thiol group leading to the diselenide f, which may form ebselen again after oxidation by* H_2O_2 *and intramolecular rearrangement. This picture has been adapted from* [72].

In contrast to Se-compounds, Te-compounds have long and widely been believed to be biologically "useless" and even toxic for humans. Recently, however, several organic tellurium compounds have been reported as promising anti-cancer drugs [13, 65, 74-76]. A widely accepted mechanism proposes that those Te compounds may show similar biological activities as their analogues Se compounds, because, chemically, Te is mostly relative of Se [75]. The activities of these Te-compounds, however, still remain elusive. Some organic phenyl telluride (oxidation state -2) derivates have been reported to generate ROS, which causes cancer cells to undergo apoptosis by halting cell proliferation or by inducing DNA damage in HL-60 cells (chemical structures of such compounds as shown in Fig 11. a)) [77]. Furthermore, inorganic Te-compounds also seem to contribute to the modulation of the intracellular redox balance, such as potassium tellurite (K_2TeO_3, oxidation state of tellurium +4) [78].

Organic quinone-telluride derivates (oxidation state of tellurium -2) designed by Jacob and co-workers, such as 2,3-bis(phenyltellanyl)naphthoquinone and 2-(phenyltellanyl)-3-methylnaphthoquinone, are able to elevate intracellular ROS levels, induce apoptosis, signaling and disturb tubulin and actin structures in PtK2 potoroo and KB-3-1 cells [74, 79]. Some of these compounds, such as 2,3-bis(phenyltellanyl)naphthoquinone, also show very selective anti-proliferating effects against HT29 and CT26 human colon cancer cells but not against normal fibroblast cells like NIH-3T3. Similar effects have been observed in human chronic lymphocytic leukemia (CLL) cells [75]. The 2,3-bis(phenyltellanyl)naphthoquinone considerably reduced the viability of CLL B-cells isolated from patient blood, while healthy B-cells from the same patient were much less affected (structures shown in Fig 11 b)) [74]. It is very difficult, however, to synthesize these compounds. Furthermore, many organic tellurium-contaminating substances are insoluble in water or decompose easily. In fact, in order to increase stability, aryl- and allyl-groups need

to “flank” the reactive atom, which in turn causes issues related to solubility. Therefore, new and simple organic selenium and tellurium containing compounds have been designed and synthesized carrying these elements. These compounds have been designed to improve their water solubility, cell membrane permeability and to show an improved biological activity.

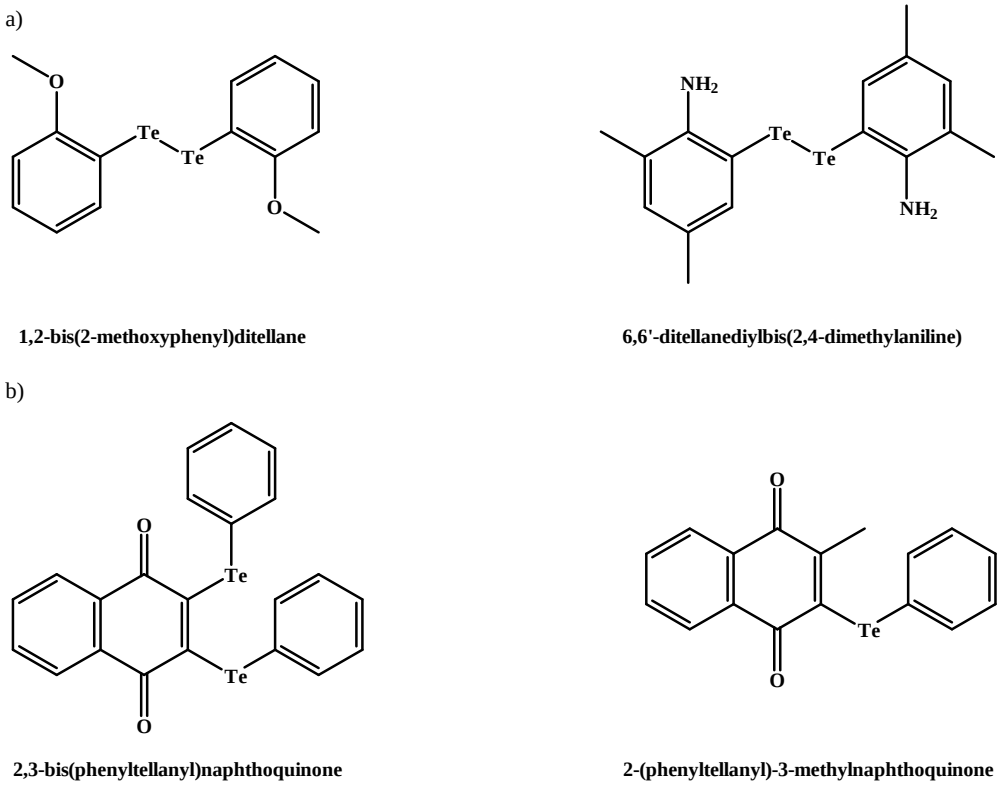

Fig 11. *Organotellurium compounds evaluated previously for redox-modulating biological activity. a) Tested with HL-60 cells based assays*. b) *Organic quinone-telluride derivates. This picture has been adapted from* [74, 79].

The compounds designed must cross the cell membrane before they can modulate the redox cycle in the cell to perform the biological activities. Therefore, the structure of cell membrane was extensively considered. The mammalian cell membrane consists of a phospholipid bilayer with embedded proteins [80]. Biophysically, a phospholipid

is a surfactant that is composed of one hydrophilic head group, and the lipophilic tail that contributes to the solubility in oil phase. Therefore, surfactants dissolve both in H_2O and in oil. Due to the high similarities with the components of the cell membrane, synthetic surfactants can interact with the cell membrane and even penetrate it [81]. To achieve water solubility and penetration of the cell membrane in one go, surfactant-like molecules with both hydrophilic and hydrophobic properties can be considered.

In the early 1980s, it has been reported already that some organic tellurium-containing derivatives of fatty acids can be taken up by cells and then trapped specifically in the myocardium. Therefore, these fatty acids could be used as a biomarker of cardiac diseases [82]. Based on the structures of these chalcogen containing fatty acids, a specific design strategy has been developed. The rationale is: 1. Se and Te (-2) are supposed to provide biological effects of modulating ROS levels in cancer cells; 2. The Alkyl chain, Se (or Te) and phenyl groups are arranged in tandem, such that the Se (or Te) atom could be stabilized by the phenyl group during the catalytic cycle in the cells; 3. Due to the replacement of the alkyl group by the phenyl group on one side of Se (or Te), the absorption by cells could be affected, hence the length of the alkyl group on the other side is varied to investigate the correlation between amphiphilicity (in respect of the critical micelle concentration (CMC)) and their biological activities to select the best compound for biological tests on cancer cells. To increase solubility in aqueous media, the sulfuric acid group was used as head group for these new amphiphilic compounds. Because sulfuric acid (a strong acid) can dissociate fully in water, the sulfuric acid group provides excellent hydrophilicity and is superiors to, for instance, the carboxylic acid group. Thus, ten compounds as shown in Fig 12 have been designed, synthesized, purified and characterized chemically. The results of subsequent biological tests indicated that these sulfates can readily penetrate the cell

membrane, induce ROS, trigger ER stress and finally induce apoptosis in HCT 116 cells.

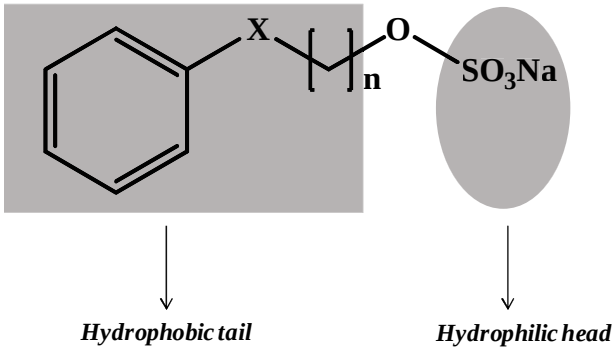

	X	n
DP 31	Se	8
DP 32	Se	9
DP 33	Se	10
DP 34	Se	11
DP 35	Se	12
DP 41	Te	8
DP 42	Te	9
DP 43	Te	10
DP 44	Te	11
DP 45	Te	12

Fig 12. *The design of the selenium- and tellurium-containing compounds based on the idea of water soluble and cell membrane penetrable at the same time. The part of Ph-Se- Alkyl chain fuctions as hydrophobic tail and the SO_3Na as hydrophilic head. See text for further details. The picture has been adapted from* [83].

Interestingly, the cellular redox state can be modulated not only by selenide compounds, but also by other seleno-compounds such as seleninic acid derivates [84]. Chemically, seleninic acid (+2) only functions as a pro-oxidant. Thus, seleninic acid can be directly reduced by thiol moieties within a few seconds [85, 86]. The reduced selenide can subsequently participate in the catalytical redox cycle as discussed above. Unfortunately, due to their chemical property of being an acid, chemically simple seleninic acid derivates cannot penetrate the cell membrane. Therefore, the usage of seleninic acid as biological redox catalysts is prevented. In order to solve this problem and turn this high hydrophilicity into an advantage, the seleninic acid has been used as a suitable head group of amphiphilic molecules. This method has shown considerable success.

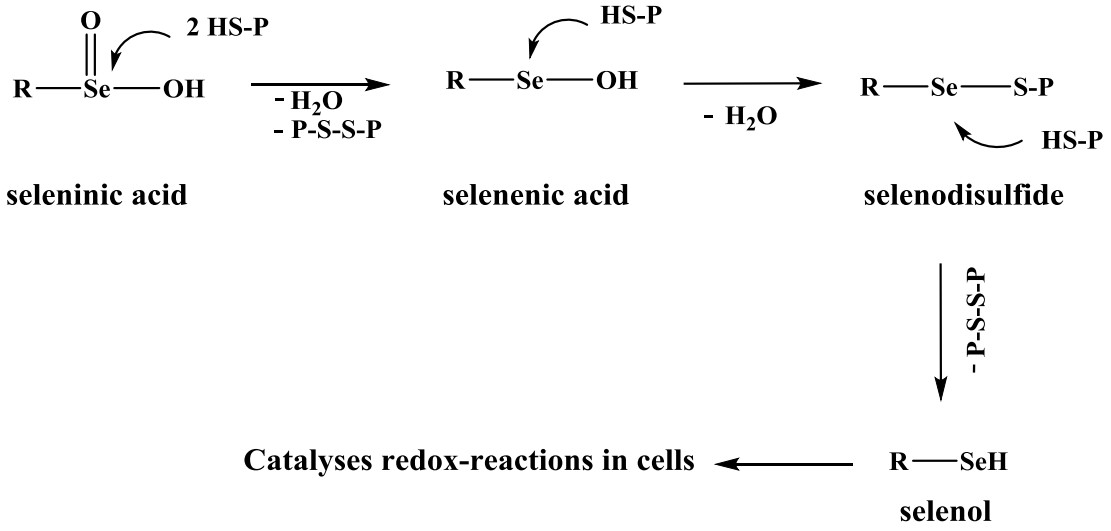

Fig 13. *The chemisty of seleninic acid derivates. The seleninic acid can be reduced by two thiol groups (HS-P) leading to selenenic acid (R-Se-OH). Further, the selenenic acid can react with another two thiol groups to form selenodisulfide (R-Se-S-R) first, and then a selenol(R-SeH), which enters into the redox catalytic cycle. This picture has been adapted from* [87].

Based on similar rationales in designing selenide surfactants, new series of seleninic acid derivates has been designed to the deliver seleninic acid moiety into cells, as shown in Fig 14. In this case, seleninic acid is used directly as the head group. This head combines two functions: hydrophilicity and biological activity.

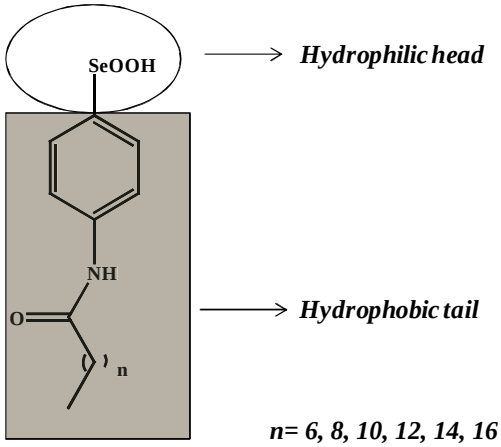

Fig 14. The *design of seleninic acid derivates based on the idea of a surfactant. The seleninic acid acts both as hydrophilic head and carrier of selenium specific biological activity. See the text for further details. This picture has been adapted from* [88].

1.7 References

[1] Australian Institute of Health and Welfare & Australasian Association of Cancer Registries 2012. Cancer in Australia: an overview, 2012. Cancer series no. 74. Cat. no. CAN 70.

[2] R. Siegel, D. Naishadham, A. Jemal, Cancer statistics, 2013, CA: A Cancer Journal for Clinicians, 63 (2013) 11-30.

[3] M. Malvezzi, P. Bertuccio, F. Levi, C. La Vecchia, E. Negri, European cancer mortality predictions for the year 2013, Annals of Oncology / Official Journal of the European Society for Medical Oncology, 24 (2013) 792-800.

[4] J.R. Knowles, Enzyme-catalyzed phosphoryl transfer reactions, Annual Review of Biochemistry, 49 (1980) 877-919.

[5] D. Trachootham, J. Alexandre, P. Huang, Targeting cancer cells by ROS-mediated mechanisms: a radical therapeutic approach?, Nature Reviews. Drug Discovery, 8 (2009) 579-591.

[6] B. D'Autreaux, M.B. Toledano, ROS as signalling molecules: mechanisms that generate specificity in ROS homeostasis, Nature Reviews / Molecular Cell Biology, 8 (2007) 813-824.

[7] T. Fiaschi, P. Chiarugi, Oxidative stress, tumor microenvironment, and metabolic reprogramming: a diabolic liaison, International Journal of Cell Biology, 2012 (2012) Article ID:762825.

[8] H. Sies, Strategies of antioxidant defense, European Journal of Biochemistry / FEBS, 215 (1993) 213-219.

[9] M. Valko, D. Leibfritz, J. Moncol, M.T. Cronin, M. Mazur, J. Telser, Free radicals and antioxidants in normal physiological functions and human disease, The International Journal of Biochemistry & Cell Biology, 39 (2007) 44-84.

[10] M. Valko, C.J. Rhodes, J. Moncol, M. Izakovic, M. Mazur, Free radicals, metals and antioxidants in oxidative stress-induced cancer, Chemico-biological Interactions, 160 (2006) 1-40.

[11] J. Fang, T. Seki, H. Maeda, Therapeutic strategies by modulating oxygen stress in cancer and inflammation, Advanced Drug Delivery Reviews, 61 (2009) 290-302.

[12] D. Ivanova, R. Bakalova, D. Lazarova, V. Gadjeva, Z. Zhelev, The impact of reactive oxygen species on anticancer therapeutic strategies, Advances in Clinical and Experimental Medicine, 22 (2013) 899-908.

[13] V. Jamier, L.A. Ba, C. Jacob, Selenium- and tellurium-containing multifunctional redox agents as biochemical redox modulators with selective cytotoxicity, Chemistry, 16 (2010) 10920-10928.

[14] D. Trachootham, W. Lu, M.A. Ogasawara, R.D. Nilsa, P. Huang, Redox regulation of cell survival, Antioxidants & Redox Signaling, 10 (2008) 1343-1374.

[15] W.C. Burhans, N.H. Heintz, The cell cycle is a redox cycle: linking phase-specific targets to cell fate, Free Radical Biology & Medicine, 47 (2009) 1282-1293.

[16] J. Boonstra, J.A. Post, Molecular events associated with reactive oxygen species and cell cycle progression in mammalian cells, Gene, 337 (2004) 1-13.

[17] S. Fourquet, M.E. Huang, B. D'Autreaux, M.B. Toledano, The dual functions of thiol-based peroxidases in H2O2 scavenging and signaling, Antioxidants & Redox Signaling, 10 (2008) 1565-1576.

[18] C. Nicco, A. Laurent, C. Chereau, B. Weill, F. Batteux, Differential modulation of normal and tumor cell proliferation by reactive oxygen species, Biomedicine & Pharmacotherapy, 59 (2005) 169-174.

[19] A.A. Starkov, The role of mitochondria in reactive oxygen species metabolism and signaling, Annals of the New York Academy of Sciences, 1147 (2008) 37-52.

[20] B. Halliwell, Reactive species and antioxidants. Redox biology is a fundamental theme of aerobic life, Plant Physiology, 141 (2006) 312-322.

[21] C. Jacob, P.G. Winyard, in: Redox Signaling and Regulation in Biology and Medicine, Wiley-VCH Verlag GmbH & Co. KGaA, 2009, pp. 1-11.

[22] S. Elmore, Apoptosis: a review of programmed cell death, Toxicologic Pathology, 35 (2007) 495-516.

[23] L. Galluzzi, K. Blomgren, G. Kroemer, Mitochondrial membrane permeabilization in neuronal injury, Nature Reviews / Neuroscience, 10 (2009) 481-494.

[24] F.H. Igney, P.H. Krammer, Death and anti-death: tumour resistance to apoptosis, Nature Reviews / Cancer, 2 (2002) 277-288.

[25] S. Fulda, Tumor resistance to apoptosis, International Journal of Cancer, 124 (2009) 511-515.

[26] R.J. Youle, A. Strasser, The BCL-2 protein family: opposing activities that mediate cell death, Nature Reviews / Molecular Cell Biology, 9 (2008) 47-59.

[27] D.B. Zorov, M. Juhaszova, S.J. Sollott, Mitochondrial ROS-induced ROS release: an update and review, Biochimica et Biophysica Acta, 1757 (2006) 509-517.

[28] J.D. Malhotra, R.J. Kaufman, Endoplasmic reticulum stress and oxidative stress: a vicious cycle or a double-edged sword?, Antioxidants & Redox Signaling, 9 (2007) 2277-2293.

[29] J.D. Malhotra, H. Miao, K. Zhang, A. Wolfson, S. Pennathur, S.W. Pipe, R.J. Kaufman, Antioxidants reduce endoplasmic reticulum stress and improve protein secretion, Proceedings of the National Academy of Sciences of the United States of America, 105 (2008) 18525-18530.

[30] M. Schroder, R.J. Kaufman, ER stress and the unfolded protein response, Mutation Research, 569 (2005) 29-63.

[31] J.D. Malhotra, R.J. Kaufman, ER stress and its functional link to mitochondria: role in cell survival and death, Cold Spring Harbor Perspectives in Biology, 3 (2011) Article ID: a004424.

[32] D.R. Fels, C. Koumenis, The PERK/eIF2alpha/ATF4 module of the UPR in hypoxia resistance and tumor growth, Cancer Biology & Therapy, 5 (2006) 723-728.

[33] Y. Chen, F. Brandizzi, IRE1: ER stress sensor and cell fate executor, Trends in Cell Biology, 23 (2013) 547-555.

[34] N. Morishima, K. Nakanishi, A. Nakano, Activating transcription factor-6 (ATF6) mediates apoptosis with reduction of myeloid cell leukemia sequence 1 (Mcl-1) protein via induction of WW domain binding protein 1, The Journal of Biological Chemistry, 286 (2011) 35227-35235.

[35] W.A. Wang, J. Groenendyk, M. Michalak, Endoplasmic reticulum stress associated responses in cancer, Biochimica et Biophysica Acta, (2014). DOI: 10.1016/j.bbamcr.2014.01.012

[36] T. Verfaillie, A.D. Garg, P. Agostinis, Targeting ER stress induced apoptosis and inflammation in cancer, Cancer Letters, 332 (2013) 249-264.

[37] S.B. Cullinan, J.A. Diehl, Coordination of ER and oxidative stress signaling: the PERK/Nrf2 signaling pathway, The International Journal of Biochemistry & Cell Biology, 38 (2006) 317-332.

[38] R.C. Wek, H.Y. Jiang, T.G. Anthony, Coping with stress: eIF2 kinases and translational control, Biochemical Society Transactions, 34 (2006) 7-11.

[39] K. Ameri, A.L. Harris, Activating transcription factor 4, The International Journal of Biochemistry & Cell Biology, 40 (2008) 14-21.

[40] S. Oyadomari, M. Mori, Roles of CHOP/GADD153 in endoplasmic reticulum stress, Cell Death and Differentiation, 11 (2004) 381-389.

[41] M.C. Wei, W.X. Zong, E.H. Cheng, T. Lindsten, V. Panoutsakopoulou, A.J. Ross, K.A. Roth, G.R. MacGregor, C.B. Thompson, S.J. Korsmeyer, Proapoptotic BAX and BAK: a requisite gateway to mitochondrial dysfunction and death, Science, 292 (2001) 727-730.

[42] S. Oyadomari, K. Takeda, M. Takiguchi, T. Gotoh, M. Matsumoto, I. Wada, S. Akira, E. Araki, M. Mori, Nitric oxide-induced apoptosis in pancreatic beta cells is mediated by the endoplasmic reticulum stress pathway, Proceedings of the National Academy of Sciences of the United States of America, 98 (2001) 10845-10850.

[43] H. Zinszner, M. Kuroda, X. Wang, N. Batchvarova, R.T. Lightfoot, H. Remotti, J.L. Stevens, D. Ron, CHOP is implicated in programmed cell death in response to

impaired function of the endoplasmic reticulum, Genes & Development, 12 (1998) 982-995.

[44] R. Gold, L. Kappos, D.L. Arnold, A. Bar-Or, G. Giovannoni, K. Selmaj, C. Tornatore, M.T. Sweetser, M. Yang, S.I. Sheikh, K.T. Dawson, Placebo-controlled phase 3 study of oral BG-12 for relapsing multiple sclerosis, The New England Journal of Medicine, 367 (2012) 1098-1107.

[45] R.A. Linker, D.H. Lee, S. Ryan, A.M. van Dam, R. Conrad, P. Bista, W. Zeng, X. Hronowsky, A. Buko, S. Chollate, G. Ellrichmann, W. Bruck, K. Dawson, S. Goelz, S. Wiese, R.H. Scannevin, M. Lukashev, R. Gold, Fumaric acid esters exert neuroprotective effects in neuroinflammation via activation of the Nrf2 antioxidant pathway, Brain / A Journal of Neurology, 134 (2011) 678-692.

[46] R.H. Scannevin, S. Chollate, M.Y. Jung, M. Shackett, H. Patel, P. Bista, W. Zeng, S. Ryan, M. Yamamoto, M. Lukashev, K.J. Rhodes, Fumarates promote cytoprotection of central nervous system cells against oxidative stress via the nuclear factor (erythroid-derived 2)-like 2 pathway, The Journal of Pharmacology and Experimental Therapeutics, 341 (2012) 274-284.

[47] M.M. Sachdeva, M. Cano, J.T. Handa, Nrf2 signaling is impaired in the aging RPE given an oxidative insult, Experimental Eye Research, 119 (2014) 111-114.

[48] C. Hetz, E. Chevet, H.P. Harding, Targeting the unfolded protein response in disease, Nature reviews. Drug Discovery, 12 (2013) 703-719.

[49] M.L. Whitfield, L.K. George, G.D. Grant, C.M. Perou, Common markers of proliferation, Nature Reviews / Cancer, 6 (2006) 99-106.

[50] L.H. Hartwell, M.B. Kastan, Cell cycle control and cancer, Science, 266 (1994) 1821-1828.

[51] G.I. Evan, K.H. Vousden, Proliferation, cell cycle and apoptosis in cancer, Nature, 411 (2001) 342-348.

[52] L. Wilson, M.A. Jordan, New microtubule/tubulin-targeted anticancer drugs and novel chemotherapeutic strategies, Journal of Chemotherapy, 16 Suppl 4 (2004) 83-85.

[53] M.A. Jordan, L. Wilson, Microtubules as a target for anticancer drugs, Nature Reviews / Cancer, 4 (2004) 253-265.

[54] C. Dumontet, M.A. Jordan, Microtubule-binding agents: a dynamic field of cancer therapeutics, Nature Reviews / Drug Discovery, 9 (2010) 790-803.

[55] I. Bernhardt, L. Ivanova, P. Langehanenberg, B. Kemper, G. von Bally, Application of digital holographic microscopy to investigate the sedimentation of intact red blood cells and their interaction with artificial surfaces, Bioelectrochemistry, 73 (2008) 92-96.

[56] C.M. Haest, Distribution and Movement of Membrane Lipids, in: I. Bernhardt, J.C. Ellory (Eds.) Red Cell Membrane Transport in Health and Disease, Springer Berlin Heidelberg, 2003, pp. 1-25.

[57] G. Nelson, Lipid composition and metabolism of erythrocytes. In: Blood lipids and lipoproteins: Quantitation, composition, and metabolism, Wiley Interscience New York, (1972) 317-386.

[58] R.M. Broekhuyse, Improved lipid extraction of erythrocytes, Clinica Chimica Acta, 51 (1974) 341-343.

[59] R.M. Broekhuyse, Quantitative two-dimensional thin-layer chromatography of blood phospholipids, Clinica Chimica Acta, 23 (1969) 457-461.

[60] R.F. Zwaal, P. Comfurius, E.M. Bevers, Surface exposure of phosphatidylserine in pathological cells, Cellular and Molecular Life Sciences, 62 (2005) 971-988.

[61] E. Lang, K. Jilani, C. Zelenak, V. Pasham, D. Bobbala, S.M. Qadri, F. Lang, Stimulation of suicidal erythrocyte death by benzethonium, Cellular Physiology and Biochemistry, 28 (2011) 347-354.

[62] M. Foller, S.M. Huber, F. Lang, Erythrocyte programmed cell death, Iubmb Life, 60 (2008) 661-668.

[63] D.B. Nguyen, L. Wagner-Britz, S. Maia, P. Steffen, C. Wagner, L. Kaestner, I. Bernhardt, Regulation of phosphatidylserine exposure in red blood cells, Cellular Physiology and Biochemistry, 28 (2011) 847-856.

[64] O.A. Kofanova, N.G. Zemlyanskikh, L. Ivanova, I. Bernhardt, Changes in the intracellular Ca2+ content in human red blood cells in the presence of glycerol, Bioelectrochemistry, 73 (2008) 151-154.

[65] F.H. Fry, C. Jacob, Sensor/effector drug design with potential relevance to cancer, Current Pharmaceutical Design, 12 (2006) 4479-4499.

[66] S.E. Jackson-Rosario, W.T. Self, Targeting selenium metabolism and selenoproteins: Novel avenues for drug discovery, Metallomics, 2 (2010) 112-116.

[67] C.F. Yang, H.M. Shen, C.N. Ong, Ebselen induces apoptosis in HepG(2) cells through rapid depletion of intracellular thiols, Archives of Biochemistry and Biophysics, 374 (2000) 142-152.

[68] C.F. Yang, H.M. Shen, C.N. Ong, Intracellular thiol depletion causes mitochondrial permeability transition in ebselen-induced apoptosis, Archives of Biochemistry and Biophysics, 380 (2000) 319-330.

[69] I.J. Rzepczynska, N. Foyouzi, P.C. Piotrowski, C. Celik-Ozenci, A. Cress, A.J. Duleba, Antioxidants induce apoptosis of rat ovarian theca-interstitial cells, Biology of Reproduction, 84 (2011) 162-166.

[70] M. Yoshizumi, T. Kogame, Y. Suzaki, Y. Fujita, M. Kyaw, K. Kirima, K. Ishizawa, K. Tsuchiya, S. Kagami, T. Tamaki, Ebselen attenuates oxidative stress-induced apoptosis via the inhibition of the c-Jun N-terminal kinase and activator protein-1 signalling pathway in PC12 cells, British Journal of Pharmacology, 136 (2002) 1023-1032.

[71] L. Zhang, L. Zhou, J. Du, M. Li, C. Qian, Y. Cheng, Y. Peng, J. Xie, D. Wang, Induction of apoptosis in human multiple myeloma cell lines by ebselen via enhancing the endogenous reactive oxygen species production, BioMed Research International, 2014 (2014) Article ID: 696107.

[72] C.W. Nogueira, J.B. Rocha, Toxicology and pharmacology of selenium: emphasis on synthetic organoselenium compounds, Archives of Toxicology, 85 (2011) 1313-1359.

[73] C. Sanmartin, D. Plano, A.K. Sharma, J.A. Palop, Selenium compounds, apoptosis and other types of cell death: an overview for cancer therapy, International Journal of Molecular Sciences, 13 (2012) 9649-9672.

[74] M. Doering, L.A. Ba, N. Lilienthal, C. Nicco, C. Scherer, M. Abbas, A.A.P. Zada, R. Coriat, T. Burkholz, L. Wessjohann, M. Diederich, F. Batteux, M. Herling, C. Jacob, Synthesis and Selective Anticancer Activity of Organochalcogen Based Redox Catalysts, Journal of Medicinal Chemistry, 53 (2010) 6954-6963.

[75] L.A. Ba, M. Doring, V. Jamier, C. Jacob, Tellurium: an element with great biological potency and potential, Organic & Biomolecular Chemistry, 8 (2010) 4203-4216.

[76] R.L. Cunha, I.E. Gouvea, L. Juliano, A glimpse on biological activities of tellurium compounds, Anais da Academia Brasileira de Ciencias, 81 (2009) 393-407.

[77] B.L. Sailer, N. Liles, S. Dickerson, S. Sumners, T.G. Chasteen, Organotellurium compound toxicity in a promyelocytic cell line compared to non-tellurium-containing organic analog, Toxicology in Vitro : An International Journal Published in Association with BIBRA, 18 (2004) 475-482.

[78] J.M. Sandoval, P. Leveque, B. Gallez, C.C. Vasquez, P. Buc Calderon, Tellurite-induced oxidative stress leads to cell death of murine hepatocarcinoma cells, Biometals, 23 (2010) 623-632.

[79] T. Schneider, Y. Muthukumar, B. Hinkelmann, R. Franke, M. Doring, C. Jacob, F. Sasse, Deciphering intracellular targets of organochalcogen based redox catalysts, Medchemcomm, 3 (2012) 784-787.

[80] P.F. Devaux, A. Zachowski, Maintenance and consequences of membrane phospholipid asymmetry, Chemistry and Physics of Lipids, 73 (1994) 107-120.

[81] S. Schreier, S.V. Malheiros, E. de Paula, Surface active drugs: self-association and interaction with membranes and surfactants. Physicochemical and biological aspects, Biochimica et Biophysica Acta, 1508 (2000) 210-234.

[82] G. Kirsch, M.M. Goodman, F.F. Knapp, Organotellurium compounds of biological interest-unique properties of the N-chlorosuccinimide oxidation product of 9-telluraheptadecanoic acid, Organometallics, 2 (1983) 357-363.

[83] P. Du, U.M. Viswanathan, K. Khairan, T. Buric, N.E.B. Saidu, Z. Xu, B. Hanf, I. Bazukyan, A. Trchounian, F. Hannemann, I. Bernhardt, T. Burkholz, B. Diesel, A.K. Kiemer, K.-H. Schafer, M. Montenarh, G. Kirsch, C. Jacob, Synthesis of amphiphilic, chalcogen-based redox modulators with in vitro cytotoxic activity against cancer cells, macrophages and microbes, Medchemcomm, 5 (2014) 25-31.

[84] W. Zhong, T.D. Oberley, Redox-mediated effects of selenium on apoptosis and cell cycle in the LNCaP human prostate cancer cell line, Cancer Research, 61 (2001) 7071-7078.

[85] M. Abdo, Z. Sun, S. Knapp, Biohybrid -Se-S- coupling reactions of an amino acid derived seleninate, Molecules, 18 (2013) 1963-1972.

[86] M. Abdo, S. Knapp, Mechanism of a redox coupling of seleninic acid with thiol, The Journal of Organic Chemistry, 77 (2012) 3433-3438.

[87] P. Du, U.M. Viswanathan, Z. Xu, H. Ebrahimnejad, B. Hanf, T. Burkholz, M. Schneider, I. Bernhardt, G. Kirsch, M. Montenarh, C. Jacob, Emerging Biological Applications of Chalcogens: Amphiphilic Selenic Acids with Multiple Impact on Living Cells, in: E.R. Rene, P. Kijjanapanich, P.N. Lens (Eds.) G16 conference - Proceedings of the 3rd International Conference on Research Frontiers in Chalcogen Cycle Science & Technology, Unesco-IHE, Delft, 2013, pp. 59-68.

[88] P. Du, U.M. Viswanathan, Z. Xu, H. Ebrahimnejad, B. Hanf, T. Burkholz, M. Schneider, I. Bernhardt, G. Kirsch, C. Jacob, Synthesis of amphiphilic seleninic acid derivatives with considerable activity against cellular membranes and certain pathogenic microbes, J Hazard Mater, 269 (2014) 74-82.

2. Result and Discussion

In this chapter, three publications are described by Diplom Apotheker Peng Du as first author. The synthesis of the new selenium and tellurium containing surfactants as well as the screening of their activities with nematodes, RBCs, RAW 264.7, HCT116 and ARPE-19 cells are shown in the first publication. The signaling transduction to induce apoptosis with the tellurium compound DP41 in HCT116 cells is described in the second publication. The synthesis of seleninic acid containing surfactants and their activities against RBCs and *S. cervisiae* are summarized in the third publication.

2.1. Pulication 1

Synthesis of amphiphilic, chalcogen-based redox modulators with in vitro cytotoxic activity against cancer cells, macrophages and microbes

Peng Du, Uma M. Viswanathan, Khairan Khairan, Tomislav Buric, Nathaniel E. B. Saidu, Zhanjie Xu, Benjamin Hanf, Inga Bazukyan, Armen Trchounian, Frank Hannemann, Ingolf Bernhardt, Torsten Burkholz, Britta Diesel, Alexandra K. Kiemer, Karl-Herbert Schäfer, Mathias Montenarh, Gilbert Kirsch and Claus Jacob

This manuscript was published as an article in the following Journal:

Medicinal Chemistry Communications, 2014, 5, 25-31

DOI: 10.1039/C3MD00204G

2.1.1. Abstract

Several amphiphilic, chalcogen-based redox modulators have been synthesized which exhibit a widespread, yet in some instances also selective, biological activity which is most likely based on their ability to modulate the intracellular redox balance and to interact with cellular membranes and specific proteins.

2.1.2. Introduction

The last decade has witnessed a growing interest in the development of redox modulating agents, which are able to effectively, yet also selectively, attack cells with a disturbed redox balance, such as diverse cancer cells, macrophages and sclerodermic fibroblasts.[1–5] A similar strategy has also been employed to kill various microorganisms, which are vulnerable because of a weak antioxidant defence.[1,6–8] In many cases, catalytic selenium and tellurium agents have been at the forefront of these developments, since these compounds exploit the efficiency and selectivity of a chemical catalyst for its intracellular substrate(s) to generate pronounced cytotoxic events in specific cells.[4–6,9,10] Such compounds are, for instance, able to induce apoptosis in leukemic B-cells while healthy B-cells of the same patient remain largely unaffected.[2,11]

Unfortunately, many of the most interesting organoselenium and tellurium agents available to date are only poorly soluble in aqueous media and often unstable – and hence possess a comparably poor bioavailability and drug profile, even in cell culture. While attempting to circumvent some of the problems associated with such unfavourable physico-chemical properties, the idea of amphiphilic redox modulators has emerged, as detergent-like properties may, at least in theory, bestow such molecules with certain additional, quite beneficial aspects. Firstly, such amphiphilic

compounds should be fairly soluble in aqueous media. Secondly, amphiphilic structures should cross cell membranes and hence enter cells more easily when compared to more hydrophilic or lipophilic agents. Thirdly, amphiphilic agents should be able to interact strongly with membranes and (hydrophobic parts of) proteins. And finally, such agents may cluster together at certain cellular sites (e.g. at membranes, in hydrophobic pockets) and hence may act synergistically.

Surprisingly, only few suitable amphiphilic redox-modulating agents have been reported in the literature so far, and most of these substances have not been studied comprehensively in cell culture.[12,13] Recently, some relevant chalcogen compounds have emerged in this context in the literature, confirming that the synthesis of such structures is realistic.[13]

2.1.3. Result and discussion

We have therefore decided to synthesize a series of amphiphilic selenium and tellurium compounds with an anionic head group and hydrocarbon 'tails' of different tail lengths in order to explore the various aspects – and possible benefits – of such agents in the context of biological activity, selectivity and mode(s) of action. The compounds ultimately selected and subsequently synthesized as part of this study are shown in Fig. 1. The design of these compounds combines aspects of previously studied selenium and tellurium compounds (e.g. aryl substituents for enhanced stability) with typical features of an amphiphilic agent.[13] As for the synthesis of such compounds, once the most promising synthetic avenue was selected (see Fig. 1), the preparation of these molecules has been fairly straightforward (see the ESI†). In many instances, good yields (up to 63%) were possible even without further optimization.

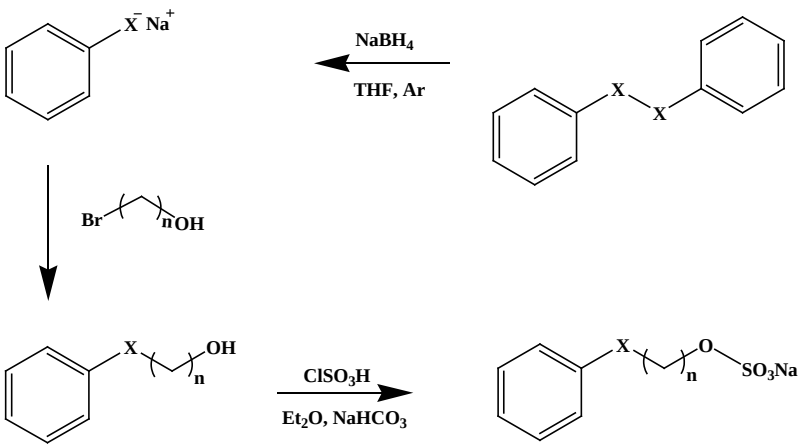

	X	n
DP 11	Se	8
DP 12	Se	9
DP 13	Se	10
DP 14	Se	11
DP 15	Se	12
DP 21	Te	8
DP 22	Te	9
DP 23	Te	10
DP 24	Te	11
DP 25	Te	12

	X	n
DP 31	Se	8
DP 32	Se	9
DP 33	Se	10
DP 34	Se	11
DP 35	Se	12
DP 41	Te	8
DP 42	Te	9
DP 43	Te	10
DP 44	Te	11
DP 45	Te	12

Fig 1. *Chemical structures of compounds selected for this study. The most successful synthetic route is provided (see text and ESI for details†)*

Once synthesized and chemically characterized, the two most interesting physico-chemical properties associated with these compounds from a biological perspective (i.e. the amphiphilic and redox properties) have been confirmed using surface tension measurements and cyclic voltammetry. The results, illustrated exemplarily for DP33 and DP43 in Fig. 2 and summarized in Table 1, confirm that the compounds selected indeed possess amphiphilic properties, with Critical Micelle Concentrations (CMCs) in water in the low millimolar range (Fig. 2a). As expected, the CMC values of these compounds generally decrease with increasing hydrocarbon chain length, and compounds DP35 and DP45, respectively, show the lowest CMC values of the selenium and tellurium compounds studied. Under these conditions, the

selenium-containing compound DP35 has a CMC of 0.7 mM and the tellurium-containing compound DP45 of just 0.3 mM, which is comparable to the CMC of sodium dodecylsulfate (SDS) under these conditions (Table 1). The latter is used here as a benchmark anionic surfactant and has a CMC of 0.9 mM under the experimental conditions used. Interestingly, there is no major difference in CMC values between the selenium and tellurium analogues.

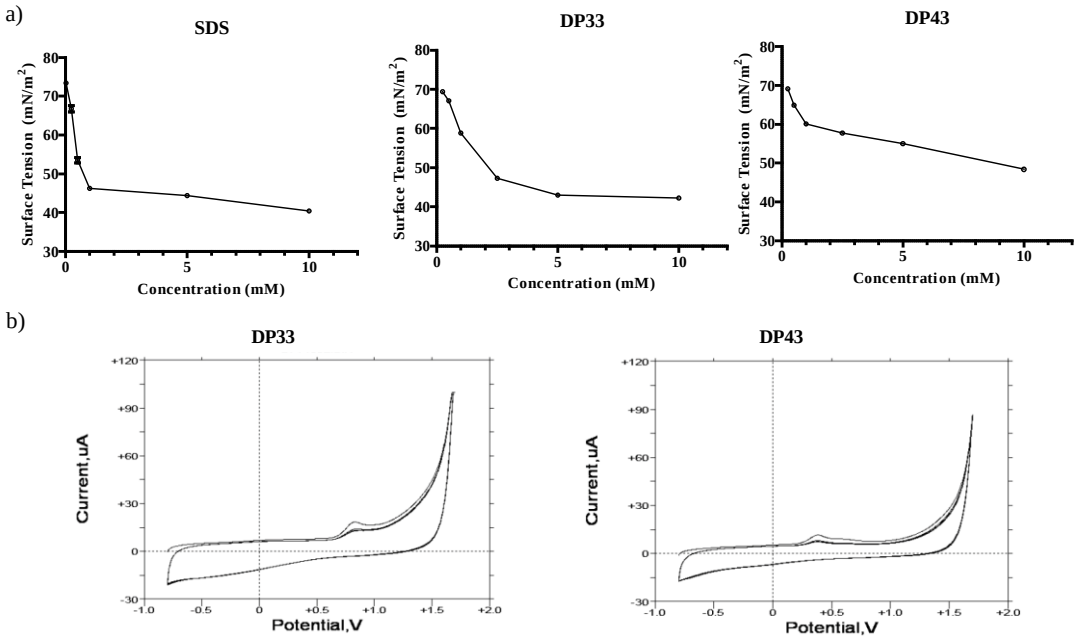

Fig 2. *Biologically relevant physico-chemical properties associated with the amphiphilic compounds investigated: (a) representative surface tension measurements of 'average tail length' (n = 10) selenium compound DP33 and tellurium compound DP43 in order to determine the CMC values of these compounds and to compare them to the benchmark surfactant SDS. (b) Cyclic voltammograms of the same compounds to demonstrate redox activity and to determine* E_{pa} *values.*

Compound	X	n	Yield (%)	CMC (mM)	Epa (mV)	Lysis of RBCs (%) at 100 µM	IC50 (µM) against HCT116	IC50 (µM) against RAW
SDS	**-**	**-**	**-**	**0.9**	**-**	**9.51 ± 1.31**	**> 100**	**> 100**
31	**Se**	**8**	**64**	**2.6**	**472.3**	**1.24 ± 0.18**	**> 100**	**> 100**
32	**Se**	**9**	**73**	**2.5**	**783.8**	**2.73 ± 0.63**	**> 100**	**> 100**
33	**Se**	**10**	**77**	**1.2**	**819.4**	**7.94 ± 1.81**	**> 100**	**> 100**
34	**Se**	**11**	**67**	**1.1**	**822.2**	**63.41 ± 4.02**	**> 100**	**> 100**
35	**Se**	**12**	**81**	**0.7**	**826.5**	**66.80 ± 2.55**	**> 100**	**> 100**
41	**Te**	**8**	**63**	**5**	**306.1**	**3.09 ± 0.07**	**5.99 ± 1.16**	**3.95 ± 1.16**
42	**Te**	**9**	**80**	**4.8**	**363.1**	**20.44 ± 0.90**	**4.99 ± 1.46**	**4.67 ± 1.01**
43	**Te**	**10**	**77**	**0.9**	**374.5**	**45.35 ± 1.35**	**7.47 ± 0.74**	**5.32 ± 1.20**
44	**Te**	**11**	**81**	**0.5**	**385.9**	**53.35 ± 3.35**	**9.73 ± 0.34**	**7.84 ± 1.22**
45	**Te**	**12**	**82**	**0.3**	**385.9**	**67.61 ± 2.04**	**19.84 ± 1.26**	**4.96 ± 1.41**

Table 1. *Overview of the most relevant physico-chemical parameters and biological activities associated with the compounds developed and evaluated as part of this study. See text and ESI for further details† (E_{pa} values vs. SSE)*

At the same time, these compounds are redox active and exhibit an electrochemical behaviour more or less typical of mono-selenides and tellurides (Fig. 2b). Here, the oxidation potentials E_{pa} are typically in the range of +472 to +827 mV vs. the standard silver/silver chloride electrode (SSE) for the selenides and +306 to +386 mV vs. SSE for the tellurides. In contrast to the CMC values, the E_{pa} values therefore do differ

significantly between the selenium and tellurium analogues, in line with previous reports pointing towards generally lower E_{pa} values for tellurium compounds compared to their selenium analogues. Interestingly, the E_{pa} values within the respective selenium and tellurium series do seem to increase with increasing hydrocarbon 'tail' length; yet these increases are in the range of a couple of tens of millivolts only and hence minor in comparison.

While it is unlikely that such amphiphilic agents form micelles under physiological conditions – the concentrations generally employed in cell culture are too low for micellation and the complexity of the biological 'buffer' also interferes with micelle formation – they should still be able to interact rather strongly with – hydrophobic parts of – biomolecules surrounding the cell or being present therein. Within this context, and in analogy to the action of SDS, interactions with cellular membranes and with proteins are of particular interest.[14] We have therefore briefly explored the potential interactions of some of our compounds with the membrane of red blood cells (RBCs) and/or whole RBCs with a representative protein, i.e. haemoglobin (Hb) (see also the ESI†).

RBCs were chosen to study compound–membrane interactions as they represent intact cells rather than just liposomes. RBCs therefore enable the study of direct effects of compounds on the cell membrane, yet do not possess the kind of signaling usually associated with dividing cells.[14] We know, for instance, that redox modulators can trigger secondary, indirect responses in dividing cells, hence complicating investigations (see also below).[9,15,16] Fig. 3 shows the pronounced effect of the selenium and tellurium containing agents on the integrity of the RBCs. This effect is concentration dependent (see Fig. S1 in the ESI†). Rather modest concentrations of compounds such as DP35, DP44 and DP45 cause significant lysis of the cell membrane, as determined by the haemoglobin release assay. Compound DP45 is the

most ‘active’ in this assay, with 67.6% lysis at 100 μM of the compound tested. This compound has also the lowest CMC value (around 300 μM), indicating that the activity on the RBC cell membrane is apparently dominated by the amphiphilic character of the compounds and is less dependent on the nature of the chalcogen involved. Indeed, there is a dramatic increase in lysis with increasing hydrocarbon chain length in the selenium as well as tellurium series, from a couple of percents in the case of short tails (DP31, DP41) to almost 70% in the case of the longest tails (DP35, DP45). There is only a slight increase in lysis when switching from selenium to tellurium (66.8% lysis in the case of DP35 and 67.6% in the case of DP45). Therefore the impact of compounds such as DP34, DP35, DP44 and DP45 on the cell membrane is driven primarily by the amphiphilic character of these agents, and is possibly slightly enhanced by the presence of tellurium. Although speculative at this time, one may envisage that the primary interaction of these compounds is indeed with the phospholipid bilayer directly, while a smaller, secondary, chalcogen-driven effect is perhaps due to yet to be specified interactions with – probably cysteine containing – membrane proteins. A similar behaviour apparently dominated by amphiphilicity rather than redox activity has also been found in the case of nematodes, whose cuticula or epidermis may be the target of such compounds (see below).

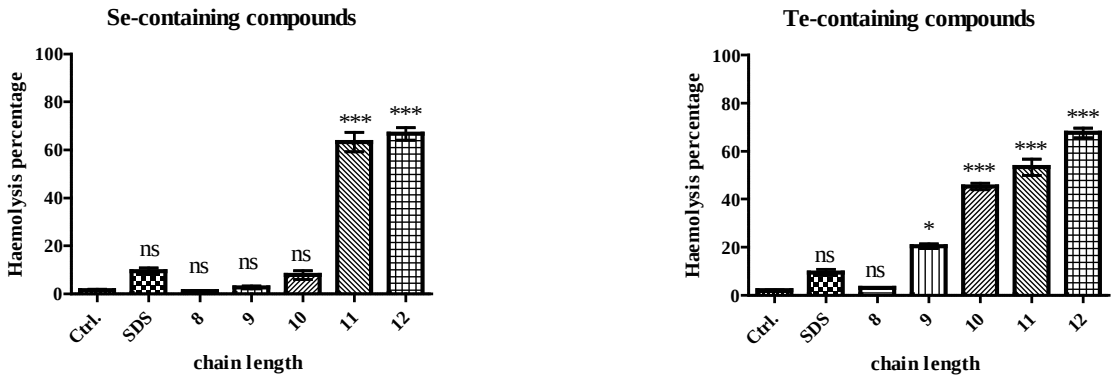

Fig 3. *Interactions of amphiphilic compounds with possible biochemical target molecules. Membrane interactions were recorded with subsequent lysis of RBCs*

(at a compound concentration of 100 μM). The chain lengths refer to n, the number of carbon atoms in the hydrophobic tail, as defined in Fig. 1. Lysis of RBCs increases with increasing tail length from n = 8 (DP31 and DP41) to n = 12 (DP35 and DP45). Data are presented as mean ± SD, and one-way ANOVA test (Dunnett) is used: p < 0.05 (*), p < 0.01 (**) or p < 0.001 (***).

In the next step, we have turned our attention to possible (non-covalent) interactions with proteins. Here, Hb has been used as the initial choice as this protein occurs commonly in RBCs, exhibits distinct signals in CD and, as a metalloprotein, also accounts for possible chalcogen–metal interactions (the iron–sulfur cluster containing protein Adx has been used as a further control). Indeed, the studies employing circular dichroism (CD) in order to determine possible interactions of the amphiphilic agents with Hb indicate rather pronounced effects of these compounds on the secondary structure of such proteins. At 50 μM concentrations, most of the compounds studied showed some impact on the Hb structure, which was comparable to that of SDS at the same concentration. The underlying interaction(s) were not particularly specific and seemed to be dominated by the amphiphilic character of the molecules (see Fig. S2 in the ESI†). SDS and DP31 had pronounced effects on the structure of Hb, while the impact of DP41 was less apparent. Interactions of such compounds with the protein structure could also be observed in the case of the reference protein Adx, where DP41 was slightly more potent than DP31 (see the ESI†).

Encouraged by these results, which clearly support the notion of possible multiple interactions of such compounds with various types of biomolecules, we have turned our attention towards potential biological targets. In the first part of the evaluation of biological activity, two different epithelial human cell lines have been chosen: human colon cancer cells (HCT116 cells, ATCC® CCL-247™) represent a well established cancer cell model, while human retinal pigment epithelia cells (ARPE-19, ATCC®

CRL-2302™) provide a suitable and often acceptable control as they exhibit many features of non-cancerous, primary cells, yet do not result in the various practical and ethical issues associated with using primary human colon cells obtained, for instance, from biopsies. ARPE-19 cells are particularly suited as control cells when the activity of redox modulating agents is investigated, as such epithelial cells are fairly resilient towards oxidative stress.[15] Hence screening compounds against HCT116 and ARPE-19 cells in tandem often allows a first but certainly preliminary glance at cytotoxicity against human cells and also a comparison of a cancer cell line with 'normal' cells.[2,15–17]

Fig. 4 shows the results obtained for a set of amphiphilic compounds against HCT116 and ARPE-19 cells (for IC_{50} values see Table 1). While the selenium-containing compounds and SDS were more or less inactive against HCT116 cells at the concentrations used, all of the tellurium containing compounds showed considerable cytotoxic activity against these cancer cells with IC_{50} values in the range of 5 to 20 μM. Interestingly, a small but consistent and statistically significant, ultimately around 3–4-fold, increase in IC_{50} values was observed when the hydrocarbon tail length was increased, from 6.0 μM in the case of DP41 to 19.8 μM in the case of DP45. In line with the notable absence of any observable cytotoxicity associated with the selenium compounds (DP31 to DP35) up to a concentration of 100 μM, this trend in IC_{50} values obviously counts against (purely) amphiphilic (inter-)actions of such compounds.

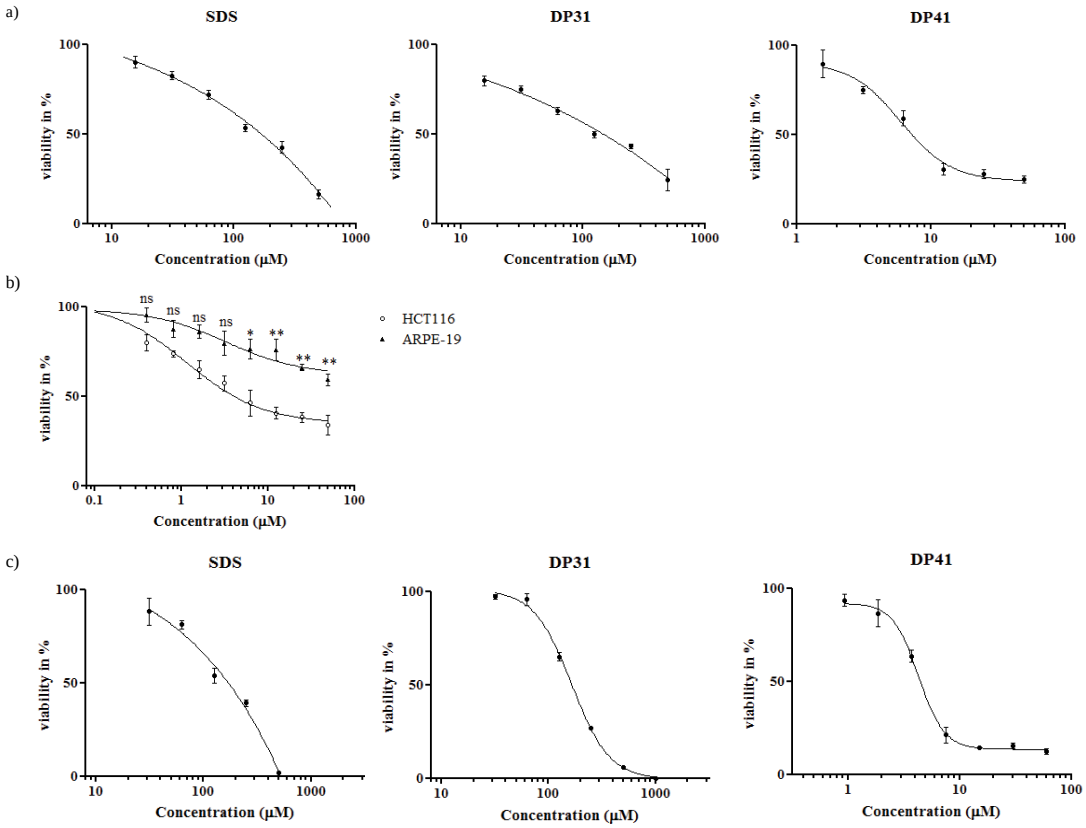

Fig 4. *Selective cytotoxicity of tellurium compound DP41. Panel (a): cytotoxicity of DP41 in HCT116 cells compared to the less cytotoxic selenium analogue DP31 and SDS. Panel (b): cytotoxicity of DP41 in HCT116 cells compared to ARPE-19 cells. Data are presented as mean ± SD, t-test is used, $p < 0.05$ (*), $p < 0.01$ (**) or $p < 0.001$ (***). Panel (c): cytotoxicity of DP41 in RAW 264.7 cells compared to the less cytotoxic selenium analogue DP31 and SDS.*

Here, one must bear in mind, of course, that the IC_{50} values (below or around 20 µM) are considerably lower than the concentrations employed for lysis of RBCs (100 µM), which in turn are lower than the CMCs (300 µM in the case of DP45). It is therefore likely that most of the most dramatic amphiphilic effects of such compounds only come to bear at concentrations which are 10-fold or even higher than the ones required to kill a human cell. In the case of the most cytotoxic compound DP42, the

IC_{50} value in HCT116 cells is around 1000 times lower than the CMC of this compound.

In fact, while longer chain lengths may promote interactions with cell membranes (as seen in the case of RBCs), they may also prevent compounds from ultimately crossing such membranes, i.e. from leaving the membrane again and entering the cytosol. In the case of one of the most active compounds, DP41, we have therefore used Energy-dispersive X-ray spectroscopy (EDX) to confirm the presence of tellurium inside (washed) HCT116 cells (see Fig. S3 in the ESI†). While it is not possible to confirm the exact location and chemical state of tellurium inside these cells using this method, EDX nonetheless confirms that the compound has crossed the cell membrane and indeed is ultimately present inside the cell.

Amazingly, the IC_{50} values of some of these tellurium agents were consistently lower in HCT116 cells when compared to the IC_{50} values of the same compounds in ARPE-19 cells (the latter were usually around 50 μM), pointing towards a high and, in this case, also selective activity in the HCT116 cell line. While it is premature to speculate why such tellurium compounds may be particularly active in HCT116 cells – and not to the same extent in ARPE-19 cells, and why the selenium analogues are not active in HCT116 cells, these findings are in excellent agreement with previous results obtained for organotellurium compounds in such cell lines.[10] They also confirm once more the significantly higher cytotoxicity associated with tellurium compounds when compared to their selenium analogues.[1,3,4,10,17] As for the possible underlying biochemical causes of such high activity and selectivity (for tellurium as well as for HCT116 cells), a specific interaction of tellurium compounds with cellular targets, such as individual components of the intracellular thiolstat, or burst of reactive oxygen species (ROS) is most likely.[1,2,4,5,10,15,16,18–22] Indeed, there are numerous reports that selenium as an antioxidant seems to be unable to induce a ROS

generating chemistry, which may also explain the rather low activity of the selenium compounds in our assays.[1,3,23,24]

We have therefore investigated this possible 'redox link' between a tellurium compound and apoptosis in HCT116 cells in more detail.[15] In the first instance, fluorescent staining of intracellular superoxide anion radicals ($O_2^{\cdot -}$) was performed using dihydroethidium (DHE) as a fairly specific probe for this particular radical.[15] As expected, initial results confirm a sharp increase in intracellular $O_2^{\cdot -}$ levels in response to compounds such as DP41. At a concentration of 50 μM and within 40 min of application, this tellurium compound causes a significant increase of $O_2^{\cdot -}$ levels (in our preliminary experiments, the $O_2^{\cdot -}$ concentration measured by this method almost doubles). Similar increases in intracellular ROS levels have already been observed for quinone-containing organotellurium agents, and ultimately may lead to cell death via apoptosis.[5,10,15] Indeed, our subsequent investigation of the effects of DP41 on the mitochondrial membrane potential $\Delta\Psi_M$ using JC-1 as a dual colour red/green fluorescent reporter dye revealed a significant, time- and concentration-dependent decrease of $\Delta\Psi_M$ in response to this tellurium compound (see Fig. 5 for a graphic evaluation of fluorescent data). Such a loss of mitochondrial membrane potential may form an important part of apoptotic processes resulting in cell death. It should be emphasized, however, that any – causal – relationship(s) between $O_2^{\cdot -}$ levels on the one side and $\Delta\Psi_M$, on the other, are not immediately obvious and require further investigation. Considering the timing of these events, i.e. less than 1 h for the increase in $O_2^{\cdot -}$ levels and evidently more than 2 h for the decrease in $\Delta\Psi_M$, it appears that the increase in ROS occurs prior to mitochondrial damage. This in turn points towards a redox event as the initial cause of activity and counts against a decisive amphiphilic interaction of compounds such as DP41 with the mitochondrial membrane. Indeed, the selenium-analogue of DP41, i.e. compound DP31, did not cause any significant increases in $O_2^{\cdot -}$ levels and also did not cause a major decrease in $\Delta\Psi_M$, hence

supporting the notion of a tellurium-specific activity which is linked to the generation of intracellular ROS. DP41 differs from previously used quinone-containing organotellurium compounds, and the build-up of $O_2^{\cdot -}$ occurs in the absence of a radical-generating quinone moiety. It may not be caused directly by the redox chemistry of DP41, but by a more indirect, secondary event, possibly mediated by cellular processes, such as ER stress.

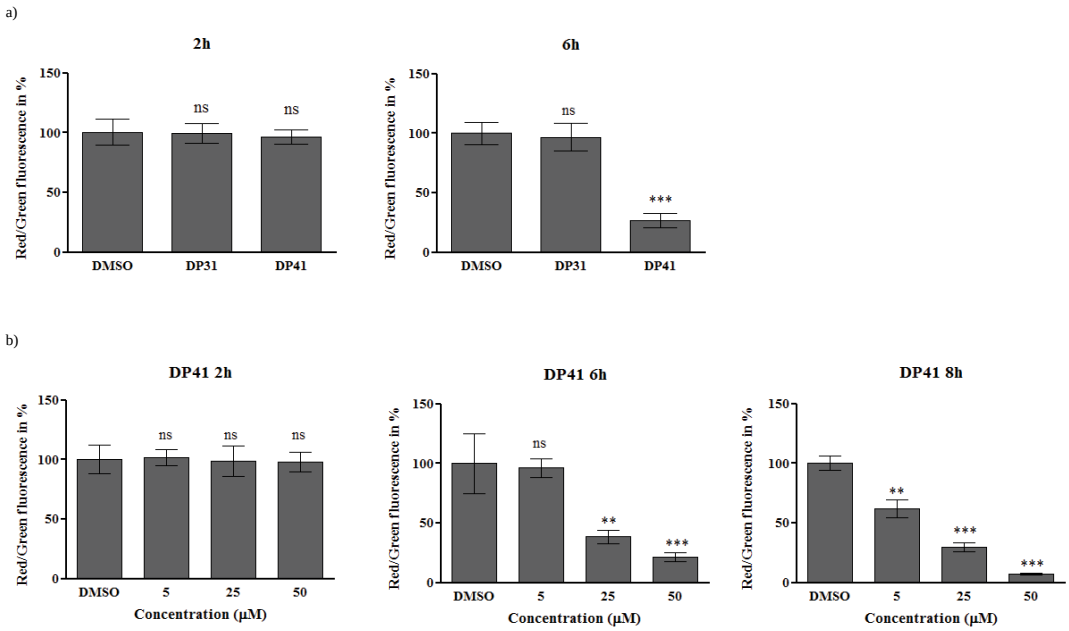

Fig 5. *Time- and dose-dependent impact of DP31 and DP41 on the mitochondrial membrane potential (DMSO as the negative control). The fluorescent intensities of the green and red channels from 150 cells were integrated and final ratios of red to green calculated. Panel (a): DP41 (at 50 µM), but not DP31, causes a significant decrease in $\Delta\Psi_M$ after 6 h of incubation. Panel (b): the impact of DP41 on $\Delta\Psi_M$ is time- and dose-dependent. It manifests itself after around 6 to 8 h and at concentrations from around 5 µM upwards. Data are presented as mean ± SD, one-way ANOVA test (Dunnett), $p < 0.05$ (*), $p < 0.01$ (**) or $p < 0.001$ (***).*

While the initial results obtained in human RBCs, HCT116 and ARPE-19 cells are rather instructive, they may be due to specific interactions which occur – perhaps solely – in those cell types. We have therefore also considered the impact of such selenium and tellurium compounds on cultured RAW 264.7 macrophages (ATCC® TIB-71™). Macrophages were selected as an additional cell system because these immune cells naturally produce high levels of ROS and hence should provide a suitable target for compound-induced redox modulation.[1] The results obtained in RAW 264.7 cells are summarized in Table 1 and shown for DP31 and DP41 in Fig. 4c. These results confirm the considerable cytotoxicity of DP41 (IC_{50} = 3.95 μM). Indeed, it seems that the macrophages are even slightly more sensitive to DP41 when compared to the HCT116 cells (IC_{50} = 5.99 μM), which may be due to the high ROS levels present naturally in and near such immune cells. A similar activity of tellurium-based redox modulators on macrophages has been observed previously.[1] While the precise cause of such activity is speculative at this time, it should be noted that the selenium analogue of DP41, i.e. DP31, as well as SDS, are both considerably less active against RAW 264.7 cells with IC_{50} values of over 100 μM. These findings support further the notion of a tellurium-based, redox modulating activity of compounds such as DP41, which is notably absent in the case of the corresponding selenium compounds or SDS. The specific activity of DP41, together with the low concentrations of this compound required, once more count against an amphiphilic interaction as the main cause of (cytotoxic) activity in proliferating human cell lines.

The results obtained in isolated or cultured human cells may only provide a partial picture of the various biological activities and biochemical mode(s) of action associated with these compounds. It is known, for instance, that many chalcogen-based compounds also exhibit a pronounced activity against various bacteria and some redox sensitive parasites. Therefore initial screens for antibiotic activity against Staphylococcus aureus and Escherichia coli were performed, which

point towards some activity of the tellurium compounds when used at higher micromolar concentrations, which exceed the activity of the selenium analogues and SDS. DP41, which was among the most cytotoxic compounds in the case of cultured human cells, was also the most active compound against E. coli with an IC_{50} of around 550 μM. Nonetheless, antibacterial activity was weak when compared to the cytotoxicity against human cells.

When DP31 and DP41 were tested in the context of the agricultural nematode Steinernema feltiae, a rather different picture emerged. S. feltiae is a parasitic nematode often used in initial toxicity screens, as this organism is easy to cultivate and also fairly reliable in producing representative and reproducible results.[25] The nematicidal activities associated with DP31, DP41 and SDS are shown in Fig. S4 in the ESI.† SDS is only weakly active against S. feltiae (LD_{50} > 400 μM), counting against a particular sensitivity of this organism towards surfactants. Perhaps surprisingly, therefore, DP41 and especially DP31 are quite active against this organism. Interestingly, the selenium compound DP31 (LD_{50} = 30 μM) is even more active when compared to its tellurium analogue, DP41 (LD_{50} = 78 μM). The exact causes for this pronounced activity of DP31 – compared to DP41 – are still unclear. One may speculate that the selenium compound is taken up and metabolized to toxic metabolites more readily, as most organisms possess pathways for the metabolism of selenium compounds, but not for tellurium compounds. Indeed, the results obtained for our compounds in the four human cell models, the bacteria and nematodes confirm that such agents are not merely globally toxic but possess some selectivity which may result from their ability to enter cells and to act on particular cellular targets, be it on specific proteins or on a local or global redox state.

Ultimately, our studies have shown that it is possible to synthesize a range of selenium- and tellurium-containing surfactants with comparable ease. As expected,

these molecules combine redox activity with amphiphilic properties and hence exhibit several advantages when compared to traditional redox modulators or surfactants. The compounds reported here are easy to handle, fairly soluble in aqueous solutions and endowed with considerable biological activity against a range of important therapeutic targets, such as certain cancer cells, macrophages, bacteria and a representative nematode. In fact, the activity determined so far compares well with that of so-called 'multifunctional' redox modulators which combine a selenium or tellurium redox moiety with a quinone.[1,26] While the latter require the presence of a radical generating quinone for adequate activity in the high nanomolar to low micromolar range, the compounds discussed here exhibit a similar, slightly lower activity yet do not require the presence of a cytotoxic quinone moiety. At the same time, the tellurium compounds, which are often more active than their selenium counterparts, show activity not only against HCT116 cancer cells, but also against RAW 264.7 macrophages, *S. feltiae* and *E. coli.*

This raises the question, why such compounds are active, and possibly even show some selectivity. Our initial experiments conducted to explore the underlying biochemical mode(s) of action point towards a combination of two activities. On the one hand, there is clearly an amphiphilic, probably non-covalent and disruptive interaction of these agents with membranes and proteins; on the other hand, the presence of tellurium (and less so selenium) seems to directly or indirectly enable these compounds to affect the cellular redox balance (as seen for $O_2^{\cdot -}$ levels) and maybe also cause a covalent modification of key proteins of the cellular thiolstat. While the amphiphilic events seem to occur only at higher concentrations (50 to 100 μM and above) and do not discriminate significantly between the presence of selenium and tellurium, the redox interactions seem to be more or less specific for tellurium and occur at lower concentrations (10 to 50 μM in cultured human cells).

Extensive future studies are obviously required to investigate further the exact underlying biochemical mode(s) of action and to identify possible intracellular targets (such as specific organelles, membranes or proteins). At this point, the intracellular pathways triggered or influenced by such compounds also need to be mapped out in more detail. Ultimately, it will also be necessary to produce a wider range of such compounds, including some sulfur-containing analogues, and to screen for further activities and selectivity, also in order to derive reliable structure–activity relationships. Our initial results point towards a particularly promising spectrum of activities associated with the tellurium compounds, especially compound DP41, which may be considered as a lead compound emerging from these studies. As the structure of this compound provides considerable scope for modifications, and the synthesis of derivatives is now straightforward, a wider spectrum of additional compounds based on this initial lead appears possible. Here, it will be interesting to see if the presence of a quinone helper group will further enhance activity and/or selectivity, as has already been observed for a previous generation of such redox modulating compounds.[1,2,4,5,9,26]

In the future, such compounds will be evaluated extensively for possible anticancer and antimicrobial activity. Cells and organisms which naturally produce high amounts of ROS (such as certain cancer or immune cells), or exhibit a weak antioxidant defence (such as certain parasites, including nematodes and Plasmodium falciparum), will obviously form the prime targets of such redox modulating agents.[6] In any case, our findings bode well for the further development of such amphiphilic redox modulators as lead structures for the treatment of a range of human diseases and for possible agricultural applications.

2.1.4. Acknowledgements

The authors acknowledge financial support from Saarland University, the Landesforschungsfoerderungsprogramm Saarland (T/1-14.2.1.1.-LFFP 12/23) and the BMBF (grant number 01DK12002). The authors would like to thank Dr Josef Zapp from Saarland University and Ms Veronique Poddig from the University Lorraine for NMR measurements.

2.1.5. Notes and references

1. M. Doering, B. Diesel, M. C. H. Gruhlke, U. M. Viswanathan, D. Manikova, M. Chovanec, T. Burkholz, A. J. Slusarenko, A. K. Kiemer and C. Jacob, *Tetrahedron*, 2012, **68**, 10577-10585.

2. N. Lilienthal, C. Prinz, A. A. Peer-Zada, M. Doering, L. A. Ba, M. Hallek, C. Jacob and M. Herling, *Leukemia & Lymphoma*, 2011, **52**, 1407-1411.

3. V. Jamier, L. A. Ba and C. Jacob, *Chem-Eur J*, 2010, **16**, 10920-10928.

4. W. K. Marut, N. Kavian, A. Servettaz, C. Nicco, L. A. Ba, M. Doering, C. Chereau, C. Jacob, B. Weill and F. Batteux, *J Invest Dermatol*, 2012, **132**, 1125-1132.

5. M. Doering, L. A. Ba, N. Lilienthal, C. Nicco, C. Scherer, M. Abbas, A. A. P. Zada, R. Coriat, T. Burkholz, L. Wessjohann, M. Diederich, F. Batteux, M. Herling and C. Jacob, *Journal of Medicinal Chemistry*, 2010, **53**, 6954-6963.

6. S. Mecklenburg, S. Shaaban, L. A. Ba, T. Burkholz, T. Schneider, B. Diesel, A. K. Kiemer, A. Roseler, K. Becker, J. Reichrath, A. Stark, W. Tilgen, M. Abbas, L.

A. Wessjohann, F. Sasse and C. Jacob, *Organic & Biomolecular Chemistry*, 2009, **7**, 4753-4762.

7. C. Jacob, *Biochemical Society Transactions*, 2011, **39**, 1247-1253.

8. T. Schneider, A. Baldauf, L. A. Ba, V. Jamier, K. Khairan, M. B. Sarakbi, N. Reum, M. Schneider, A. Roseler, K. Becker, T. Burkholz, P. G. Winyard, M. Kelkel, M. Diederich and C. Jacob, *Journal of Biomedical Nanotechnology*, 2011, **7**, 395-405.

9. S. Shaaban, R. Diestel, B. Hinkelmann, Y. Muthukumar, R. P. Verma, F. Sasse and C. Jacob, *Eur J Med Chem*, 2012, **58**, 192-205.

10. T. Schneider, Y. Muthukumar, B. Hinkelmann, R. Franke, M. Doring, C. Jacob and F. Sasse, *Medchemcomm*, 2012, **3**, 784-787.

11. N. Lilienthal, A. A. Peer-Zada, L. A. Ba, H. Liu, C. Jacob, M. Hallek and M. Herling, *Onkologie*, 2010, **33**, 240-240.

12. L. B. Xing, S. Yu, X. J. Wang, G. X. Wang, B. Chen, L. P. Zhang, C. H. Tung and L. Z. Wu, *Chem Commun (Camb)*, 2012, **48**, 10886-10888.

13. P. Han, N. Ma, H. Ren, H. Xu, Z. Li, Z. Wang and X. Zhang, *Langmuir : the ACS journal of surfaces and colloids*, 2010, **26**, 14414-14418.

14. T. Schneider, L. A. Ba, K. Khairan, C. Zwergel, N. D. Bach, I. Bernhardt, W. Brandt, L. Wessjohann, M. Diederich and C. Jacob, *Med Chem Comm*, 2011, **2**, 196-200.

15. N. E. B. Saidu, R. Touma, I. Abu Asali, C. Jacob and M. Montenarh, *Bba-Gen Subjects*, 2013, **1830**, 2214-2225.

16. C. Busch, C. Jacob, A. Anwar, T. Burkholz, L. A. Ba, C. Cerella, M. Diederich, W. Brandt, L. Wessjohann and M. Montenarh, *International Journal of Oncology*, 2010, **36**, 743-749.

17. L. A. Ba, M. Doring, V. Jamier and C. Jacob, *Org Biomol Chem*, 2011, **8**, 4203-4216.

18. K. K. Bhasin, E. Arora, A. S. Grover, Jyoti, H. Singh, S. K. Mehta, A. K. K. Bhasin and C. Jacob, *J Organomet Chem*, 2013, **732**, 137-141.

19. C. Jacob, E. Battaglia, T. Burkholz, D. Peng, D. Bagrel and M. Montenarh, *Chemical Research in Toxicology*, 2012, **25**, 588-604.

20. C. Scherer, C. Jacob, M. Dicato and M. Diederich, *Phytochemistry Reviews*, 2009, **8**, 349-368.

21. F. H. Fry and C. Jacob, *Current Pharmaceutical Design*, 2006, **12**, 4479-4499.

22. N. M. Giles, N. J. Gutowski, G. I. Giles and C. Jacob, *Febs Letters*, 2003, **535**, 179-182.

23. C. A. Collins, F. H. Fry, A. L. Holme, A. Yiakouvaki, A. Al-Qenaei, C. Pourzand and C. Jacob, *Organic & Biomolecular Chemistry*, 2005, **3**, 1541-1546.

24. G. I. Giles, F. H. Fry, K. M. Tasker, A. L. Holme, C. Peers, K. N. Green, L. O. Klotz, H. Sies and C. Jacob, *Organic & Biomolecular Chemistry*, 2003, **1**, 4317-4322.

25. B. Czepukojc, U. M. Viswanathan, A. Raza, S. Ali, T. Burkholz and C. Jacob, *Phosphorus Sulfur and Silicon and the Related Elements*, 2013, **188**, 446-453.

26. F. H. Fry, A. L. Holme, N. M. Giles, G. I. Giles, C. Collins, K. Holt, S. Pariagh, T. Gelbrich, M. B. Hursthouse, N. J. Gutowski and C. Jacob, *Organic & Biomolecular Chemistry*, 2005, **3**, 2579-2587.

2.1.6. Supplementary Information

Synthesis of amphiphilic, chalcogen-based redox modulators with in vitro cytotoxic activity against cancer cells, macrophages and microbes

2.1.6.1. *Experimental Section*

All chemicals and solvents used were purchased from Acros Organic, Alfa Aesar or Sigma Aldrich as reagent grade and used without further purification. Melting points were determined with a Thermo Scientific Electrothermal Digital Melting Point Apparatus and are provided as uncorrected values. ^{1}H and ^{13}C NMR spectra were recorded with a Bruker AC or a Bruker Avance 500 spectrometer at 250 or 500 MHz in $CDCl_3$ or DMSO-d_6 as specified. ^{77}Se spectra were measured with a Bruker Avance 500 at 92.5 MHz in $CDCl_3$ or DMSO-d_6. All chemical shifts are reported in parts per million (ppm). Tetramethylsilane (TMS) and dimethylselenide were used as standard reference for ^{1}H and ^{13}C (δ 0 ppm) and for ^{77}Se, respectively. MS spectra were recorded on an Agilent Technologies GC-MS instrument equipped with a 7683 injector, 6890N gas chromatograph and a 5973 mass selective detector. The mass spectrometer was operated in EI mode at 70 eV, and MS spectra were recorded from m/z 50 to 650. All reactions were routinely checked by TLC analysis on an Alugram SIL G/UV254 plate (Macherey-Nagel) with spots visualized by UV light.

2.1.6.1.1. **General Procedure for Synthesis of 1-Hydroalkylphenyl Selenide (Telluride)**

1-Hydroalkylphenyl selenide was synthesized according to Han *et al*, with some modifications.[1] Briefly, diphenyl diselenide or diphenyl ditelluride (1 eq.) was dissolved in 20 ml of anhydrous THF under argon, and then 20 ml of an aqueous solution of 5.0 eq. sodium borohydride was added. The reaction mixture was stirred for 10 min until the solution turned colourless, indicating the formation of PhSeNa or PhTeNa, respectively. The PhSeNa or PhTeNa solution was stirred for a further 20 min. A solution of a bromoalkylalcohol (2 eq.) in 5ml THF was then added to the reaction mixture and the reaction was kept at 50 ℃ for 12 h under argon flow (for the telluride compound at 40 ℃). Then 50 ml of saturated aqueous NH_4Cl solution was added to the reaction mixture and the product was extracted with CH_2Cl_2 (3×50ml). The organic layers were combined and dried with $MgSO_4$, filtered, and the solvent was evaporated under vacuum. The oily solid obtained was purified by column chromatography with CH_2Cl_2 as the eluent. (R_f values of all compounds were between 0.2 to 0.3)

8-(phenylselanyl)octan-1-ol (DP11). Yield: 92%; white powder; mp 41 ℃; ^{1}H NMR (500 MHz, $CDCl_3$) δ 7.45-7.47 (m, 2H, benzene protons), 7.20-7.25 (m, 3H, benzene protons), 3.60-3.62 (t, 2H, *J* = 7Hz, -C*H*$_2$OH), 2.87-2.90 (t, 2H, *J* = 7.5Hz, -SeC*H*$_2$-), 1.65-1.71 (m, 2H, -C*H*$_2$CH$_2$OH), 1.50-1.55 (m, 2H, -SeCH$_2$C*H*$_2$-), 1.25-1.40 (m, 8H, -(C*H*$_2$)$_4$CH$_2$CH$_2$OH) ppm; ^{13}C NMR (125 MHz, $CDCl_3$) δ 132.37 (2C), 130.64, 128.96 (2C), 126.58, 63.01, 32.73, 30.09, 29.71, 29.23, 29.00, 27.90, 25.63 ppm; ^{77}Se NMR (92.5 MHz, CDCl3) δ 291.02 ppm; HRMS (ESI) $[M+H]^+$ $C_{14}H_{23}OSe$ calcd 287.0909, found 287.0916.

9-(phenylselanyl)nonan-1-ol (DP12). Yield: 87%; white powder; mp 46 ℃; ^{1}H NMR (500 MHz, $CDCl_3$) δ 7.45-7.47 (m, 2H, benzene protons), 7.20-7.25 (m, 3H, benzene protons), 3.60-3.63 (t, 2H, *J* = 6.5Hz, -C*H*$_2$OH), 2.87-2.90 (t, 2H, *J* = 7.5Hz, -SeC*H*$_2$-), 1.65-1.71 (m, 2H, -CH$_2$C*H*$_2$OH), 1.50-1.56 (m, 2H, -SeCH$_2$C*H*$_2$-), 1.25-1.39 (m, 10H,

-(C*H*$_2$)$_5$CH$_2$CH$_2$OH) ppm; ^{13}C NMR (125 MHz, CDCl$_3$) δ 132.37 (2C), 130.68, 128.96 (2C), 126.58, 63.05, 32.77, 30.12, 29.78, 29.42, 29.32, 28.99, 27.93, 25.69 ppm; ^{77}Se NMR (92.5 MHz, CDCl$_3$) δ 290.94 ppm; HRMS (ESI) $[M+Na]^+$ $C_{15}H_{24}NaOSe$ calcd 323.0885, found 323.0917.

10-(phenylselanyl)decan-1-ol (DP13). Yield: 96%; white powder; mp 52 ℃; ^{1}H NMR (500 MHz, CDCl$_3$) δ 7.45-7.47 (m, 2H, benzene protons), 7.20-7.25 (m, 3H, benzene protons), 3.60-3.63 (t, 2H, *J* = 6.5Hz, -C*H*$_2$OH), 2.87-2.90 (t, 2H, *J* = 7.5Hz, -SeC*H*$_2$-), 1.65-1.71 (m, 2H, -CH$_2$C*H*$_2$OH), 1.51-1.55 (m, 2H, -SeCH$_2$C*H*$_2$-), 1.25-1.39 (m, 12H, -(C*H*$_2$)$_6$CH$_2$CH$_2$OH) ppm; ^{13}C NMR (125 MHz, CDCl$_3$) δ 132.35 (2C), 130.69, 128.95 (2C), 126.56, 63.06, 32.78, 30.12, 29.79, 29.48, 29.38, 29.36, 29.03, 27.93, 25.70 ppm; ^{77}Se NMR (92.5 MHz, CDCl$_3$) δ 290.96 ppm; HRMS (ESI) $[M+H]^+$ $C_{16}H_{27}OSe$ calcd 315.1222, found 315.1223.

11-(phenylselanyl)undecan-1-ol (DP14). Yield: 92%; white powder; mp 58 ℃; ^{1}H NMR (500 MHz, CDCl$_3$) δ 7.45-7.47 (m, 2H, benzene protons), 7.20-7.25 (m, 3H, benzene protons), 3.60-3.63 (t, 2H, *J* = 6.5Hz, -C*H*$_2$OH), 2.87-2.90 (t, 2H, *J* = 7.5Hz, -SeC*H*$_2$-), 1.65-1.71 (m, 2H, -CH$_2$C*H*$_2$OH), 1.51-1.57 (m, 2H, -SeCH$_2$C*H*$_2$-), 1.24-1.39 (m, 14H, -(C*H*$_2$)$_7$CH$_2$CH$_2$OH) ppm; ^{13}C NMR (125 MHz, CDCl$_3$) δ 132.34 (2C), 130.70, 128.95 (2C), 126.56, 63.06, 32.79, 30.12, 29.80, 29.54, 29.46, 29.44, 29.39, 29.05, 27.94, 25.71 ppm; ^{77}Se NMR (92.5 MHz, CDCl$_3$) δ 290.94 ppm; HRMS (ESI) $[M+H]^+$ $C_{17}H_{29}OSe$ calcd 329.1379, found 329.1384.

12-(phenylselanyl)dodecan-1-ol (DP15). Yield: 85%; white powder; mp 63 ℃, ^{1}H NMR (500 MHz, CDCl$_3$) δ 7.45-7.47 (m, 2H, benzene protons), 7.20-7.24 (m, 3H, benzene protons), 3.60-3.63 (t, 2H, *J* = 6.5Hz, -C*H*$_2$OH), 2.87-2.90 (t, 2H, *J* = 6.5Hz, -SeC*H*$_2$-), 1.65-1.69 (m, 2H, -CH$_2$C*H*$_2$OH), 1.53-1.56 (m, 2H, -SeCH$_2$C*H*$_2$-), 1.23-1.39 (m, 16H, -(C*H*$_2$)$_8$CH$_2$CH$_2$OH) ppm; ^{13}C NMR (125 MHz, CDCl$_3$) δ

132.34 (2C), 130.70, 128.95 (2C), 126.56, 63.08, 32.80, 30.13, 29.81, 29.56, 29.52 (2C), 29.46, 29.41, 29.05, 27.94, 25.72; ^{77}Se NMR (92.5 MHz, $CDCl_3$) δ 290.94 ppm; HRMS (ESI) $[M+H]^+$ $C_{18}H_{31}OSe$ calcd 343.1535, found 343.1539.

8-(phenyltellanyl)octan-1-ol (DP21). Yield: 97%; orange oil; ^{1}H NMR (500 MHz,$CDCl_3$) δ 7.75-7.77 (m, 2H, benzene protons), 7.23-7.33 (m, 3H, benzene protons), 3.64-3.67 (t, 2H, *J* = 6.5Hz, -C*H*$_2$OH), 2.93-2.96 (t, 2H, *J* = 7.5Hz, -TeC*H*$_2$-), 1.81-1.87 (m, 2H, -C*H*$_2$CH$_2$OH), 1.62-1.56 (2H, m, -TeCH$_2$C*H*$_2$-), 1.32-1.44 (m, 8H, - (C*H*$_2$)$_4$CH$_2$CH$_2$OH) ppm; ^{13}C NMR (125 MHz, $CDCl_3$) δ 138.11 (2C), 128.99 (2C), 127.31, 111.73, 62.78, 32.60, 31.74, 31.63, 29.15, 28.74, 25.56, 8.67 ppm; HRMS (ESI) $[M+H]^+$ $C_{14}H_{23}OTe$ calcd 337.0806, found 337.0812.

9-(phenyltellanyl)nonan-1-ol (DP22). Yield: 95%; orange oil; ^{1}H NMR (500 MHz, $CDCl_3$) δ 7.75-7.77 (m, 2H, benzene protons), 7.23-7.33 (m, 3H, benzene protons), 3.66-3.68 (t, 2H, *J* = 6.5Hz, -C*H*$_2$OH), 2.93-2.96 (t, 2H, *J* = 7.5Hz, -TeC*H*$_2$-), 1.83-1.87 (m, 2H, -C*H*$_2$CH$_2$OH), 1.57-1.63 (m, 2H, -TeCH$_2$C*H*$_2$-), 1.31-1.43 (m, 10H, -(C*H*$_2$)$_5$CH$_2$CH$_2$OH) ppm; ^{13}C NMR (125 MHz, $CDCl_3$) δ 138.17 (2C), 129.04 (2C), 127.36, 111.78, 62.80, 32.70, 31.84, 31.69, 29.36, 29.27, 28.76, 25.65, 8.74 ppm. HRMS (ESI) $[M+H]^+$ $C_{15}H_{25}OTe$ calcd 351.0962, found 351.0958.

10-(phenyltellanyl)decan-1-ol (DP23). Yield: 96%; orange oil; ^{1}H NMR (250 MHz, $CDCl_3$) δ 7.69-7.73 (m, 2H, benzene protons), 7.16-7.30 (m, 3H, benzene protons), 3.62-3.66 (t, 2H, *J* = 5Hz, -C*H*$_2$OH), 2.87-2.93 (t, 2H, *J* = 7.5Hz, -TeC*H*$_2$-), 1.74-1.85 (m, 2H, -C*H*$_2$CH$_2$OH), 1.51-1.59 (m, 2H, -TeCH$_2$C*H*$_2$-), 1.26-1.43 (m, 12H, -(C*H*$_2$)$_6$CH$_2$CH$_2$OH) ppm; ^{13}C NMR (62.5 MHz, $CDCl_3$) δ 138.37 (2C), 128.73 (2C), 126.85, 111.82, 63.05, 32.78, 31.90, 31.75, 29.49, 29.38, 28.86, 29.37, 25.70, 8.78 ppm; HRMS (ESI) $[M+H]^+$ $C_{16}H_{27}OTe$ calcd 365.1119, found 365.1120.

11-(phenyltellanyl)undecan-1-ol (DP24). Yield: 98%; white powder; mp 39 ℃;^{1}H NMR (500 MHz, DMSO-d_6) δ 7.63-7.65 (m, 2H, benzene protons), 7.20-7.28 (m, 3H, benzene protons), 3.35-3.38 (m, 2H, -C*H*$_2$OH), 2.88-2.91 (t, 2H, *J* = 7Hz, -TeC*H*$_2$-), 1.69-1.75 (m, 2H, -C*H*$_2$CH$_2$OH), 1.36-1.41 (m, 2H, -TeCH$_2$C*H*$_2$-), 1.21-1.34 (m, 14H, -(C*H*$_2$)$_7$CH$_2$CH$_2$OH) ppm; ^{13}C NMR (125 MHz, DMSO-d_6) δ 137.06 (2C), 129.24 (2C), 127.18, 112.06, 60.71, 32.52, 31.15 (2C), 29.02, 28.91, 28.88, 28.84, 28.21, 25.47, 8.21 ppm; HRMS $[M+H]^+$ $C_{17}H_{29}OTe$ calcd 379.1275, found 379.1266.

12-(phenyltellanyl)dodecan-1-ol (DP25). Yield: 90%; yellow powder; mp 43 ℃; ^{1}H NMR (250 MHz, $CDCl_3$) δ 7.69-7.72 (m, 2H, benzene protons), 7.16-7.30 (m, 3H, benzene protons), 3.62-3.67 (t, 2H, *J* = 7.5Hz, -C*H*$_2$OH), 2.87-2.93 (t, 2H, *J* = 7.5Hz, -TeC*H*$_2$-), 1.74-1.85 (2H, m, -C*H*$_2$CH$_2$OH), 1.51-1.57 (m, 2H, -TeCH$_2$C*H*$_2$-), 1.25-1.43 (m, 16H, -(C*H*$_2$)$_8$CH$_2$CH$_2$OH) ppm; ^{13}C NMR (62.5 MHz, $CDCl_3$) δ 138.21 (2C), 129.07 (2C), 127.39, 111.82, 63.09, 32.80, 31.92, 29.56, 29.45, 29.40, 29.29, 29.13, 29.04, 28.88, 25,72, 8.79 ppm; HRMS (ESI) $[M+H]^+$ $C_{18}H_{31}OTe$ calcd 393.1432, found 393.1428.

2.1.6.1.2. **General Procedure for Synthesis of sodium phenylselanyl-alkyl sulfate.**

1-Hydroalkylphenyl selenide or telluride (1eq.) was dissolved in 25ml anhydrous diethyl ether, then 1.5 eq. chlorosulfonic acid was added dropwise cautiously under nitrogen gas at 0 ℃ for 10 min. The reaction mixture was stirred for a further 30 min. 1.0 eq of $NaHCO_3$ powder was added to the reaction mixture, then water was added dropwise until no further gas developed. The organic mixture was dried with $MgSO_4$. The remaining solid was separated, washed with anhydrous diethyl ether several times and the compound contained therein was resolubilized using 250 ml ethanol. The residual $MgSO_4$ and $NaHCO_3$ were removed by filtration. The solvent was evaporated and the product collected.

Sodium 8-(phenylselanyl)octyl sulfate (DP31). Yield: 69%; white powder; mp 112 ℃; ^{1}H NMR (500 MHz, DMSO-d_6) δ 7.44-7.46 (m, 2H, benzene protons), 7.21-7.30 (m, 3H, benzene protons), 3.34-3.38 (m, 2H, -C*H*$_2$OSO$_3$Na), 2.92-2.95 (t, 2H, *J* = 7.5Hz, -SeC*H*$_2$-), 1.59-1.62 (m, 2H, -C*H*$_2$CH$_2$OSO$_3$Na, 1.33-1.42 (m, 2H, -SeCH$_2$C*H*$_2$-), 1.20-1.26 (m, 8H, -(C*H*$_2$)$_5$CH$_2$CH$_2$OSO$_3$Na) ppm; ^{13}C NMR (125 MHz, DMSO-d_6) δ 131.29 (2C), 130.28, 129.15 (2C), 126.37, 60.69, 29.50, 28.97, 28.90, 28.84, 28.40, 26.65, 25.47; ^{77}Se NMR (92.5 MHz, DMSO-d_6) δ 283.17 ppm; HRMS (ESI) [M-Na]$^-$ $C_{14}H_{21}O_4SSe$ calcd 365.0331, found 365.0337.

Sodium 9-(phenylselanyl)nonyl sulfate (DP32). Yield, 84%; white powder; mp 122 ℃; ^{1}H NMR (500 MHz, DMSO-d_6) δ:7.43-7.46 (m, 2H, benzene protons), 7.21-7.30 (m, 3H, benzene protons), 3.64-3.67 (t, 2H, *J* = 6.5Hz, -C*H*$_2$OSO$_3$Na), 2.92-2.95 (t, 2H, *J* = 7.5Hz, -SeC*H*$_2$-), 1.59-1.65 (m, 2H, -C*H*$_2$CH$_2$OSO$_3$Na), 1.42-1.51 (2H, m, -SeCH$_2$C*H*$_2$-), 1.18-1.36 (m, 10H, -(C*H*$_2$)$_5$CH$_2$CH$_2$OSO$_3$Na) ppm; ^{13}C NMR (125 MHz, DMSO-d_6) δ 131.31 (2C), 130.26, 129.17 (2C), 126.38, 65.41, 29.51, 29.04, 29.01, 28.84, 28.64, 28.35, 26.64, 25.46 ppm;^{77}Se NMR (92.5 MHz, DMSO-d_6) δ 283.17 ppm; HRMS (ESI) [M-Na]$^-$ $C_{15}H_{23}O_4SSe$ calcd 365.0337, found 365.0331.

Sodium 10-(phenylselanyl)decyl sulfate (DP33). Yield, 81%; white powder; mp 125 ℃; ^{1}H NMR (500 MHz, DMSO-d_6) δ 7.43-7.45 (m, 2H, benzene protons), 7.22-7.29 (m, 3H, benzene protons), 3.65-3.68 (t, 2H, *J* = 6.5Hz, -C*H*$_2$OSO$_3$Na), 2.91-2.94 (t, 2H, *J* = 7.5Hz, -SeC*H*$_2$-), 1.58-1.64 (m, 2H, -C*H*$_2$CH$_2$OSO$_3$Na), 1.43-1.48 (m, 2H, -SeCH$_2$C*H*$_2$-), 1.22-1.36 (m, 12H, -(C*H*$_2$)$_6$CH$_2$CH$_2$OSO$_3$Na) ppm; ^{13}C NMR (125 MHz, DMSO-d_6) δ: 131.30 (2C), 130.25, 129.17 (2C), 126.38, 65.45, 29.49, 29.03, 28.88, 28.82, 28.71, 28.37, 26.64, 25.48; ^{77}Se NMR (92.5 MHz, DMSO-d_6) δ 283.15 ppm; HRMS (ESI) [M-Na]$^-$ $C_{16}H_{25}O_4SSe$ calcd 393.0644, found 393.0671.

Sodium 11-(phenylselanyl)undecyl sulfate (DP34). Yield, 73%; white powder; mp 130 ℃; ^{1}H NMR (500 MHz, DMSO-d_6) δ 7.44-7.46 (m, 2H, benzene protons), 7.21-7.30 (m, 3H, benzene protons), 3.65-3.67 (t, 2H, *J* = 7Hz, -C*H*$_2$OSO$_3$Na), 2.92-2.95 (t, 2H, *J* = 7.5Hz, -SeC*H*$_2$-), 1.65-1.57 (m, 2H, -C*H*$_2$CH$_2$OSO$_3$Na), 1.44-1.49 (m, 2H, -SeCH$_2$C*H*$_2$-), 1.19-1.37 (m, 14H, -(C*H*$_2$)$_7$CH$_2$CH$_2$OSO$_3$Na) ppm; ^{13}C NMR (125 MHz, DMSO-d_6) δ , 132.61, 131.30, 130.67, 129.94, 129.61, 128.67, 65.33, 32.49, 28.97, 28.79, 28.74, 28.60, 28.56, 28.49, 28.20, 28.08, 25.40 ppm; ^{77}Se NMR (92.5 MHz, DMSO-d_6) δ 283.24 ppm; HRMS (ESI) [M-Na]$^-$ $C_{17}H_{27}O_4SSe$ calcd 407.0801, found 407.0815.

Sodium 12-(phenylselanyl)dodecyl sulfate (DP35). Yield: 96%; colourless solid; mp 137 ℃; ^{1}H NMR (500 MHz, DMSO-d_6) δ 7.43-7.46 (m, 2H, benzene protons), 7.21-7.31 (m, 3H, benzene protons), 3.65-3.68 (t, 2H, *J* = 6.5Hz, -C*H*$_2$OSO$_3$Na), 2.92-2.95 (t, 2H, *J* = 7.5Hz, -SeC*H*$_2$-), 1.58-1.64 (m, 2H, -C*H*$_2$CH$_2$OSO$_3$Na), 1.44-1.50 (m, 2H, -SeCH$_2$C*H*$_2$-), 1.22-1.36 (m, 14H, -(C*H*$_2$)$_7$CH$_2$CH$_2$OSO$_3$Na) ppm; ^{13}C NMR (125 MHz, DMSO-d_6) δ 131.29 (2C), 130.27, 129.16 (2C), 126.37, 65.42, 29.49, 29.05, 29.00, 28.99, 28.95, 28.90, 28.86, 28.75, 28.38, 26.64, 25.50 ppm; ^{77}Se NMR (92.5 MHz, DMSO-d_6) δ 283.15 ppm; HRMS (ESI) [M-Na]$^-$ $C_{18}H_{29}O_4SSe$ calcd 421.0957, found 421.1003.

Sodium 8-(phenyltellanyl)octyl sulfate (DP41). Yield: 65%; orange powder; mp 108 ℃; ^{1}H NMR (250 MHz, $CDCl_3$) δ 8.17-8.15 (m, 2H, benzene protons), 7.59-7.54 (m, 3H, benzene protons), 4.38-4.25 (m, 2H, -C*H*$_2$OSO$_3$Na), 3.86-3.57 (m, 2H, -TeC*H*$_2$-), 2.26-2.23 (m, 2H, -C*H*$_2$CH$_2$OSO$_3$Na), 1.80-1.77 (m, 2H, -TeCH$_2$C*H*$_2$-), 1.43-1.27 (m, 8H, -(C*H*$_2$)$_5$CH$_2$CH$_2$OSO$_3$Na) ppm; ^{13}C NMR (125 MHz, DMSO-d_6) δ 133.01, 132.75, 132.57, 129.31, 128.96, 128.72, 65.42, 30.97, 30.67, 29.07, 28.61, 28.47, 28.39, 25.42, 25.38 HRMS (ESI) [M-Na]$^-$ $C_{14}H_{21}O_4STe$ calcd 415.0227, found 415.0248.

Sodium 9-(phenyltellanyl)nonyl sulfate (DP42). Yield: 85%; orange powder; mp 124 ℃; ^{1}H NMR (250 MHz, $CDCl_3$) δ 8.16 (m, 2H, benzene protons), 7.58 (m, 3H, benzene protons), 4.35 (m, 2H, -C*H*$_2$OSO$_3$Na), 3.79 (m, 2H, -TeC*H*$_2$-), 2.28 (m, 2H, -C*H*$_2$CH$_2$OSO$_3$Na), 1.80 (m, 2H, -TeCH$_2$C*H*$_2$-), 1.57-1.39 (m, 10H, -(C*H*$_2$)$_5$CH$_2$CH$_2$OSO$_3$Na); ^{13}C NMR (62.5 MHz, $CDCl_3$) δ 133.28 (2C), 131.87, 131.77, 130.13-129.89 (2C), 70.48, 31.01, 30.79, 29.16, 28.82, 28.68, 25.54, 25.27, 25.10; HRMS (ESI) $C_{15}H_{23}O_4STe$ calcd [M-Na]$^-$ 429.0383, found 429.0380.

Sodium 10-(phenyltellanyl)decyl sulfate (DP43). Yield: 81%; orange powder; mp 127 ℃; ^{1}H NMR (250 MHz, $CDCl_3$) δ 8.17-8.15 (m, 2H, benzene protons), 7.83-7.56 (m, 3H, benzene protons), 4.22 (m, 2H, -C*H*$_2$OSO$_3$Na), 3.79-3.75 (t, 2H, *J* = 5 Hz, -TeC*H*$_2$-), 2.27-2.24 (m, 2H, -C*H*$_2$CH$_2$OSO$_3$Na), 1.74 (m, 2H, -TeCH$_2$C*H*$_2$-), 1.55-1.33 (m, 12H, -(C*H*$_2$)$_6$CH$_2$CH$_2$OSO$_3$Na) ppm; ^{13}C NMR (62.5 MHz, $CDCl_3$) δ 133.26, 133.09, 132.16, 131.78, 130.53, 130.07, 70.17, 31.05, 29.37, 29.27, 29.17, 28.89, 25.64, 25.27, 24.67; HRMS (ESI) [M-Na]- $C_{16}H_{25}O_4STe$ calcd 443.0540, found 443.0530.

Sodium 11-(phenyltellanyl)undecyl sulfate (DP44). Yield: 83%; orange powder; mp 131 ℃; ^{1}H NMR (250 MHz, $CDCl_3$) δ 8.17-8.16 (m, 2H, benzene protons), 7.58-7.57 (m, 3H, benzene protons), 4.31 (m, 2H, -C*H*$_2$OSO$_3$Na), 3.80-3.76 (t, 2H, *J* = 5 Hz, -TeC*H*$_2$-), 2.27-2.24 (m, 2H, -C*H*$_2$CH$_2$OSO$_3$Na), 1.78 (m, 2H, -TeCH$_2$C*H*$_2$-), 1.42-1.26 (m, 14H, -(C*H*$_2$)$_7$CH$_2$CH$_2$OSO$_3$Na) ppm; ^{13}C NMR (62.5 MHz, $CDCl_3$) δ 133.28, 133.19, 132.01, 131.77, 130.21, 130.07, 70.48, 31.05, 30.71, 29.41, 29.33, 29.21, 28.90, 28.65, 25.51, 25.28, 24.96 ppm; HRMS (ESI) [M-Na]$^-$ $C_{17}H_{27}O_4STe$ calcd 457.0696, found 457.0676.

Sodium 12-(phenylselanyl)dodecyl sulfate (DP45). Yield: 92%; orange powder; mp 135 ℃; ^{1}H NMR (250 MHz, $CDCl_3$) δ 8.18-8.15 (m, 2H, benzene protons), 7.58-7.56

(m, 3H, benzene protons), 4.26 (m, -C*H*$_2$OSO$_3$Na), 3.79-3.76 (t, 2H, *J* = 5 Hz, -TeC*H*$_2$-), 2.27-2.24 (t, 2H, *J* = 5 Hz, -C*H*$_2$CH$_2$OSO$_3$Na), 1.76 (m, 2H, -TeCH$_2$C*H*$_2$-), 1.41-1.31 (m, 16H, -(C*H*$_2$)$_8$CH$_2$CH$_2$OSO$_3$Na) ppm; ^{13}C NMR (62.5 MHz, CDCl$_3$) δ 137.73, 133.76, 133.10 (2C), 132.61, 130.54, 70.05, 35.14 (2C), 31.10, 30.50, 29.71, 29.43 (2C), 29.28, 28.53, 24.76 (2C) ppm; HRMS (ESI) [M-Na]$^-$ $C_{18}H_{29}O_4STe$ calcd 471.0853 found 471.0837.

2.1.6.2. *Surface activity and Critical Micelle Concentration (CMC) measurements*

Compounds were dissolved in double-distilled water and the final concentrations used for this experiment were as follows: 0.025 mM, 0.25 mM, 0.5 mM, 1 mM, 5 mM and 10 mM. This experiment was carried out with a KRÜSS Tensiometer K6 (KRÜSS GmbH, Hamburg) according to the manufacturer's instructions.

2.1.6.3. *Cyclic voltammetry*

Cyclic Voltammograms were recorded at a BAS CV-100W electrochemical workstation. In all electrochemical experiments, a glassy carbon electrode was used as a working electrode, an Ag/AgCl electrode (SSE) as reference and a platinum spiral as counter electrode. For the electrochemical studies, the electrolysis cell containing 33% methanolic 50 mM potassium phosphate buffer, pH 7.4, with in a final concentration of 250 µM of compound was used. The potential range was varied between -800 to 800 mV, with a scan rate of 500 mVs^{-1}. Four full cycles were recorded and the first cycle was used to identify the respective peak potentials. All experiments were preformed in triplicate at room temperature. To obtain oxygen-poor conditions, the electrolysis cell was purged with nitrogen before each measurement.

2.1.6.4. *Haemolysis Assay*

Drabkin's reagent kit (Sigma) was used for the haemolysis assay. All compounds were dissolved in DMSO (100 mM stock solutions). Stock solutions were diluted with DMSO to obtain a dilution series of 100 µM, 1 mM and 10 mM. The RBCs sample consisted of 990µl HPS buffer (NaCl 145 mM, KCl 7.5 mM, glucose 10 mM, HEPES 10 mM, pH 7.4). 10 µl of each compound were tested with 2.5 % haematocrit. The final concentrations of the compounds tested were 1 µM, 10 µM, 100 µM and 1 mM. The DMSO concentration in every sample was 1%. A negative control was used consisting of 990 µl HPS buffer and 10 µl DMSO with 2.5 % haematocrit. SDS served as a positive control. The RBC samples were incubated for 30 min at 37 °C in a water bath. After incubation, the samples were centrifuged at 12,000 g for 30 s, the 500 µl supernatant for each concentration was transferred into 2 ml of Drabkin's solution. The supernatant of the positive control was transferred into 2 ml of Drabkin's solution with detergent to lyse all RBCs in the sample. After incubation of the samples at room temperature for 30 min in the dark, the absorption at 540 nm was measured with a UV-Vis spectrophotometer (UV mini 1240, UV-Vis Spectrophotometer, Shimadzu). Three different whole blood samples were used for each experiment.

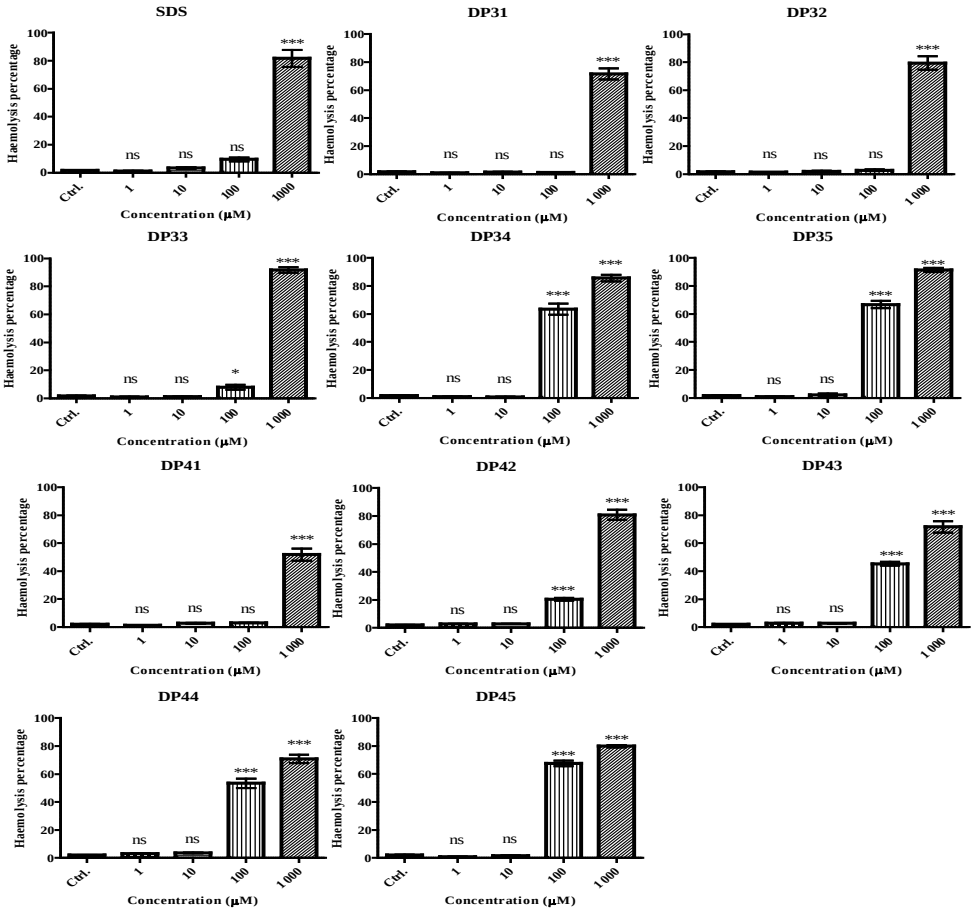

Fig S1. *Impact of compounds on the membranes of RBCs. SDS was used as a positive control.*

2.1.6.5. *Circular dichroism measurement (CD)*

CD spectra were measured at 20 ℃ on a Jasco J720 spec-tropolarimeter (Jasco Corporation, Tokyo, Japan). For the determination of the interaction between compounds and proteins, samples contained 50 µM haemoglobin (Sigma) in 995 µl potassium phosphate buffer (10mM, pH 7.4) and 5 µl of each compound in DMSO (10mM) or 20 µM Adx in 995 µl potassium phosphate buffer (10mM, pH 7.4) and 5 µl of each compound in DMSO (1mM stock solution) as well as 5 µl DMSO as negative control in 1 cm cuvette for measurements in the range of 250 to 650 nm. The

spectra were accumulated 3 times and then smoothed. The spectrum of the potassium phosphate buffer was recorded in each case and respectively saved as a baseline.

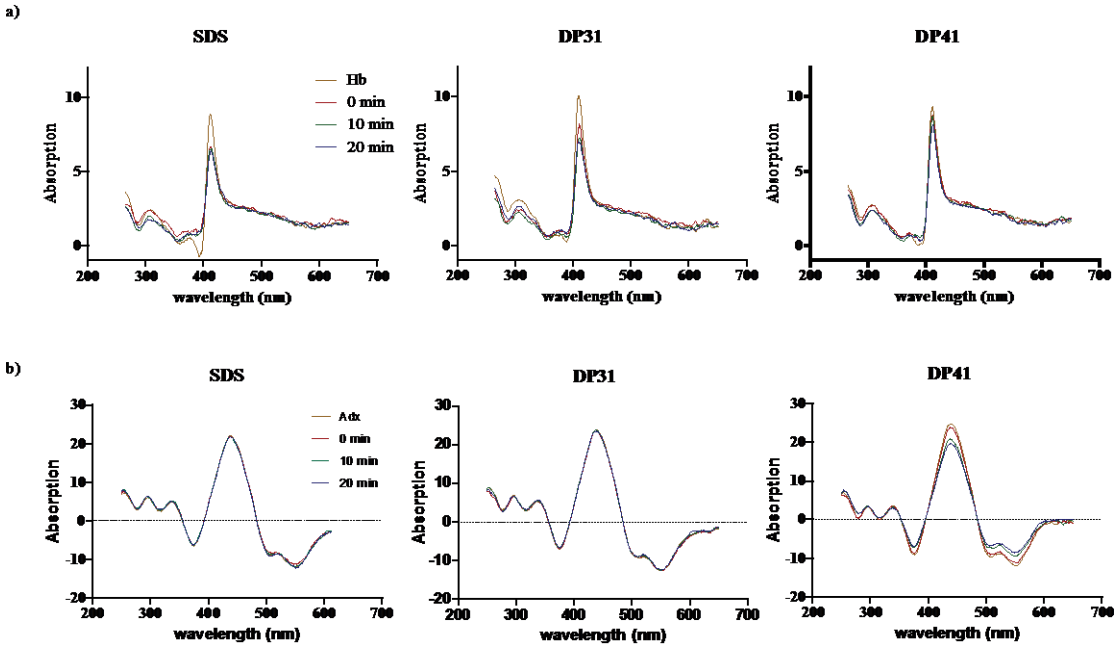

Fig S2. *Interaction of selected compounds with proteins. SDS was used as positive control. a) haemoglobin b) Adx.*

2.1.6.6. *Cell culture*

p53-Positive HCT116 wt cells were maintained at 37 ℃ and 5% CO_2 in McCoy's 5A medium (PromoCell, Heidelberg, Germany) with 10% fetal calf serum (FCS). ARPE-19 cells were maintained at 37 ℃ and 5% CO_2 in DMEM medium (PromoCell, Heidelberg, Germany) with 10% fetal calf serum (FCS). RAW 264.7 cells were cultured at 37 ℃ and 5% CO2 in RPMI 1640 medium (PromoCell, Heidelberg,

Germany). Organic selenide and telluride compounds were dissolved in DMSO as a 100 mM stock solution which was freshly prepared before use.

2.1.6.7. *Reflection electron microscope (REM) and Energy-dispersive X-ray spectroscopy (EDX)*

HCT116 cells were grown on coverslips until they were 50% confluent, washed with warm PBS (PH 7.4), treated with 50 μM organic selenide and telluride compounds and as negative control with same amount of DMSO. After incubations for 48 h, cells were fixed with 0.2 M cacodylate buffer containing 1% formaldehyde. Continuously increasing concentrations of ethanol were used for dehydration for 24 h. The fixed cells were coated with gold on a coverslip. REM and EDX analyses were recorded with a SUPRA^{TM} 40 (Carl Zeiss AG, Germany).

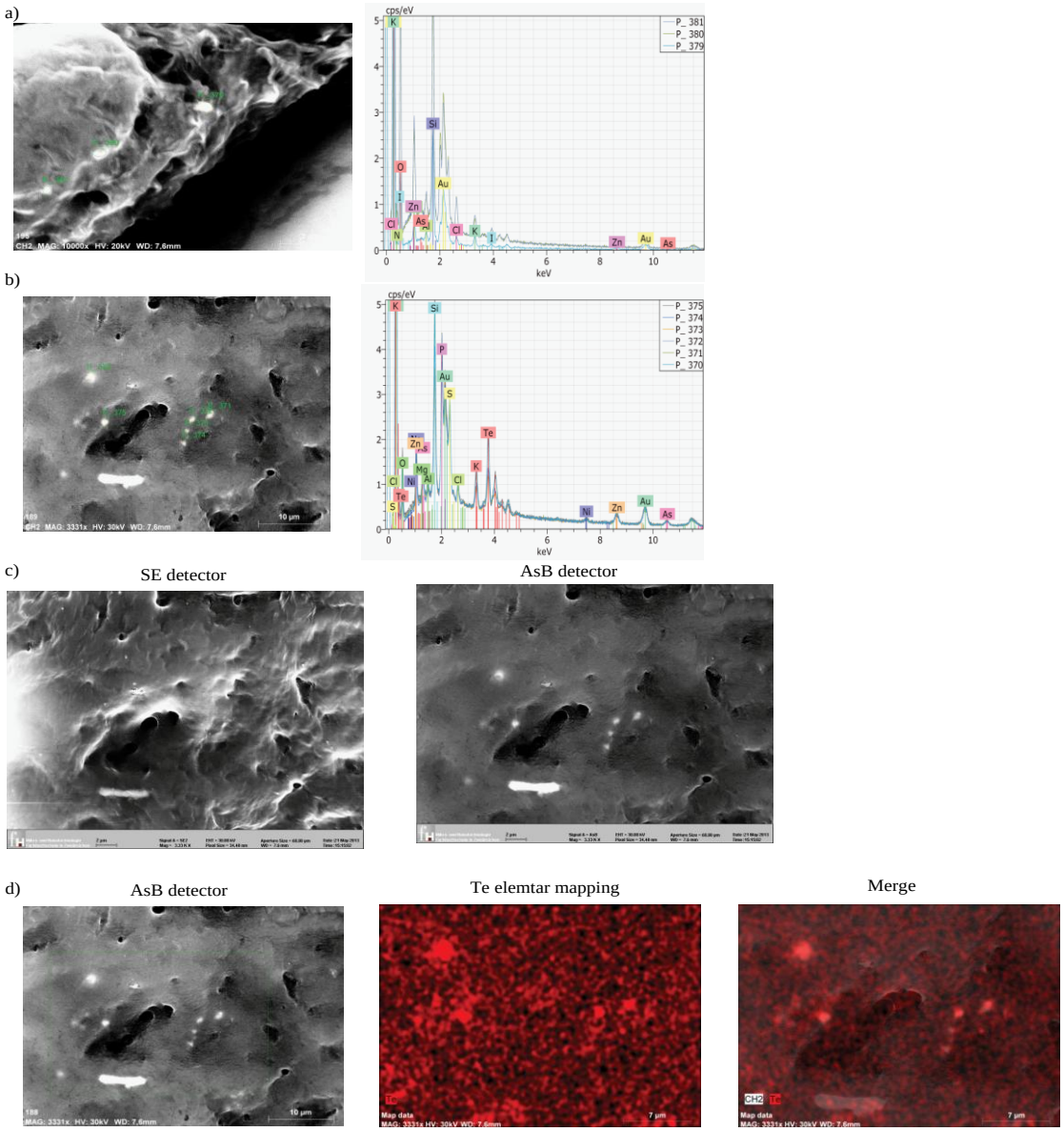

Fig S3. *HCT 116 cells were treated with compound DP41 for 48 h as well as with DMSO as negative control. a) and b) REM analysis with EDX analysis to detect Te atoms in the cells. Cells were treated with DMSO (a) as well as with DP41 (b). c) Detection of tellurium inside the cell using two different detectors (the SE-detector is used for cell surface imaging, the AsB detector for crystallographic contrast). d) Tellurium mapping to show the distribution of the tellurium in the cells.*

2.1.6.8. *Evaluation of cell viability*

In order to determine the effect of organic selenide and telluride compounds on HCT116, ARPE-19 cells or RAW 264.7, cells were seeded at 10^4 cells per well to a final volume of 200 µl in a 96-well plate and incubated overnight. Cells were then incubated with various concentrations of organic selenide and telluride compounds for 24h. Viability of the cells was determined by a colorimetric MTT (3-(4,5-dimethylthiazol-2-yl)-2,5-diphenyltetrazolium, Sigma) assay according to the manufacturer's instructions. 1 hour before the end of treatment, 50 µl MTT (5 mg/ml PBS) were added at 37 ℃ in a humified atmosphere. Following 1 h MTT treatment, the medium was removed and disposed and cells solubilized by adding 200 µl pure DMSO each well to allow the formazan crystals to dissolve completely. The spectrophotometrical absorbance of the purple-blue formazan dye was determined with an absorbance reader at 595 nm. [2]

2.1.6.9. *JC-1 assay for estimating the mitochondrial membrane potential* $\Delta\Psi_M$

Cells were plated onto coverslips with a density of 5×10^3 cells/coverslip and cultured for 24 h before further treatment. At this point, cells were treated with different concentrations of compounds for 2, 6 or 8 h. After cells were washed three times with Tyrode buffer (see above), they were incubated with 10 µg/ml JC-1 dye for 30 min. Subsequently, cells were washed three times with Tyrode buffer to remove any excess of dye. The coverslips were then mounted on a microscope (Karl Zeiss, Germany) and illuminated at 488 nm and 519 nm. The green and red channels of the fluorescence emitted were recorded. The fluorescence intensities of green and red channels from 150 cells were integrated, respectively, and the final ratios of red to green fluorescence were calculated for further statistic analysis.

2.1.6.10.*Nematode Assay*

The nematode assay based on *S. feltiae* is used to screen the toxicity of compounds against smaller organisms, especially against nematodes. *S. feltiae* were purchased from Sautter & Stepper, Germany. The nematodes were prepared and assayed as described previously. [3] Different concentrations of compounds were added (final concentrations of 50, 100, 200, and 400 µM in 1 % of DMSO in water). The viability of the nematodes was determined after 24 h of treatment, the control containing 1 % DMSO was set at 100 % viability and LD_{50} values were calculated accordingly.

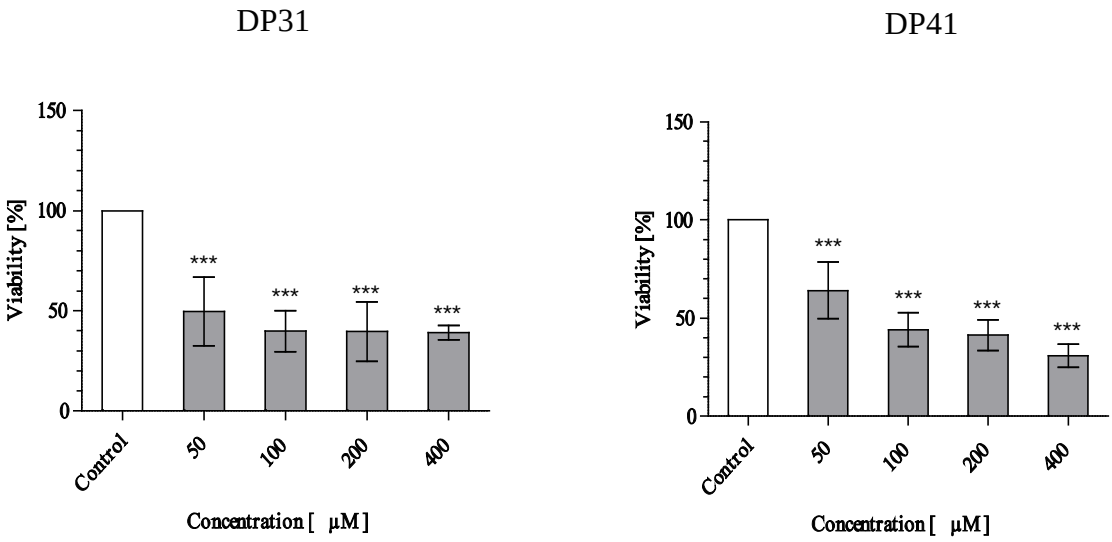

Fig S4. *Nematicidal activity of selected compounds against S. feltiae. Nematodes were treated with different concentrations of SDS, DP31 and DP41 for 24 h. Significances are expressed to the control (1% DMSO in water). Data shown as means of three independent experiments. (* $p \leq 0.05$; ** $p \leq 0.01$; *** $p \leq 0.001$).*

2.1.6.11.*Bacterium-Inhibition Assay*

Staphyllococcus aureus WDCM 5233 was obtained from Microbiological Depository Centre, Armenia and *Escherichia coli* M17 VKPM-B8208 from the Russian National Collection of Industrial Microorganisms. Bacteria were cultured on agar plates according to standard procedures. The diameters of the inhibitory zones were measured in mm. The minimal antibacterial activity was taken according to the diameter of the absence of bacterial growth zones, not less than 12 mm. The MIC (minimum inhibitory concentrations) was calculated with the corresponding optical density measurements at 595nm.

2.1.6.12.*Statistics*

GraphPad Prism software (GraphPad Inc., USA) was used for statistical analysis. Results were expressed as the mean ±SEM. Differences between the experimental groups were analyzed using one-way ANOVA test (Dunnett) or Student's t-test (two-tail, unpaired). Statistical significance categories are shown as: $p < 0.05$ (*), $p < 0.01$ (**) or $p < 0.001$ (***).

2.1.6.13.*Additional Literature for the ESI*

1. P. Han, N. Ma, H. Ren, H. Xu, Z. Li, Z. Wang and X. Zhang, Langmuir : the ACS journal of surfaces and colloids, 2010, 26, 14414-14418. 50

2. M. Doering, B. Diesel, M. C. H. Gruhlke, U. M. Viswanathan, D. Manikova, M. Chovanec, T. Burkholz, A. J. Slusarenko, A. K. Kiemer and C. Jacob, Tetrahedron, 2012, 68, 10577-10585.

3. B. Czepukojc, U. M. Viswanathan, A. Raza, S. Ali, T. Burkholz and C. Jacob, Phosphorus Sulfur and Silicon and the Related Elements, 2013, 188, 446-453.

2.2. Publication 2

A new tellurium-containing amphiphilic molecule induces apoptosis in HCT116 colon cancer cells

Peng Du, Nathaniel Edward Bennett Saidu, Johanna Intemann, Claus Jacob, Mathias Montenarh

This manuscript was published as an article in the following Journal:

Biochimica et Biophysica Acta 1840 (2014) 1808–1816

DOI: 10.1016/j.bbagen.2014.02.003

2.2.1. Abstract

2.2.1.1. *Background*

Chalcogen-based redox modulators over the years have attracted considerable attention as anti-cancer agents. New selenium- and tellurium-containing compounds with a polar head group and aryl-groups of various lengths have recently been reported as biologically active in several organisms. In the present study, we used the most active of the tellurium compound DP41, and its selenium counterpart DP31 to investigate their effects on the human cancer cell line HCT116.

2.2.1.2. *Methods*

Cells were treated with DP41 or DP31 and the formation of superoxide radicals was determined using dihydroethidium. Cell cycle analysis and apoptosis was determined by cytofluorimetry. Proteins involved in ER signaling and apoptosis were determined by Western blot analysis and fluorescence microscopy.

2.2.1.3. *Results*

With 50 μM of DP41, we observed an increase in $O_2^{\cdot -}$ formation. There was, however, no such increase in $O_2^{\cdot -}$ after treatment with the corresponding selenium compound under the same conditions. In the case of DP41, the production of $O_2^{\cdot -}$ radicals was followed by an up-regulation of Nrf2, HO-1, phospho-eIF2α and ATF4. CHOP was also induced and cells entered apoptosis. Unlike the cancer cells, normal retinal epithelial ARPE-19 cells did not produce elevated levels of $O_2^{\cdot -}$ radicals nor did they induce the ER signaling pathway or apoptosis.

2.2.1.4. *Conclusions*

The tellurium-containing compound DP41, in contrast to the corresponding selenium compound, induces $O_2^{\cdot -}$ radical formation and oxidative and ER stress responses, including CHOP activation and finally apoptosis.

2.2.1.5. *General significance*

These results indicate that DP41 is a redox modulating agent with promising anti-cancer potentials.

2.2.2. Introduction

Organosulfur-containing compounds have had a prominent role in medicine since ancient times [1-3]. There is a comprehensive literature in particular on sulfur-containing compounds derived from garlic, onions and leek [4-7]. Against this background, the medicinal applications of other members of the chalcogen family, namely selenium and tellurium compounds, are clearly still in their infancy. Selenium is an essential trace element which is involved in a variety of different functions in the human body [8]. Furthermore, selenium seems to play a role in cancer prevention and treatment. In contrast to selenium, tellurium does not have any known natural biological function in the human body. One of the reasons for this difference may be that tellurium–carbon bonds are more labile than their selenium counterparts and so bond cleavage occurs much more readily [9]. There are many reports on efforts which have been directed towards the evaluation of synthetic selenium compounds for pharmaceutical applications [10], but only a very limited number of attempts are known for synthetic tellurium compounds. Some of the compounds studied so far exhibit anti-fungal, anti-bacterial and anti-malarial activities [11-12] . Many of these applications, but not all, rely on an inherent redox modulating ability of selenium and tellurium. Unfortunately, many of the most interesting organoselenium or organotellurium compounds are poorly water soluble and unstable and hence inappropriate to test in a biological context. On the other hand, highly water-soluble compounds have only a limited capability to cross the plasma membrane and to penetrate into cells. Thus, bioavailability of such agents is usually limited. About a decade ago, first attempts on the synthesis of amphiphilic selenium and tellurium compounds with an anionic head group and different hydrophilic tail lengths were published. These compounds were tested for their protective activity against oxidation and nitration reactions caused by peroxynitrite [13]. Furthermore, the catalytic activity of these compounds towards the peroxidation of the zinc-containing protein

metallothionein was investigated. Recently, newly designed tellurium-containing compounds were used to monitor *in vivo* redox reactions between peroxynitrite and glutathione [14]. Other new tellurium compounds have also been used for the detection of reactive oxygen species [15]. Both these detection systems utilize the redox properties of the tellurium atom. On the other hand, new tellurium-containing pyrylium compounds were tested as modulators of the activity of multidrug resistance proteins [16-17]. It turned out that the electronegativity of the chalcogen determines whether these compounds act as inhibitors or activators of the multidrug resistance proteins. A whole series of new organoselenium and organotellurium compounds with different aryl-side chains have recently been synthesized and initially characterized [18]. At the same time, chalcogen nanoparticles have been used successfully providing further impetus for the development of more sophisticated self-assembling tellurium agents. In general, it was found that the tellurium compounds are more potent than the corresponding selenium compounds with regard to a reduction in cell viability and killing of bacteria. In the present study, we used the most potent compounds and tested their ability to induce cell death in cancer cells. Moreover, we analyzed cellular signaling pathways leading to growth arrest and eventually to apoptosis. We found that the organotellurium compound DP41 generates $O_2^{\cdot -}$ radicals in cancer cells. The production of $O_2^{\cdot -}$ radicals is followed by the activation of the ER signaling pathway which finally results in the induction of apoptosis. In contrast, normal retinal pigment epithelial (ARPE-19) cells failed to produce any significant amounts of $O_2^{\cdot -}$ radicals in response to DP41 treatment and consequently there was no induction of apoptosis in these cells.

2.2.3. Materials and methods

2.2.3.1. *Reagents and antibodies*

Protease inhibitor cocktail Complete™ (Roche Diagnostics, Mannheim, Germany), ascorbic acid (ASC) and anti-α-tubulin antibodies were obtained from Sigma-Aldrich (Munich, Germany). DMSO was from Merck (Darmstadt, Germany). Antibodies against CHOP (GADD153), cytochrome c, γH_2AX, GAPDH and Nrf2 were purchased from Santa Cruz Biotechnology (Heidelberg, Germany). Anti-poly(ADP-ribose) polymerase (anti-PARP), anti-ATF4, anti-eIF2α, anti-phospho-eIF2α (Ser 51) and anti-HO-1 antibodies were purchased from Cell Signaling Technology (Frankfurt, Germany), while the caspase 3 antibody was purchased from Promega (Mannheim, Germany). Goat, mouse and rabbit secondary antibodies were all bought from Dianova (Hamburg, Germany). Organic selenide DP31 and telluride DP41 compounds were synthesized and described recently [18]. They were dissolved in DMSO to a 100 mM stock solution which was freshly prepared before use. Ascorbic acid was dissolved in distilled water to a 100 mM stock solution and applied to the cell culture medium 0.5 h (unless stated otherwise) before treatment with chalcogen compounds.

2.2.3.2. *Cell culture*

HCT116 cells were maintained at 37 ℃ and 5% CO_2 in McCoy's 5A medium (PromoCell, Heidelberg, Germany) with 10% fetal calf serum (FCS). ARPE-19 cells were maintained at 37 ℃ and 5% CO_2 in DMEM medium (PromoCell, Heidelberg, Germany) with 10% FCS. The androgen-sensitive prostate cancer cells, LNCaP, were maintained at 37 ℃ in RPMI 1640 media, supplemented with 10% FCS in an atmosphere enriched with 5% CO_2.

2.2.3.3. *Tubulin immunofluorescence analysis*

HCT116 cells were grown on coverslips until they were 70% confluent. They were washed with PBS (pH 7.4), treated with DP41 at 50 μM and with DMSO as solvent control. After incubation for various time periods, cells were washed with PBS, fixed in 3% (v/v) formaldehyde in PBS at room temperature for 20 min and permeabilized on ice for 5 min with 0.2% (v/v) Triton X-100. This was followed by another washing step with PBS, blocking with 2% (w/v) bovine serum albumin (BSA) for 3 × 10 min at room temperature on a shaker. Cells were then incubated with a primary antibody against α-tubulin for 30 min at 37 ℃ in a humidified chamber. They were further washed with PBS for 3 × 10 min, incubated with secondary antibody (ALEXA-Fluor™ 488) at 37 ℃ for 30 min in the dark, then washed under the same conditions as above. This was followed by another treatment with 0.5 μM 4′,6-diamidino-2-phenylindole (DAPI) at 37 ℃ for 15 min in a humidified chamber and another washing step with PBS on a shaker. Cells on the coverslips were fixed with a drop of mounting medium and were analyzed using the QLC-100 microscope equipped with a 60 × oil immersion objective (NA 1.4; Nikon, Japan).

2.2.3.4. *Cell cycle analysis*

HCT116 cells (5×10^5) were seeded on a 10 cm Petri dish and grown overnight. The medium was changed and cells were treated with DMSO (solvent control) or 50 μM DP41 and incubated for 24 h. Media and trypsinized cells were subsequently collected from a Petri dish, and centrifuged with 200 ×*g* at 4 ℃ for 7 min. Cells were washed with cold PBS then centrifuged under the same conditions as above twice before being re-suspended in PBS and fixed with 70% ethanol. The cells were incubated further with 1 mg/ml RNase (Sigma-Aldrich, Taufkirchen, Germany) and 400 μM propidium iodide (1 mg/ml, Sigma-Aldrich) to label DNA. Cells were then analyzed

in a flow cytometer (FACSCalibur, 4CS E4021, Becton and Dickinson, Heidelberg, Germany). 10,000 events were counted for each sample. Data were analyzed using FlowJo software (FlowJo, USA).

2.2.3.5. *Analysis of apoptosis*

HCT116 cells or ARPE-19 cells (5×10^5) were seeded and grown on a 10 cm Petri dish overnight. The medium was changed and cells were treated with 50 µM DP41 and incubated for 24 h. Cells were trypsinized and collected along with media from the Petri dish, then centrifuged with 200 ×*g* at 4 ℃ for 7 min. Cells were washed with binding buffer (BioLegend, Fell, Germany), centrifuged twice and then resuspended in 100 µl binding buffer. They were stained with 5 µl annexin V FITC (BioLegend) and 10 µl of 0.1 mg/ml propidium iodide (1 mg/ml, Sigma-Aldrich). Cells were then analyzed in a cytofluorimeter (FACSCalibur, 4CS E4021, Becton and Dickinson). 10,000 events were counted for each sample. The data were analyzed using FlowJo software (FlowJo).

2.2.3.6. *ROS assay*

HCT116 or ARPE cells (2×10^4) were seeded in 96 black/transparent wells from Becton and Dickinson overnight. Medium was removed and cells were washed 3 times with Tyrode's buffer (10 mM HEPES, 140 mM NaCl, 5 mM KCl, 10 mM glucose, 1.8 mM $CaCl_2$, 1 mM $MgCl_2$, pH 7.4) for 3 times. For ROS staining, 3.2 mg dihydroethidium (DHE, Sigma-Aldrich) was dissolved in 100 µl DMSO as stock solution, and diluted with Tyrode's buffer to 25 µM as working solution. 100 µl DHE-working solution was added to each well. After cells were incubated with DHE for 30 min at 37 ℃ in the dark, they were washed again 3 times with Tyrode's buffer. 100 µl Tyrode's buffer containing 50 mM DP31 or DP41 was then added directly into

each well. The fluorescence (Ex/Em: 518 ± 9/606 ± 20 nm) per each well was measured with a plate reader (Tecan Infinite M200, Crailsheim, Germany) every 5 min to determine the concentration of $O_2^{\cdot -}$ inside the cells.

2.2.3.7. *Extraction of cellular proteins*

Following incubation of HCT116 cells or ARPE-19 cells with the test compounds, cells were collected in cold PBS, pH 7.4 and centrifuged together with the cell culture medium at 4 ℃ and 250 ×*g* for 7 min. After one washing step with cold PBS, cells were lysed with 100 µl of RIPA buffer (50 mM Tris–HCl, pH 8.0, 150 mM NaCl, 0.5% sodium desoxycholate, 1% Triton X-100, 0.1% sodium dodecyl sulfate (SDS)) supplemented with the protease inhibitor cocktail Complete™ according to manufacturer's instructions (Roche Diagnostics, Mannheim, Germany). The cell lysate was left on ice for 15 min, subjected to sonification (3 × 1 min) at 4 ℃ and then cell debris was removed by centrifugation at 16,250 ×*g* at 4 ℃ for 30 min. The protein content of the supernatant was determined according to the Bradford method using the Bio-Rad protein assay reagent (Bio-Rad, Munich, Germany).

2.2.3.8. *SDS polyacrylamide gel electrophoresis and Western blot analysis*

Proteins were separated on either a 10 or 12.5% sodium dodecyl sulfate-polyacrylamide gel and transferred onto a polyvinylidene difluoride membrane (PVDF) by tank blotting using a transfer buffer containing 20 mM Tris–HCl, pH 8.8 and 150 mM glycine. The membrane was blocked with 5% dry milk in PBS containing 0.1% Tween-20 for 1 h at room temperature and then incubated with the specific antibody which was diluted in PBS with 0.1% Tween-20 containing 1% dry milk powder. The membrane was washed with PBS Tween-20 containing 1% skimmed milk (3 × 10 min), before being incubated with a peroxidase-coupled

secondary antibody (anti-rabbit 1:30,000 or anti-mouse 1:10,000) for 1 h at room temperature. The membrane was washed again in PBS Tween-20 (3 × 10 min). Signals were developed and visualized by the Lumilight system from Roche Diagnostic (Mannheim, Germany).

2.2.3.9. *Treatment with antioxidant*

In order to estimate antioxidant effects on the cellular process triggered by the organotellurium compound DP41, and hence, to establish a possible redox-link between this compound and its biological activity, HCT116 cells were pretreated with 100 μM ascorbic acid for 0.5 h and then washed with PBS twice prior to treatment with the organochalcogen compounds as described above.

2.2.3.10.*Statistics*

GraphPad Prism software (GraphPad Inc., USA) was used for statistical analysis. Results were expressed as arithmetic mean ± s.d. Differences between the experimental groups were analyzed using one-way ANOVA or Student's *t*-test (two-tail, unpaired), and statistical significance differences were shown as follows: $p<0.05$ (*), $p<0.01$ (**) or $p < 0.001$ (***).

2.2.4. Results

2.2.4.1. *DP41 induces $O2^{\cdot-}$ radical formation*

Organoselenium and organotellurium compounds have been known for quite some time and their biological functions were tested in fungi, bacteria and some mammalian cells. One of the main disadvantages of many of these molecules,

however, is the poor solubility in water while others, such as inorganic tellurium salts are poorly bioavailable. To circumvent these problems, novel amphiphilic selenium- and tellurium-containing compounds have been synthesized and initially characterized biophysically [18]. Here, we attempted to analyze two of these compounds, one selenium compound (DP31) and the corresponding tellurium compound (DP41) in mammalian cells. The structure of these two compounds is shown in Fig. 1. Since both, selenium as well as tellurium can act as redox modulators, we first asked whether treatment of the human cancer cell line HCT116 might induce the formation of $O_2^{\cdot -}$ radicals. We analyzed the generation of $O_2^{\cdot -}$ radicals with a dihydroethidium (DHE) assay according to the manufacturer's instructions. As shown in Fig. 2A, treatment of HCT116 cells with the selenium compound DP31 did not result in an increase in $O_2^{\cdot -}$ radical formation, whereas, the tellurium compound DP41 clearly induced the formation of $O_2^{\cdot -}$ radicals. As a control, cells were incubated with the solvent dimethyl sulfoxide (DMSO) alone and with H_2O_2 as a positive control. In order to confirm these results, we repeated the experiment with the active compound DP41 in the presence of the antioxidant ascorbic acid. As shown in Fig. 2B, ascorbic acid led to a down-regulation of the $O_2^{\cdot -}$ radicals after treatment of the cells with DP41. Thus, in contrast to the selenium compound the tellurium compound induces the formation of reactive oxygen species.

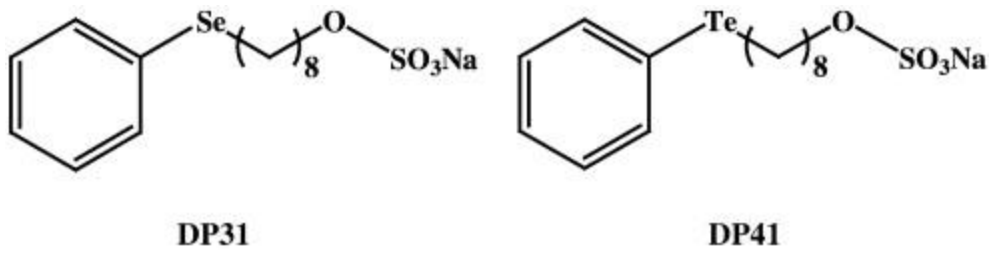

DP31 DP41

***Fig 1**. Chemical structures of selenium- and tellurium-containing compounds, DP31 and DP41, respectively.*

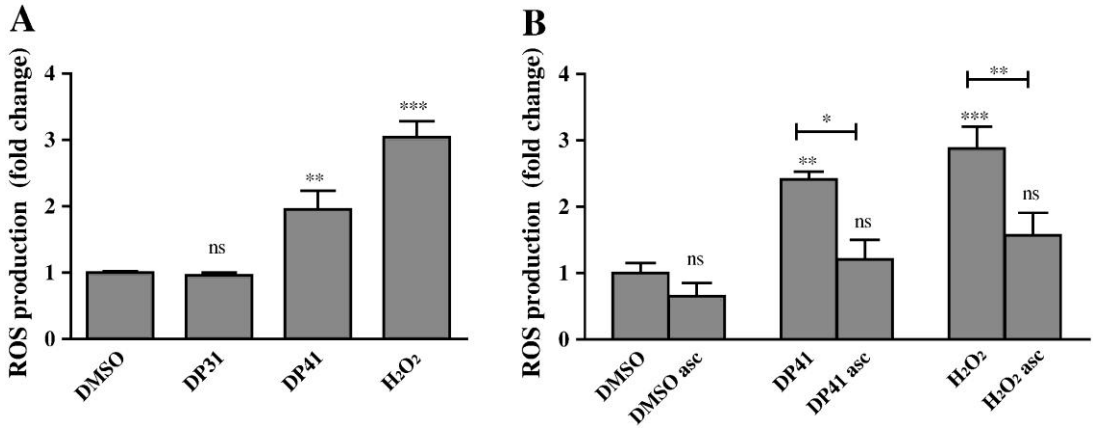

***Fig 2**. DP41 induces generation of $O_2^{\cdot-}$. (A) Relative increases in DHE oxidation in HCT116 cells, indicative of $O_2^{\cdot-}$ radical formation following treatment with DMSO (solvent control), 50 μM DP31, 50 μM DP41 or 50 μM H_2O_2 for 45 min. (B) Pre-treatment of HCT116 cells with ascorbic acid reduces the DP41- or H_2O_2-induced formation of $O_2^{\cdot-}$. Data are expressed as a relative increase in DHE oxidation in relation to solvent control and depicted as means ± s.d. (n = 3). **p<0.01 or *p<0.05.*

2.2.4.2. *DP41 up-regulates the antioxidant response proteins Nrf2 and HO-1*

Under normal physiological conditions, cells respond to reactive oxygen species (ROS) with enzymatic and non-enzymatic defense and signaling mechanisms. One of the key players in the antioxidant response in eukaryotic cells is the transcription factor nuclear factor erythroid 2-related factor 2 (Nrf2), which is complexed with Keap1 in the cytoplasm [19]. ROS induces the liberation of Nrf2 from Keap1 repression with a subsequent translocation of Nrf2 into the nucleus where it binds to the antioxidant response element (ARE) for transcription of various genes. In order to

analyze a possible activation of Nrf2 by DP41, cells were treated with these compounds for various periods of time. Afterwards, nuclear extracts were prepared and analyzed by sodium dodecyl sulfate (SDS) polyacrylamide gel electrophoresis followed by Western blot with an Nrf2 specific antibody. As shown in Fig. 3A, there was an increase in the nuclear Nrf2 protein starting at 1 h and reaching a maximum at 2 h after treatment with DP41. After 2 h Nrf2 was still present but at a much lower level than before.

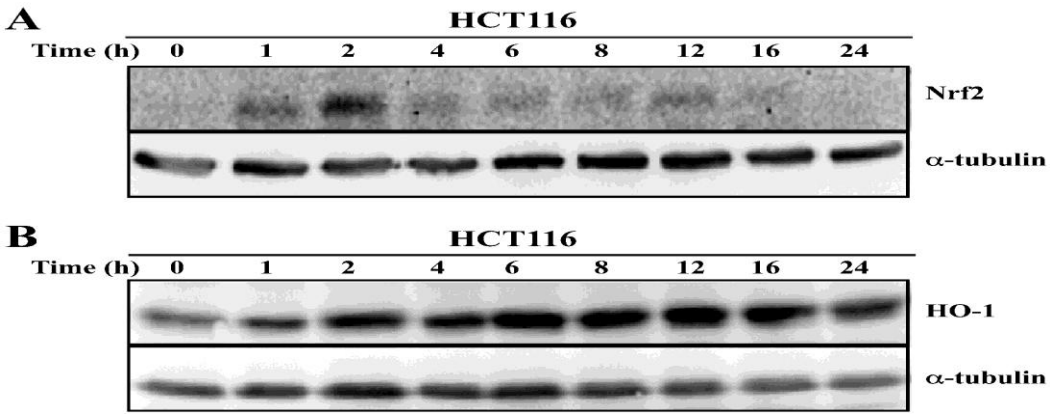

Fig 3*. DP41 induces Nrf2 and HO-1 protein expressions in HCT116 cells. Cells were untreated (0 h) or treated with 50 μM DP41 for the indicated period of time. Cell lysates were prepared and analyzed on a 10% (A) or a 12.5% (B) SDS-polyacrylamide gel followed by Western blotting using an anti-Nrf2 (A) or an anti-HO-1 (B) specific antibody. α-Tubulin was used as a loading control. One representative of at least 2 Western blots is shown here.*

One of the down-stream targets of Nrf2 is the heme oxygenase 1 (*HO-1*) gene whose gene product is a sensitive and reliable indicator of cellular stress [20]. Therefore, in the next step, we were interested in evaluating the effect of DP41 on the HO-1 protein levels following treatment of HCT116 cells. As shown in Fig. 3B, there was a steady increase in HO-1 levels after 2 h of treatment of HCT116 cells with DP41. Thus, from

these results it is clear that treatment of HCT116 cells with the tellurium compound DP41 resulted in the formation of $O_2^{\cdot -}$ radicals, which is followed by an antioxidant response including Nrf2 and HO-1 activation.

2.2.4.3. *DP41 induces other ER stress proteins but not CHOP*

It is well established that $O_2^{\cdot -}$ radicals cause an endoplasmic reticulum (ER) stress response [21]. In ER stress response signaling, phosphorylation of the eukaryotic initiation factor 2α (eIF2α) is one of the early events. This specific phosphorylation is a signal for the attenuation of protein synthesis in ER stressed cells. In order to analyze whether treatment of HCT116 cells with the tellurium compound DP41 might induce this particular kind of ER stress signaling, cells were treated with DP41 for various time intervals. Cells were subsequently lysed and the cell extract analyzed on an SDS polyacrylamide gel followed by a Western blot with antibodies against total eIF2α or the phosphorylated form of eIF2α. As shown in Fig. 4A, the overall amount of eIF2α in the cells remained constant over the time period analyzed. In contrast, we noticed a transient increase in the level of phosphorylated eIF2α, commencing after 1 h of treatment of HCT116 cells with DP41 and remaining at an elevated level for up to 6 h after treatment.

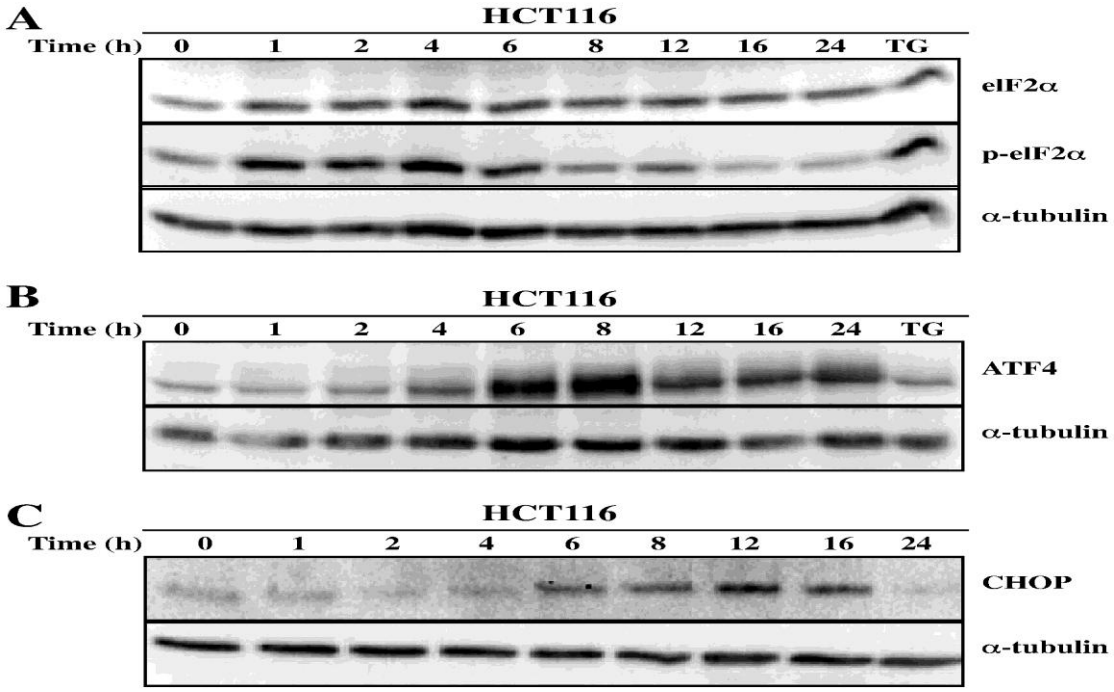

Fig 4*. DP41 induces the expression of proteins related to ER stress in HCT116 cells. Cells were untreated (0 h) or treated with 50 μM DP41 for the indicated period of time. For phospho-eIF2α and ATF4 positive controls, HCT116 cells were treated with 1 μM thapsigargin (TG) for 4 h. Cell lysates were prepared and analyzed on a 12.5% SDS-polyacrylamide gel followed by Western blotting using anti-p-eIF2 or anti-eIF2α (A), anti-ATF4 (B) or anti-CHOP (C) specific antibody. α-Tubulin was used as a loading control. One representative of at least three Western blots is shown here.*

Although ER stress signaling leads to a general repression of protein synthesis, it also induces the expression of the activating transcription factor 4 (ATF4). ATF4 is a transcription activator of genes which are involved in protein folding and assembly, metabolism and antioxidation [22]. Therefore, in the next step, we analyzed the expression of ATF4 after treatment of HCT116 cells with DP41. As shown in Fig. 4B, we observed an increase in the level of ATF4 after 4 h treatment.

One of the down-stream targets of ATF4 is the C/EBP homologous protein (CHOP) which is also known as growth arrest- and DNA damage-inducible gene 153 (GADD153) [23-24]. CHOP is considered an inducer of stress mediated apoptosis. After incubation of HCT116 cells with DP41 for various periods of time, we lysed the cells and the cell extract was subsequently analyzed on an SDS polyacrylamide gel followed by a Western blot with a CHOP specific antibody. Fig. 4C shows an increase in the level of CHOP 6 h after treatment of HCT116 cells with DP41. The level of CHOP remained elevated up to 16 h after treatment.

2.2.4.4. *DP41 causes cell cycle arrest in the G2/M-phase of the cell cycle and apoptosis*

Ultimately, CHOP induction after treatment of HCT116 cells with DP41 may result in cell cycle arrest and/or apoptosis. Therefore, in the next step, we analyzed the cell cycle distribution after treatment of HCT116 cells with DP41 using flow cytometry. After treatment of the cells for 24 h, we observed a G_2-arrest (Fig. 5). In addition to the G_2-arrest, we also observed an increase in the number of cells in the subG_1-phase, which might indicate the beginning of apoptosis. In order to confirm a possible induction of apoptosis, we analyzed HCT116 cells with annexin V and propidium iodide staining (Fig. 6A). Quantification of apoptotic cells revealed that 24 h after treatment, around 20% of the cells were already present in the apoptotic fraction (Fig. 6B). To further confirm induction of apoptosis, we analyzed the expression of the anti-apoptotic bcl-2 protein. Here, cells were treated with DP41 or with DMSO (solvent control) alone for 24 h or 48 h. Cell extracts were analyzed on a SDS polyacrylamide gel followed by Western blot with a bcl-2 specific antibody. As shown in Fig. 6C, there was a significant down-regulation of bcl-2 after 24 h which became even more pronounced after 48 h treatment of HCT116 cells with DP41. In the next step, we analyzed the release of cytochrome c from mitochondria into the

cytosol as an additional marker of the apoptotic process. Cells were treated as described above and cytosolic extracts were analyzed on an SDS-polyacrylamide gel followed by Western blot with a cytochrome c specific antibody. Fig. 6D shows an increase of cytosolic cytochrome c after treatment of the cells with DP41, whereas there was no such increase in DMSO treated control cells. Next, we analyzed the cells for caspase 3 cleavage as an even further proof for apoptosis. Cells were treated as described earlier and caspase 3 cleavage was analyzed with a caspase 3 specific antibody. The caspase 3 cleavage product was detected in DP41 treated cells but not in the control cells treated with DMSO alone (Fig. 6E). To further confirm this result, we looked for the cleavage of poly-ADP-ribose polymerase (PARP), which is a well known substrate for caspase 3/7. We again treated HCT116 cells with DP41 for 24 h or for 48 h. Cells were lysed and the cell extract was analyzed on an SDS polyacrylamide gel followed by Western blot with a PARP specific antibody. As shown in Fig. 6F, after 24 h and 48 h of treatment, there was a band for the PARP cleavage product. Thus, all these results show that treatment of HCT116 cells with DP41 results in a G_2-arrest of the cell cycle, and the induction of apoptosis.

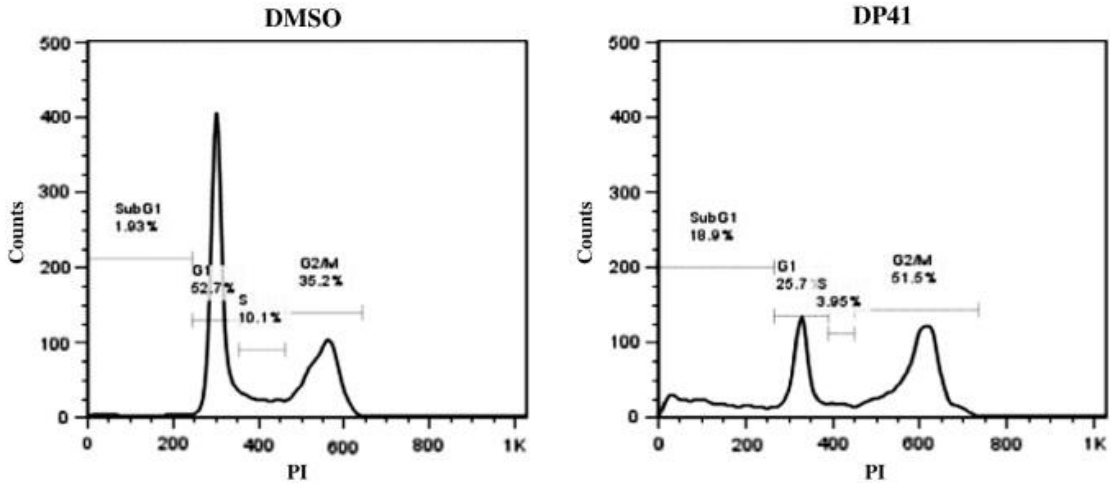

Fig 5*. Influence of DP41 on cell cycle distribution. HCT116 cells were treated for 24 h with DMSO (solvent control) or 50 μM DP41 and then analyzed by*

FACS. Cytofluorimetric analysis of treated cells. One representative of at least three independent experiments is shown here.

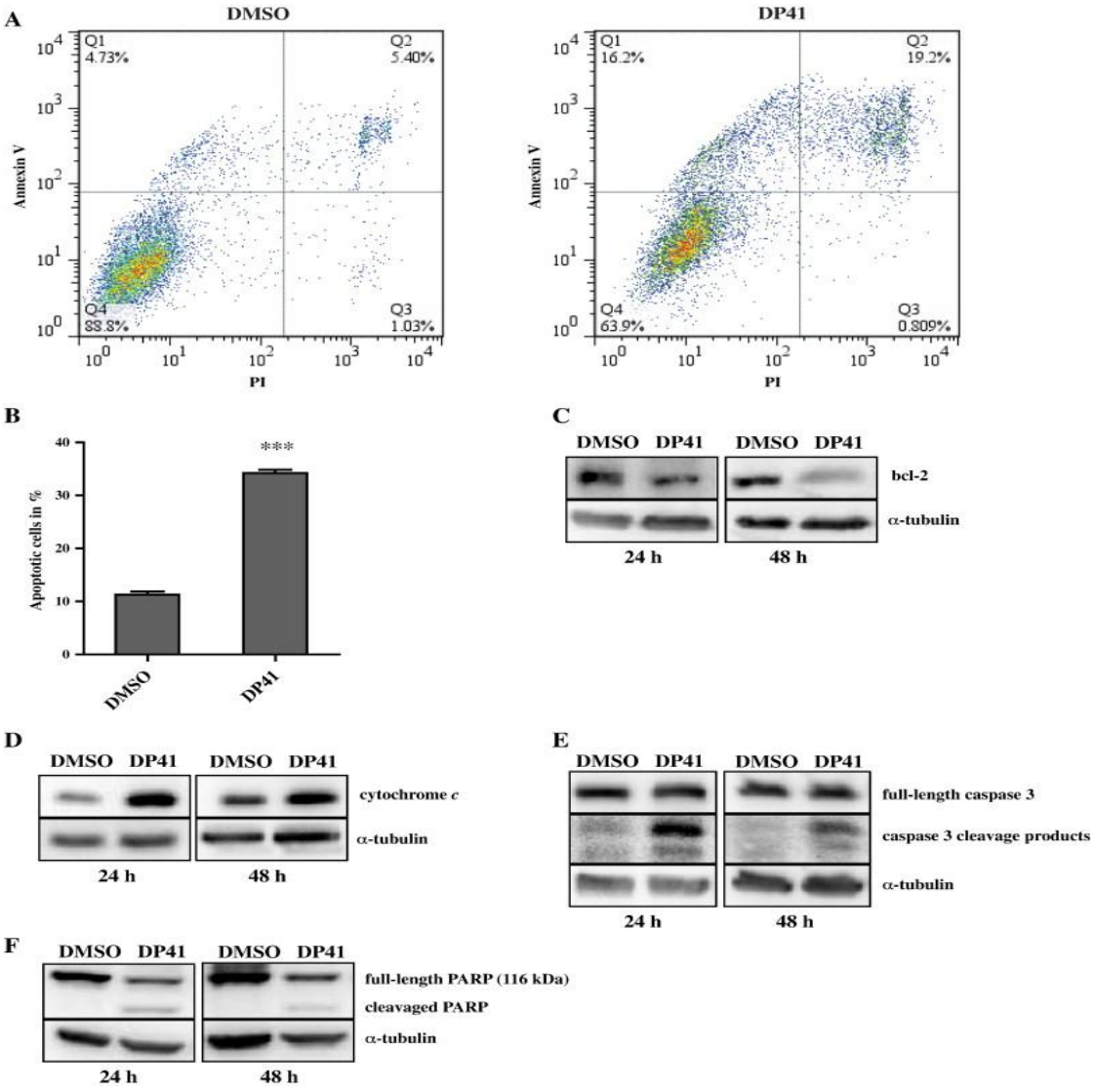

Fig 6*. DP41 induces apoptosis in HCT116 cells by modulating bcl-2 protein expression, inducing cytochrome c release and activation of both, caspase 3 and PARP cleavage. (A) Cells were treated for 24 h with either DMSO (solvent control) or 50 μM DP41 and then stained with annexin-V and*

*propidium iodide (PI) before being analyzed by FACS for apoptotic cell death. Viable cells are presented as both annexin-V and PI negative. (B) Percentage distribution of DP41-induced apoptotic cell death relative to DMSO control. One representative of at least three independent experiments is shown here. Means ± s.d. (n = 3). **p < 0.01 or *p < 0.05. (C–F) HCT116 cells were treated with either DMSO or 50 μM DP41 for 24 and 48 h, and protein expressions, PARP cleavage and caspase 3/7 activation and cleavage were subsequently studied and analyzed by Western blot. Proteins were separated on a 12.5% SDS-polyacrylamide gel and blotted on a PVDF membrane. Bcl-2 (C), cytochrome c (D) or PARP cleavage (F) was visualized with the appropriate antibody, while full-length caspase 3/7 and its cleavage products (E) were detected with a caspase 3-specific antibody (8G10). α-Tubulin was used as a loading control. One representative of at least three Western blots is shown here.*

Based on the finding that DP41 arrested HCT116 cells in the G_2-phase of the cell cycle, we next examined the effect of DP41 on the microtubule organization by immunostaining of α-tubulin. A normal microtubule distribution in HCT116 cells and network formation were observed in the cytoplasm of HCT116 cells treated with DMSO alone. In sharp contrast, taxol as a positive control caused a disruption of the microtubule network and a very similar result was obtained with DP41 (Fig. 7). Thus, DP41 destroys the microtubulin network in HCT116 cells.

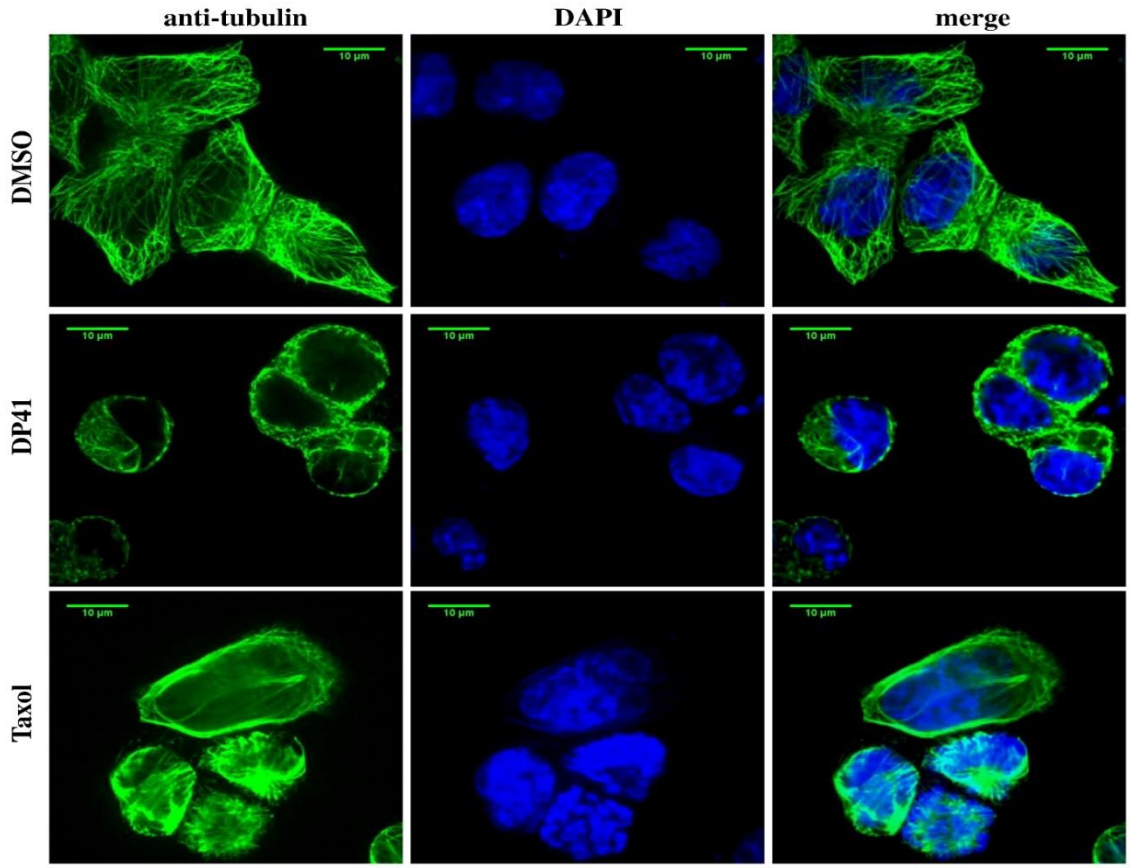

Fig 7*. Treatment of HCT116 cells with DP41 affects the organization of the cells' microtubule network. HCT116 cells were cultured overnight before incubation with DMSO (solvent control), 50 µM DP41 or 50 µM taxol (positive control) for 24 h. Cells were fixed with formaldehyde before being incubated with monoclonal anti-α-tubulin for 30 min at 37 ℃ followed by 30 min incubation at 37 ℃ with the ALEXA-Fluor™ 488 secondary antibody. After three washing steps, the cells were briefly stained with DAPI. The organization of the microtubule network (green) and nucleus (blue) was visualized with a Zeiss Axioskop fluorescence microscope.*

All experiments described so far were performed with the cancer cell line HCT116. In order to evaluate whether the effects seen with DP41 are restricted to such cancer cells, we analyzed the effect of DP41 on normal retinal epithelium ARPE-19 cells.

ARPE-19 cells were treated with DP41 and cells were analyzed for ROS production as described above for HCT116 cells. The results are shown in Fig. 8A. In the control experiment with H_2O_2, we found a clear induction of ROS production, whereas, with the tellurium compound DP41, ROS induction was notably absent in these cells. Since there is no notable increase in ROS levels in normal cells, we wonder whether normal cells would also avoid apoptosis under these conditions. Apoptosis was analyzed by annexin V and propidium iodide staining after treatment of ARPE-19 cells with DP41 for 48 h. Fig. 8B and the statistical analysis presented in Fig. 8C reveal no induction of apoptosis in ARPE-19 cells. In order to support these findings by another method, we treated ARPE-19 cells with DP41. As a positive control, HCT116 cells were treated with 5-fluorouracil (5-FU). The cell extract was analyzed on an SDS-polyacrylamide gel followed by Western blot with an anti-PARP antibody. As shown in Fig. 8D, there was a clear signal for the PARP cleavage product at a molecular weight of 89 kDa in 5-FU treated cells, whereas, no such signal was observed in DMSO or DP41 treated cells. Thus, these results demonstrate that in contrast to HCT116 cells, ARPE-19 cells are resistant against apoptosis after treatment with DP41.

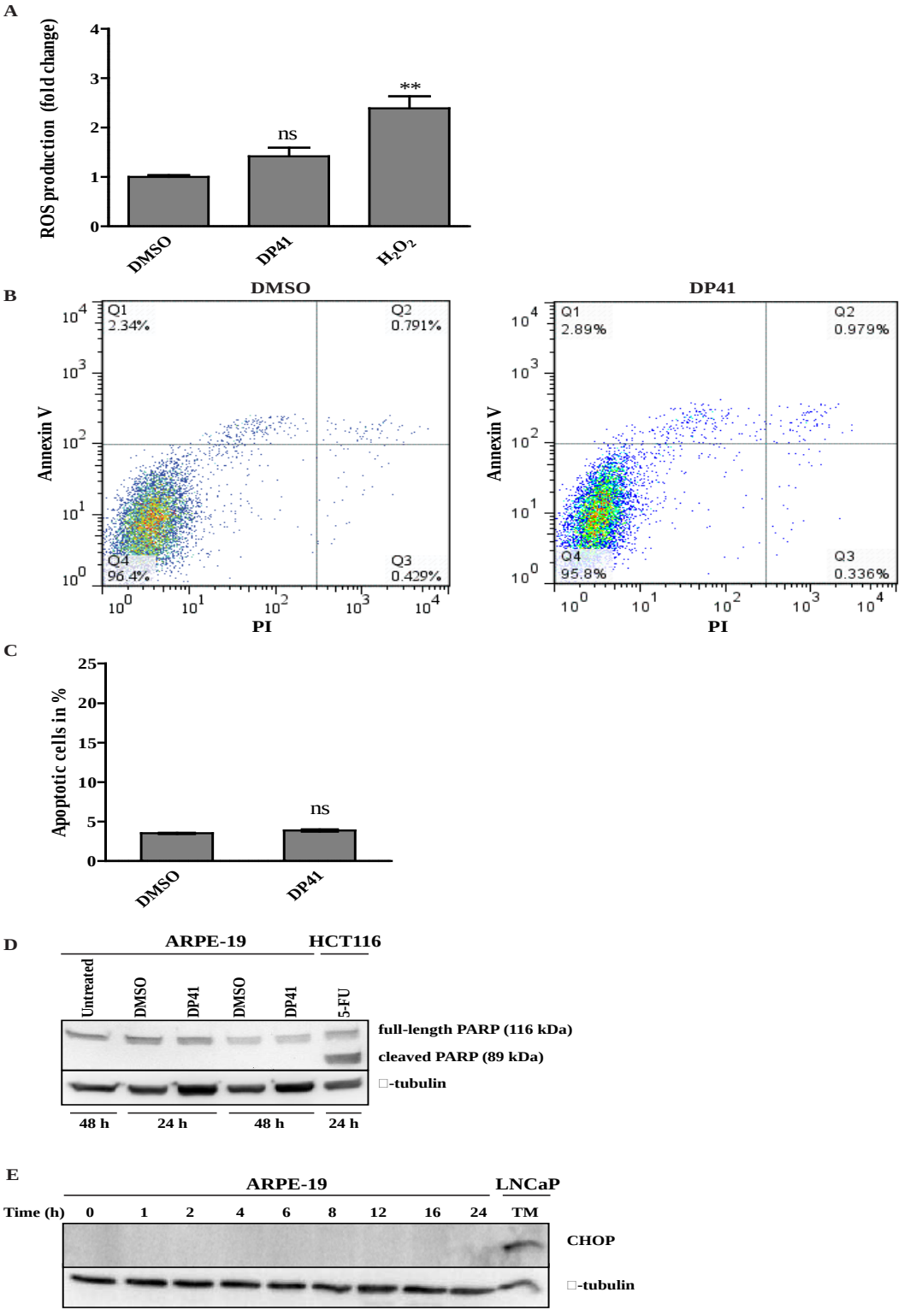

Fig. 8. Impact of DP41 on non-cancerous ARPE-19 cells. (A) DHE oxidation in ARPE-19 cells, indicative of $O_2^{\cdot-}$ radical formation as a result of treatment with 0.05%

*DMSO, 50 μM DP41 or 50 μM H_2O_2 for 45 min. Data are expressed as a fold increase in DHE oxidation rate in relation to solvent control and are depicted as means ± s.d. (n = 3). *p < 0.05, **p < 0.01 or ***p < 0.001. (B) Cells were treated for 24 h with either DMSO or 50 μM DP41 and then stained with annexin-V and propidium iodide (PI) before being analyzed by FACS for apoptotic cell death. Viable cells are presented as both annexin V and PI negative. (C) Percentage distribution of DP41-induced apoptotic cells relative to DMSO control. One representative of at least three similar independent experiments is shown here. Means ± s.d. (n = 3). *p < 0.05, **p < 0.01 or ***p < 0.001. (D) ARPE-19 cells were either left untreated, treated with 0.05% DMSO or treated with 50 μM DP41 for 24 and 48 h. As a positive reference, HCT116 cells were treated with 50 μg/μl 5-fluorouracil (5-FU) for 24 h and PARP cleavage was then studied by Western blotting. Cells were untreated (0 h) or treated with 50 μM DP41 for the indicated period of time. For a positive control, LNCaP cells were treated with 2 μg/ml tunicamycin (TM) for 24 h. Cell lysates were prepared and analyzed on a 12.5% SDS-polyacrylamide gel followed by Western blotting using anti-CHOP specific antibody (E). α-Tubulin was used as a loading control in both (D) and (E). One representative of at least three Western blots is shown here.*

Since CHOP is a critical factor in ER stress induced apoptosis in cancer cells (Fig. 4C), we next analyzed ARPE-19 cells for CHOP induction after DP41 treatment. Cell extracts were analyzed on an SDS-polyacrylamide gel followed by Western blot with a CHOP specific antibody. As shown in Fig. 8E, we could not detect the expression of CHOP in DP41 treated ARPE-19 cells, whereas, in the positive control, there was a clear signal for the CHOP protein.

2.2.5. Discussion

The unique redox and catalytic properties of organoselenium and organotellurium compounds turn these compounds into attractive molecules for pharmaceutical studies. Previously, two major drawbacks of these compounds included the poor water solubility on the one hand and the limited penetration of the compounds through membranes into the cells on the other hand. These drawbacks were mainly solved by the recently published synthesis of amphiphilic organoselenium and organotellurium compounds with an anionic head group and different hydrophobic tail lengths [13] and [18]. In these studies, it turned out that the selenium compounds were less cytotoxic than the corresponding tellurium compounds. Yet at the time, the intracellular process responsible for this activity remained mostly speculative. We, therefore, selected the most active tellurium compound DP41 to study its influence on some of the most relevant cellular signaling events. We found that the organotellurium compound DP41 induced the production of reactive oxygen species $O_2^{\cdot -}$, which was prevented by the simultaneous application of ascorbic acid. In contrast, the corresponding organoselenium compound DP31 failed to induce $O_2^{\cdot -}$ radical production. Thus, the organotellurium compound DP41 is more redox active in cancer cells than in the corresponding organoselenium compound DP31, which supports previous findings [18]. Based on these results, we decided to analyze the cellular signaling pathways, which are triggered by DP41. Due to the fact that DP41 induced the production of reactive oxygen species, it was not surprising that DP41 also activated the Keap1–Nrf2 pathway, which is the major regulator of the cytoprotective response to endogenous and exogenous stresses caused by ROS and electrophiles [25]. Nrf2 is a transcription factor that binds to the antioxidant response element (ARE) in the regulatory regions of target genes. One of the Nrf2 target genes is heme oxygenase1 (*HO-1*), whose protein was here found to be up-regulated as well after treatment of HCT116 cells with DP41. Gene transcription of HO-1 is inducible

by a broad spectrum of stimuli. Such agents include a large number of pharmacological agents as well as heat shock and other forms of extracellular and intracellular stresses [26]. A number of studies have demonstrated that HO-1 can confer protective *i.e.* anti-apoptotic and anti-proliferative effects on various cellular systems, where the underlying mechanisms, however, have not been completely elucidated. Yet, interestingly, the ER stress signaling pathway can also activate an antioxidant program by preferentially inducing the expression of the mRNA encoding ATF4 and by phosphorylation of Nrf2 [27]. Furthermore, Nrf2 activation has been implicated in the promotion of cell survival following ER stress [28]. Interestingly, we also observed an induction of the ER signaling pathway by an elevated level of phosphorylated eIF2α and an elevated level of ATF4 which is followed by an activation of CHOP. In mice liver, it has been shown that CHOP expression in Nrf2 deficient cells is constitutively higher than in wild-type cells, whereas, Nrf2 over-expression attenuates CHOP accumulation during ER stress [29]. It is also known that the ATF4 gene product binds to the amino acid response element (AARE) in the CHOP promoter after severe ER stress and activates CHOP transcription. Induction of CHOP is reported to be essential for the apoptotic response after extended ER stress [30]. According to our present results, HCT116 cells start to go into apoptosis after treatment with DP41. Thus, ER stress induced by DP41 on the one hand seems to be so severe that the antioxidant mechanism leading to a HO-1 mediated down-regulation of CHOP resulting in cell survival fails in the cells, while the pro-apoptotic ER stress signaling *via* p-eIF2α/ATF4 and CHOP activation dominates leading to apoptosis on the other hand.

All of the experiments discussed above were performed with HCT116 colon carcinoma cells. It was therefore a very interesting observation that normal ARPE-19 cells did not respond with an increase in the level of $O_2^{\cdot -}$ radicals and also did not induce apoptosis when subjected to DP41 under the same experimental conditions as

with HCT116 cells. Thus, we conclude that normal cells are more resistant to the organotellurium compound DP41 compared to cancer cells. This resistance is probably due to the fact that normal cells do not respond with an increased level of ROS when treated with DP41, or alternatively, keep such an increase under control, for instance by a strong antioxidant response. It has been shown earlier that red blood cells were comparably lysed by the organoselenium and by the organotellurium compound which seems to be independent from the redox activity of the compound and is more likely due to the amphiphilic character of these compounds which is similar to that of sodium dodecylsulfate [18]. HCT116 cells and also ARPE-19 cells are clearly resistant to this lytic function. The fact that cancer cells go into apoptosis and normal cells are apparently resistant to treatment with DP41 might indicate a future potential application of this organotellurium compound in cancer therapy.

2.2.6. Acknowledgement

The authors acknowledge financial support from the Saarland University and the Landesforschungsförderungsprogramm of the Saarland (T/1-14.2.1.1.-LFFP 12/23). We also thank Claudia Götz for her helpful comments.

2.2.7. References

[1] E. Block, Garlic and Other Alliums, The Royal Society of Chemistry, Cambridge, 2010.

[2] U. Munchberg, A. Anwar, S. Mecklenburg, C. Jacob, Polysulfides as biologically active ingredients of garlic, Org. Biomol. Chem. 5 (2007) 1505–1518.

[3] C. Jacob, A. Anwar, The chemistry behind redox regulation with a focus on sulphur redox systems, Physiol. Plant. 133 (2008) 469–480.

[4] M. Corzo-Martinez, N. Corzo, M. Villamiel, Biological properties of onions and garlic, Trends Food Sci. Technol. 18 (2007) 609–625.

[5] M. Iciek, I. Kwiecien, L. Wlodek, Biological properties of garlic and garlic-derived organosulfur compounds, Environ. Mol. Mutagen. 50 (2009) 247–265.

[6] J.A. Milner, Mechanisms by which garlic and allyl sulfur compounds suppress carcinogen bioactivation. Garlic and carcinogenesis, Adv. Exp. Med. Biol. 492 (2001) 69–81.

[7] Y. Shukla, N. Kalra, Cancer chemoprevention with garlic and its constituents, Cancer Lett. 247 (2007) 167–181.

[8] M. Bodnar, P. Konieczka, J. Namiesnik, The properties, functions, and use of selenium compounds in living organisms, J. Environ. Sci. Health C. Environ. Carcinog. Ecotoxicol. Rev. 30 (2012) 225–252.

[9] S.E. Ramadan, A.A. Razak, A.M. Ragab, M. el-Meleigy, Incorporation of tellurium into amino acids and proteins in a tellurium-tolerant fungi, Biol. Trace Elem. Res. 20 (1989) 225–232.

[10] G. Mugesh, W.W. du Mont, H. Sies, Chemistry of biologically important syntheticorganoselenium compounds, Chem. Rev. 101 (2001) 2125–2179.

[11] D. Zannoni, F. Borsetti, J.J. Harrison, R.J. Turner, The bacterial response to the chalcogen metalloids Se and Te, Adv. Microb. Physiol. 53 (2008) 1–72.

[12] E.R. Tiekink, Therapeutic potential of selenium and tellurium compounds: opportunities yet unrealised, Dalton Trans. 41 (2012) 6390–6395.

[13] C. Jacob, G.E. Arteel, T. Kanda, L. Engman, H. Sies, Water-soluble organotellurium compounds: catalytic protection against peroxynitrite and release of zinc from metallothionein, Chem. Res. Toxicol. 13 (2000) 3–9.

[14] F. Yu, P. Li, B. Wang, K. Han, Reversible near-infrared fluorescent probe introducing tellurium to mimetic glutathione peroxidase for monitoring the redox cycles between peroxynitrite and glutathione in vivo, J. Am. Chem. Soc. 135 (2013) 7674–7680.

[15] Y. Koide, M. Kawaguchi, Y. Urano, K. Hanaoka, T. Komatsu, M. Abo, T. Terai, T. Nagano, A reversible near-infrared fluorescence probe for reactive oxygen species based on Te-rhodamine, Chem. Commun. (Camb.) 48 (2012) 3091–3093.

[16] S.P. Ebert, B. Wetzel, R.L. Myette, G. Conseil, S.P. Cole, G.A. Sawada, T.W. Loo, M.C. Bartlett, D.M. Clarke, M.R. Detty, Chalcogenopyrylium compounds as modulators of the ATP-binding cassette transporters P-glycoprotein (P-gp/ABCB1) and multidrug resistance protein 1 (MRP1/ABCC1), J. Med. Chem. 55 (2012) 4683–4699.

[17] R.L. Myette, G. Conseil, S.P. Ebert, B. Wetzel, M.R. Detty, S.P. Cole, Chalcogenopyrylium dyes as differential modulators of organic anion transport by multidrug resistance protein 1 (MRP1), MRP2, and MRP4, Drug Metab. Dispos. 41 (2013) 1231–1239.

[18] P. Du, U. Viswanathan, K. Kairan, T. Buric, N.E.B. Saidu, Z. Xu, B. Hanf, I. Bazukyan, A. Trchounian, F. Hannemann, I. Bernhardt, T. Burkholz, B. Diesel, A. Kiemer, K.H. Schäfer, M. Montenarh, G. Kirsch, C. Jacob, Synthesis of amphiphilic, chalcogenbased redox modulators with in vitro cytotoxic activity against cancer cells, macrophages and microbes, MedChemComm 5 (2014) 25–31.

[19] N.K. Zenkov, E.B. Menshchikova, V.O. Tkachev, Keap1/Nrf2/ARE redox-sensitive signaling system as a pharmacological target, Biochemistry (Mosc) 78 (2013) 19–36.

[20] M. Bauer, K. Huse, U. Settmacher, R.A. Claus, The heme oxygenase–carbon monoxide system: regulation and role in stress response and organ failure, Intensive CareMed. 34 (2008) 640–648.

[21] A. Higa, E. Chevet, Redox signaling loops in the unfolded protein response, Cell. Signal. 24 (2012) 1548–1555.

[22] H.P. Harding, Y. Zhang, H. Zeng, I. Novoa, P.D. Lu,M. Calfon, N. Sadri, C. Yun, B. Popko, R. Paules, D.F. Stojdl, J.C. Bell, T. Hettmann, J.M. Leiden, D. Ron, An integrated stress response regulates amino acid metabolism and resistance to oxidative stress, Mol. Cell 11 (2003) 619–633.

[23] S. Oyadomari, M. Mori, Roles of CHOP/GADD153 in endoplasmic reticulum stress, Cell Death Differ. 11 (2004) 381–389.

[24] I. Tabas, D. Ron, Integrating the mechanisms of apoptosis induced by endoplasmic reticulum stress, Nat. Cell Biol. 13 (2011) 184–190.

[25] E. Kansanen, H.K. Jyrkkanen, A.L. Levonen, Activation of stress signaling pathways by electrophilic oxidized and nitrated lipids, Free Radic. Biol. Med. 52 (2012) 973–982.

[26] S.W. Ryter, J. Alam, A.M. Choi, Heme oxygenase-1/carbon monoxide: from basic science to therapeutic applications, Physiol. Rev. 86 (2006) 583–650.

[27] S.B. Cullinan, J.A. Diehl, Coordination of ER and oxidative stress signaling: the PERK/Nrf2 signaling pathway, Int. J. Biochem. Cell Biol. 38 (2006) 317–332.

[28] S.B. Cullinan, J.A. Diehl, PERK-dependent activation of Nrf2 contributes to redox homeostasis and cell survival following endoplasmic reticulum stress, J. Biol. Chem. 279 (2004) 20108–20117.

[29] S. Nair, C. Xu, G. Shen, V. Hebbar, A. Gopalakrishnan, R. Hu, M.R. Jain, C. Liew, J.Y. Chan, A.N. Kong, Toxicogenomics of endoplasmic reticulum stress inducer tunicamycin in the small intestine and liver of Nrf2 knockout and C57BL/6J mice, Toxicol. Lett. 168 (2007) 21–39.

[30] I. Kim, W. Xu, J.C. Reed, Cell death and endoplasmic reticulum stress: disease relevance and therapeutic opportunities, Nat. Rev. Drug Discov. 7 (2008) 1013–1030.

2.3. Publication 3

Synthesis of amphiphilic seleninic acid derivatives with considerable activity against cellular membranes and certain pathogenic microbes

Peng Du, Uma M. Viswanathan, Zhanjie Xu, Hadi Ebrahimnejad, Benjamin Hanf, Torsten Burkholz, Marc Schneider, Ingolf Bernhardt, Gilbert Kirsch, Claus Jacob

This manuscript was published as an article in the following Journal:

Journal of Hazardous Materials 269 (2014) 74–82

DOI: 10.1016/j.jhazmat.2014.01.014

2.3.1. Abstract

Selenium compounds play a major role in Biology, where they are often associated with pronounced antioxidant activity or toxicity. Whilst most selenium compounds are not necessarily hazardous, their often selective cytotoxicity is interesting from a biochemical and pharmaceutical perspective. We have synthesized a series of amphiphilic molecules which combine a hydrophilic seleninic acid head group – which at the same time serves as thiol-specific warhead – with a hydrophobic tail. These molecules possess a surface activity similar to the one of SDS, yet their biological activity seems to exceed by far the one of a simple surfactant (e.g. SDS) or seleninic acid (e.g. phenyl seleninic acid). Such compounds effectively haemolyse Red Blood Cells and exhibit pronounced activity against *Saccharomyces cerevisiae*. From a chemical perspective, the seleninic warheads are likely to attack crucial cysteine proteins of the cellular thiolstat.

2.3.2. Introduction

In Biology, redox active Group 16 compounds are often able to modulate the intracellular redox balance of living cells and hence play a major role in biological processes, medicine and drug development [1–6]. Nonetheless, such compounds are not outrightly hazardous but often possess a certain selectivity. Their inherent (cyto-)toxicity may even be used to single out and selectively kill certain target cells. For instance, naturally occurring sulfur-based pro-oxidants, such as allicin from garlic, effectively kill various microorganisms and also attack cancer cells fairly selectively. Certain selenium and tellurium compounds are also effective against a range of cancer cells in cell culture, animal models and in patient-derived materials, although this kind of selective cytotoxicity is not yet fully understood [5–9]. The circumstance that such chalcogen-based agents are effective, yet also selective cytotoxic agents is probably the result of the specific reactivity of these agents towards the thiol groups found in cysteine-containing proteins. The latter become oxidized in the process and hence trigger an appropriate pro-apoptotic signal [10-12]. Indeed, a selective attack on the intracellular 'thiolstat' with subsequent apoptosis of cells with an impaired intracellular redox balance, such as diverse cancer cells, holds considerable promise, as normal cells seem to be less affected [10-13].

The last decade has therefore witnessed a growing interest in redox modulation and novel redox modulating substances, with many selenium agents at the forefront of these developments [14]. Selenium compounds generally are more reactive and hence active than their sulfur analogues, yet are less hazardous and toxic than the tellurium ones. Nonetheless, selenium compounds cannot be employed in biological systems easily due to often unfavourable physico-chemical properties, low bioavailability and the fact that such compounds tend to act 'alone', as single molecules.

We have therefore synthesized a novel class of bifunctional agents comprised of a biologically active seleninic acid moiety embedded in an overall amphiphilic structure. The latter should endow such compounds with additional properties, such as good solubility and permeability through membranes, and hence improve handling and biological activity (Fig. 1). Furthermore, such molecules can aggregate (*e.g.* in form of micelles) or attach to membranes and proteins, and hence may show synergistic or collective (re-)activities when compared to their monomeric forms. Such synergy has been seen already in the case of sulfur, selenium and tellurium nanoparticles [15-17].

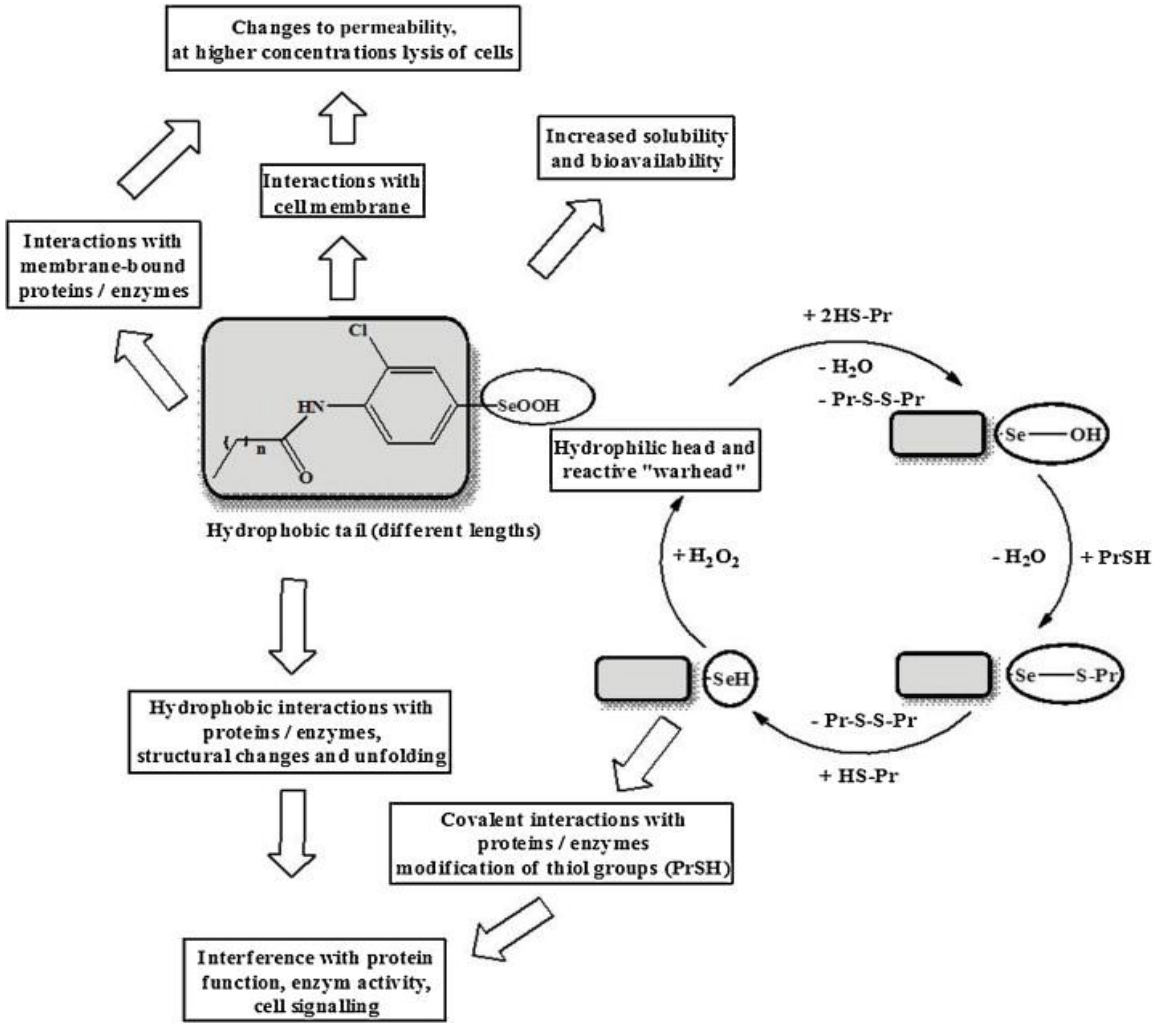

Fig 1*. Design and reactivity of amphiphilic seleninic acids which combine redox modulating properties with the ability to form aggregates (e.g. micelles), and to interact with membranes and (hydrophobic parts) of proteins. Some of the expected biological activities are highlighted.*

Whilst some amphiphilic selenium-containing agents have been reported before, such compounds had to rely on complex 'head' and 'tail' groups or on co-micellation [6] and [17]. In order to address this apparent lack of suitable molecules available, we have recently reported the synthesis and biological activity of a series of selenium- and tellurium-containing surfactants based on a hydrophilic sulfate head group [18]. The synthetic approach used by us at the time (*i.e.* a multi-step synthesis including an aggressive *O*-sulfation step) has been rather cumbersome, however, and marred by overall low yields, and difficulties to apply it to a wider range of structures. Importantly, *O*-sulfation has been achieved with the use of chlorosulfonic acid, and this final step required to introduce the hydrophilic head group can lead to an overall damage and subsequent instability of the molecule in question (including hydrolysis of the sulfate head group). Indeed, the use of common hydrophilic head groups, such as a sulfate, phosphate or ammonium group, poses certain challenges as far as their introduction and subsequent chemical stability are concerned (carboxylic acids are easier to use but often of insufficient hydrophilicity) [19-22].

As part of this study, we have therefore explored the use of a seleninic acid as 'head' group as elegant alternative to conventional approaches, hence removing the need for a separate hydrophilic head and, at the same time, endowing the head with considerable (thiol-)specific chemical reactivity (Fig. 1). Indeed, while seleninic acids have mostly been ignored in biological selenium chemistry in the past, they represent the ultimate thiol-specific cysteine-modifying agent which reacts with and hence

modifies several thiol groups and also turns catalytic once it reaches the selenylsulfide (RSeSR') or selenol (RSeH) oxidation state (Fig. 1) [23-25].

2.3.3. Experimental

2.3.3.1. *General methods for synthetic chemistry*

All starting materials and solvents used were purchased from Acros Organic (Geel, Belgium), Alfa Aesar (Karlsruhe, Germany) or Sigma Aldrich (Steinheim, Germany) as reagent grade and were used without further purification. Melting points were determined with a ThermoFisher apparatus and are uncorrected. NMR spectra were recorded with a Bruker AC 250 MHz spectrometer for ^{1}H and ^{13}C. ^{77}Se spectra were measured with a Bruker Avance 500 with 500 MHz in $CDCl_3$ or DMSO-d_6. All chemical shifts are reported in parts per million (ppm). MS spectra were recorded on an Agilent Technologies GC-MS instrument equipped with a 7683 injector, 6890 N gas chromatograph and a 5973 mass selective detector. The mass spectrometer was operated in EI mode at 70 eV, and MS spectra were recorded from *m*/*z* 50 to 650. All reactions were routinely checked by thin layer chromatography (TLC) analysis on an Alugram SIL G/UV254 plate (Macherey-Nagel) with spots visualized by UV light.

2.3.3.2. *Synthesis of 4-selenocyanatobenzenamine*

4-Selenocyanatobenzenamine was synthesized via a known procedure, according to Kachanov et al. and Plano et al. [26] and [27]. Briefly, selenium dioxide (36 mmol) was added to a solution of malononitrile (13 mmol) in DMSO (15 ml) at 0 ℃. The mixture was stirred at 0 ℃ for 30 min and the colour of the mixture subsequently

changed to dark red. Then, the reaction mixture was poured into 100 ml of cold water and the colour of the mixture instantaneously changed from red to yellow. The resulting precipitate was filtered and dried overnight. Then 2.5 g of the residue was suspended in 20 ml DMSO and aniline (18 mmol) was added. The mixture was stirred for 60 min at room temperature. After this time the reaction mixture was poured into water (150 ml) with stirring. The precipitate was filtered, washed with water and dried at room temperature overnight. The isolated solid was purified by recrystallization in isopropanol.

2.3.3.2.1. 4-Selenocyanatobenzenamine

Yield: 59%; colourless solid; mp 88 ℃; ^{1}H NMR (250 MHz, $CDCl_3$) δ 7.32–7.35 (m, 2H, benzene protons), 6.55–6.58 (m, 2H, benzene protons), 5.65 (bs, 2H, J = 6.5 Hz, $–NH_2$) ppm; ^{13}C NMR (62.5 MHz, $CDCl_3$) δ 150.62, 136.35 (2C), 114.97 (2C), 105.35, 105.03 ppm; HRMS (ESI) $[M + H]^+$ $C_7H_7N_2Se$ calc. 198.9762, found 198.9769.

2.3.3.2.2. General procedure for the synthesis of *N*-(4-selenocyanatophenyl)-alkylamide

The appropriate alkyl acid chloride (2 mmol) was added to a solution of 4-selenocyanatobenzenamine (2.2 mmol) in 50 ml of pyridine, the mixture was stirred at 110 ℃ for 1 h. After this time 30 ml of cold water was added, the reaction mixture was neutralized by 5 M HCl. The solution was extracted with ethyl acetate (3 × 40 ml), the organic layers were separated and washed with 5 M HCl (3 × 30 ml), and subsequently dried with $MgSO_4$. The solvent was removed under vacuum and the residue was washed with petrol ether (3 × 20 ml), and dried at room temperature overnight.

2.3.3.2.2.1. *N*-(4-selenocyanatophenyl)octanamide

Yield: 96%; colourless solid; mp 101 ℃; ^{1}H NMR (250 MHz, $CDCl_3$) δ 10.08 (bs, 1H, –NHCO–) 7.63 (s, 4H, benzene protons), 2.27–2.33 (t, 2H, J = 7.5 Hz, $–CH_2CO–$), 1.56 (m, 2H, $–CH_2CH_3$), 1.24–1.26 (s, 8H, $–(CH_2)_4CH_2CH_3$), 0.82–0.83 (m, 3H, $–CH_3$) ppm; ^{13}C NMR (62.5 MHz, $CDCl_3$) δ 171.68, 139.95, 134.69 (2C), 121.10 (2C), 115.07, 101.72, 37.78, 31.63, 29.16, 28.98, 25.42, 22.58, 14.03 ppm; ^{77}Se NMR (92.5 MHz, $CDCl_3$, dimethylselenide as reference δ 313.13 ppm); HRMS (ESI) $[M + H]^+$ $C_{15}H_{21}N_2OSe$ calcd. 325.0807, found 325.0814.

2.3.3.2.2.2. *N*-(4-selenocyanatophenyl)decanamide

Yield: 99%; colourless solid; mp 102 ℃; ^{1}H NMR (250 MHz, $CDCl_3$) δ 7.61 (s, 4H, benzene protons), 7.22 (bs, 1H, –NHCO–) 2.35–2.41 (t, 2H, J = 7.5 Hz, $–CH_2CO–$), 1.70–1.76 (m, 2H, –CH_2CH3), 1.27–1.33 (m, 12H, $–(CH_2)_6CH_2CH_3$), 0.85–0.90 (m, 3H, $–CH_3$) ppm; ^{13}C NMR (62.5 MHz, $CDCl_3$) δ 171.65, 139.93, 134.69 (2C), 121.08 (2C), 115.07, 101.70, 37.80, 31.83, 29.40, 29.33, 29.24, 29.21, 25.42, 22.64, 14.08 ppm; ^{77}Se NMR (92.5 MHz, $CDCl_3$, dimethylselenide as reference δ 320.71 ppm); HRMS (ESI) $[M + H]^+$ $C_{17}H_{25}N_2OSe$ calcd. 353.1125, found 353.1127.

2.3.3.2.2.3. *N*-(4-selenocyanatophenyl)dodecanamide

Yield: 98%; colourless solid; mp 109 ℃; ^{1}H NMR (250 MHz, $CDCl_3$) δ 7.51 (s, 4H, benzene protons), 7.29 (bs, 1H, –NHCO–), 2.34–2.40 (t, 2H, J = 7.5 Hz, $–CH_2CO–$), 1.63–1.72 (m, 2H, $–CH_2CH_3$), 1.22–1.32 (m, 16H, $–(CH_2)_8CH_2CH_3$), 0.85–0.88 (m, 3H, $–CH_3$) ppm; ^{13}C NMR (62.5 MHz, $CDCl_3$) δ 171.74, 139.98, 134.69 (2C), 121.11 (2C), 115.03, 101.77, 37.79, 31.88, 29.58, 29.45, 29.33 (2C), 29.31, 29.22, 25.43,

22.66, 14.10 ppm; ^{77}Se NMR (92.5 MHz, $CDCl_3$, dimethylselenide as reference δ 320.63 ppm); HRMS (ESI) $[M + H]^+$ $C_{19}H_{29}N_2OSe$ calcd. 381.1434, found 381.1440.

2.3.3.2.2.4. *N*-(4-selenocyanatophenyl)tetradecanamide

Yield: 97%; colourless solid; mp 106 ℃; ^{1}H NMR (250 MHz, $CDCl_3$) δ 7.60 (s, 4H, benzene protons), 7.32 (bs, 1H, –NHCO–), 2.34–2.40 (t, 2H, J = 7.5 Hz, $–CH_2CO–$), 1.69–1.75 (m, 2H, $–CH_2CH_3$), 1.25–1.32 (m, 20H, $–(CH_2)_{10}CH_2CH_3$), 0.85–0.90 (m, 3H, $–CH_3$) ppm; ^{13}C NMR (62.5 MHz, $CDCl_3$) δ 171.69, 139.95, 134.70 (2 C), 121.08 (2 C), 115.05, 101.75, 37.80, 31.90, 29.66 (2 C), 29.63 (2 C), 29.59, 29.45, 29.34, 29.22, 25.43, 22.67, 14.11 ppm; ^{77}Se NMR (92.5 MHz, $CDCl_3$, dimethylselenide as reference δ 320.64 ppm); HRMS (ESI) $[M + H]^+$ $C_{21}H_{33}N_2OSe$ calcd. 409.1747, found 409.1753.

2.3.3.2.2.5. *N*-(4-selenocyanatophenyl)palmitamide

Yield: 96%; colourless solid; mp 112 ℃; ^{1}H NMR (250 MHz, $CDCl_3$) δ 7.60 (s, 4H, benzene protons), 7.17 (bs, 1H –NHCO–), 2.34–2.40 (t, 2H, J = 7.5 Hz, $–CH_2CO–$), 1.70–1.76 (m, 2H, $–CH_2CH_3$), 1.23–1.34 (m, 24H, $–(CH_2)_{12}CH_2CH_3$), 0.86–0.91 (m, 3H, –CH3) ppm; ^{13}C NMR (62.5 MHz, $CDCl_3$) δ 171.64, 139.92, 134.70 (2C), 121.08 (2C), 115.09, 101.67, 37.81, 31.90, 29.67, 29.65, 29.64 (2C), 29.62 (2C), 29.59, 29.45, 29.34, 29.22, 25.42, 22.67, 14.10 ppm; ^{77}Se NMR (92.5 MHz, $CDCl_3$, dimethylselenide as reference δ 320.56 ppm); HRMS $[M + H]^+$ $C_{23}H_{37}N_2OSe$ calcd. 437.2049, found 437.2067.

2.3.3.2.3. General procedure for the synthesis of 3-chloro-4-alkylamidobenzeneseleninic acid

Sulfuryl chloride (SO_2Cl_2) (3.3 mmol) was added to a solution of *N*-(4-selenocyanatophenyl)-alkylamide (2 mmol) in 25 ml of chloroform and resulted in a yellow precipitate. The mixture was stirred under reflux for 30 min until a clear orange solution was formed. After this time the solvent was removed under vacuum. Then, 30 ml of cold water was added dropwise to the remaining oily mixture, and the resulting reaction mixture was stirred for further 20 min. 30 ml of cold water was added to the solution and the reaction mixture was neutralized with 5 M HCl. The mixture was washed with ethyl acetate (3 × 30 ml), the organic layers were separated and washed with 5 M HCl (3 × 30 ml), and subsequently dried with $MgSO_4$. The solvent was removed under vacuum and the residue was washed with petrol ether (3 × 20 ml). When the precipitate appeared, it was filtered, washed with ethyl acetate (3 × 20 ml), and dried overnight.

2.3.3.2.3.1. 3-Chloro-4-octanamidobenzeneseleninic acid (1**)**

Yield: 96%; colourless solid; mp 134 ℃; ^{1}H NMR (250 MHz, DMSO-d_6) δ 9.95 (bs, 1H, –NHCO–) 7.87–7.95 (m, 2H, benzene protons), 7.71–7.74 (m, 1H, benzene protons), 2.31–2.37 (t, 2H, J = 7.5 Hz, –$COCH_2$–), 1.55–1.58 (m, 2H, –CH_2CH_3), 1.25–1.27 (m, 8H,–$(CH_2)_4CH_2CH_3$), 0.82–0.85 (3H, m, –CH_3) ppm; ^{13}C NMR (62.5 MHz, DMSO-d_6) δ 171.81, 145.93, 137.74, 126.68, 126.25, 125.81, 125.03, 35.71, 31.13, 28.48, 28.34, 25.03, 22.00, 13.89 ppm; ^{77}Se NMR (92.5 MHz, DMSO-d_6, dimethylselenide as reference δ 1181.77 ppm); HRMS $[M + H]^+$ $C_{14}H_{21}ClNO_3Se$ calcd. 366.0362, found 366.0367.

2.3.3.2.3.2. 3-Chloro-4-decanamidobenzeneseleninic acid (2**)**

Yield: 95%; colourless solid; mp 141 ℃; ^{1}H NMR (250 MHz, DMSO-d_6) δ 9.63 (bs, 1H, –NHCO–) 7.86–7.95 (m, 2H, benzene protons), 7.70–7.74 (m, 1H, benzene

protons), 2.37–2.43 (t, 2H, J = 7.5 Hz, –$COCH_2$–), 1.55–1.61 (m, 2H, –CH_2CH_3), 1.23 (s, 12H, –$(CH_2)_6CH_2CH_3$), 0.86–0.81 (m, 3H, –CH_3); ^{13}C NMR (62.5 MHz, DMSO-d_6) δ 171.81, 145.90, 137.74, 126.69, 126.25, 125.81, 125.03, 35.71, 31.22, 28.85, 28.71, 28.61, 28.51, 25.02, 22.04. 13.90 ppm; ^{77}Se NMR (92.5 MHz, DMSO-d_6, dimethylselenide as reference δ 1181.75 ppm); HRMS $[M + H]^+$ $C_{16}H_{25}ClNO_3Se$ calcd. 394.0659, found 394.0681.

2.3.3.2.3.3. 3-Chloro-4-dodecanamidobenzeneseleninic acid (3)

Yield: 93%; colourless solid; mp 131 ℃; ^{1}H NMR (250 MHz, DMSO-d_6) δ 9.63 (bs, 1H, –NHCO–) 7.86–7.95 (m, 2H, benzene protons), 7.70–7.74 (m, 1H, benzene protons), 2.37–2.43 (t, 2H, J = 7.5 Hz, –$COCH_2$–), 1.55–1.61 (m, 2H, –CH_2CH_3), 1.24 (s, 16H, –$(CH_2)_8CH_3$), 0.81–0.86 (3H, m, –CH_3) ppm; ^{13}C NMR (62.5 MHz, DMSO-d_6) δ 171.82, 145.92, 137.73, 126.68, 126.27, 125.83, 125.03, 35.71, 31.23, 28.95, 28.93, 28.88, 28.70, 28.65, 28.50, 25.02, 22.04, 13.90 ppm; ^{77}Se NMR (92.5 MHz, DMSO-d_6, dimethylselenide as reference δ 1181.77 ppm); HRMS $[M + H]^+$ $C_{18}H_{29}ClNO_3Se$ calcd. 422.1001, found 422.0994.

2.3.3.2.3.4. 3-Chloro-4-tetradecanamidobenzeneseleninic acid (4)

Yield: 98%; colourless solid; mp 125 ℃; ^{1}H NMR (250 MHz, DMSO-d_6) δ 9.49 (bs, 1H, –NHCO–), 7.86–7.97 (m, 2H, benzene protons), 7.71–7.74 (m, 1H, benzene protons), 2.37–2.34 (t, 2H, J = 7.5 Hz, –$COCH_2$–), 1.57–1.62 (m, 2H, –CH_2CH_3), 1.24 (s, 20H, –$(CH_2)_{10}CH_2CH_3$), 0.82–0.87 (m, 3H, –CH_3) ppm; ^{13}C NMR (62.5 MHz, DMSO-d_6) δ 171.81, 145.92, 137.72, 126.67, 126.25, 125.83, 125.02, 35.70, 31.24, 29.00, 28.97 (2C), 28.95, 28.88, 28.70, 28.66, 28.51, 25.02, 22.04, 13.91 ppm; ^{77}Se NMR (92.5 MHz, DMSO-d_6, dimethylselenide as reference δ 1181.85 ppm); HRMS (ESI) $[M + H]^+$ $C_{20}H_{33}ClNO_3Se$ calcd. 450.1314, found 450.1307.

2.3.3.2.3.5. 3-Chloro-4-palmitamidobenzeneseleninic acid (5)

Yield: 99%; colourless solid; mp 116 °C; ^{1}H NMR (250 MHz, DMSO-d_6) δ 9.62 (bs, 1H, –NHCO–) 7.87–7.95 (m, 2H, benzene protons), 7.71–7.74 (m, 1H, benzene protons), 2.37–2.43 (t, 2H, J = 7.5 Hz, –$COCH_2$–), 1.55–1.58 (m, 2H, –CH_2CH_3), 1.24 (s, 24H, –$(CH_2)_{12}CH_3$), 0.81–0.86 (m, 3H, –CH_3) ppm; ^{13}C NMR (62.5 MHz, DMSO-d_6) δ 171.81, 137.14, 126.68, 126.23, 125.79, 125.02, 35.17, 31.24, 28.98 (2C), 28.95 (2C), 28.88 (2C), 28.70 (2C), 28.65 (2C), 28.51, 25.02, 22.04, 13.89 ppm; ^{77}Se NMR (92.5 MHz, DMSO-d_6), dimethylselenide as reference δ 1181.19 ppm); HRMS (ESI) $[M + H]^+$ $C_{22}H_{37}ClNO_3Se$ calcd. 478.1614, found 478.1620.

2.3.3.3. *Surface activity and critical micelle concentration (CMC) measurements*

Compounds **1**–**4** were dissolved in bidistilled water and the final concentrations used for this experiment were as follows: 0.025 mM, 0.25 mM, 0.5 mM, 1 mM, 5 mM and 10 mM. This experiment was carried out with a Krüss Schultensiometer K6 (Krüss GmbH, Hamburg) according to the manufacturer's instructions. Each experiment was carried out in triplicate, and each experiment was repeated on three separate occasions.

2.3.3.4. *Haemolysis assay and Ca^{2+}-uptake assay*

A standard method described in the literature was used for this experiment with some modifications [28-32]. Final concentrations of the compounds tested were: 1 μM, 10 μM, 100 μM and 1000 μM for haemolysis assay, and 3 μM for Ca^{2+}-uptake assay. RBCs were incubated with compounds tested for 10 min, and then analysed by FACS (FACSCalibur 4CS E4021, Becton and Dickinson and CellQuest software). Each experiment was carried out in triplicate, and each experiment was repeated on three

separate occasions. 1% DMSO was used as negative control. In the haemolysis assay, SDS was used as positive control. In the Ca^{2+}-uptake assay, the well-known calcium ionophore A23187 (abbreviated as A23) was used as positive control.

2.3.3.5. *Antifungal activity assay*

The inhibitory activity on the growth rate of *Saccharomyces cerevisiae* of compounds tested was evaluated based on the CLSI (formerly NCCLS) guidelines outlined in the M27-A2 protocol with modifications [33]. Absorbance changes were monitored continuously on a spectrophotometer (595 nm) (CARY 50*Bio* UV-Visible spectrophotometer, Varian Inc.) against the blank – DMSO (0.5%) in YPD broth – during the time until reaching the stationary phase over a period of 24 h. *S. cerevisiae* was exposed to compounds tested at the concentrations between 1 μM and 1 mM (all in 0.5% DMSO). DMSO (0.5%) and miconazole (100 μM) were used as the negative and positive controls, respectively.

2.3.4. Results

In order to investigate seleninic acid based-amphiphilic molecules, we have developed a new synthetic strategy to synthesize five new seleninic acids, whose surface activity and ability to lyse red blood cells (RBCs) has been determined. These interactions translate into a significant antimicrobial activity, as illustrated for *Saccharomyces cerevisiae.* This pronounced biological activity appears to be the result of a synergism between the reactivity of the seleninic acid and amphiphilicity of the molecule, hence exceeding the 'singular' activities associated with a simple surfactant or a simple seleninic acid.

2.3.4.1. *Chemical synthesis of new seleninic acids*

As seleninic acids are often fairly reactive and hence unstable (*e.g.* in the presence of nucleophiles such as thiols, selenols), the synthesis of appropriate derivatives is not always straight forward and requires specific considerations, especially when planning the reaction sequence and attempting to diversify the structures. We have, for instance, been unable to generate the seleninic acid forms of our compounds via the 'classic' synthetic avenue often used for simple seleninic acids, *i.e.* by oxidation of diselenides with hydrogen peroxide. Furthermore, selenium chemistry also demands certain experimental skills. To overcome these obstacles, we have developed a simple, yet effective approach for the synthesis of suitable amphiphilic derivatives based on the initial synthesis of a key amine-derivative of phenyl selenocyanate, which allows subsequent coupling of various hydrophobic tails and final oxidation of the resulting selenocyanates to seleninic acids (Fig. 2) [34]. This method intentionally keeps the seleninic acid 'under wrap' until the very last step of the synthesis, and hence provides considerable flexibility earlier on in the reaction sequence, for instance when it comes to the use of functional groups and reagents. Interestingly, it also adds an additional chlorine substituent to the phenyl ring which may be modified further later on. This method has enabled us to synthesize different seleninic acids with comparable ease and in overall yields of around 55%.

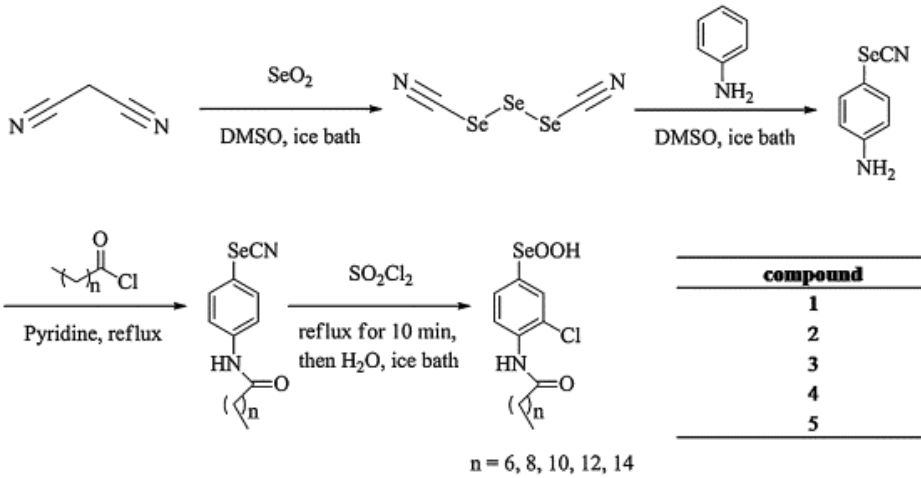

compound	n
1	6
2	8
3	10
4	12
5	14

Fig 2. *Synthesis of amphiphilic seleninic acids by initial synthesis of 4-selenocyanatobenzenamine and subsequent coupling of a hydrophobic tail and oxidation of the selenocyanate to seleninic acid.*

2.3.4.2. *Surface activity in the context of self-assembly and interactions with cell membranes*

One of the key properties associated with the new seleninic acids – besides their redox activity – is their expected amphiphilicity, which should allow such molecules to interact effectively with various biological targets, including membranes and (hydrophobic parts of) proteins. Here, the relevant physical property is surface activity, and the key quantifier is the critical micelle concentration (CMC), which has been determined using surface tensiometry [35]. A representative example of such a CMC determination is shown in Fig. 3, and the CMC values measured for the new compounds are summarized in Table 1. To the best of our knowledge, these are the first CMC values reported for seleninic acid (head) based amphiphiles. Indeed, compounds 2–4 form micelles with CMC values (2 mM for 2, 1.2 mM for 3, 1.1 mM for 4) similar to the one obtained for SDS under the same conditions (0.9 mM, which is close to its well-known literature value, *i.e.* 0.8 mM at 25 ℃). These values are also in the range of the CMC values reported by us recently for selenium- and tellurium-based surfactants bearing a sulfate head group [18]. Not surprisingly, the CMC values of 2, 3 and 4 decrease with increasing hydrocarbon-chain (‘tail’) length, although this decrease is small and within the experimental error of the surface tension method employed. While 5, the most hydrophobic compound with the longest

'tail', was not soluble enough in aqueous solution to produce micelles, 1 was too hydrophilic and did not self-assemble at concentrations up to 10 mM under the experimental conditions used.

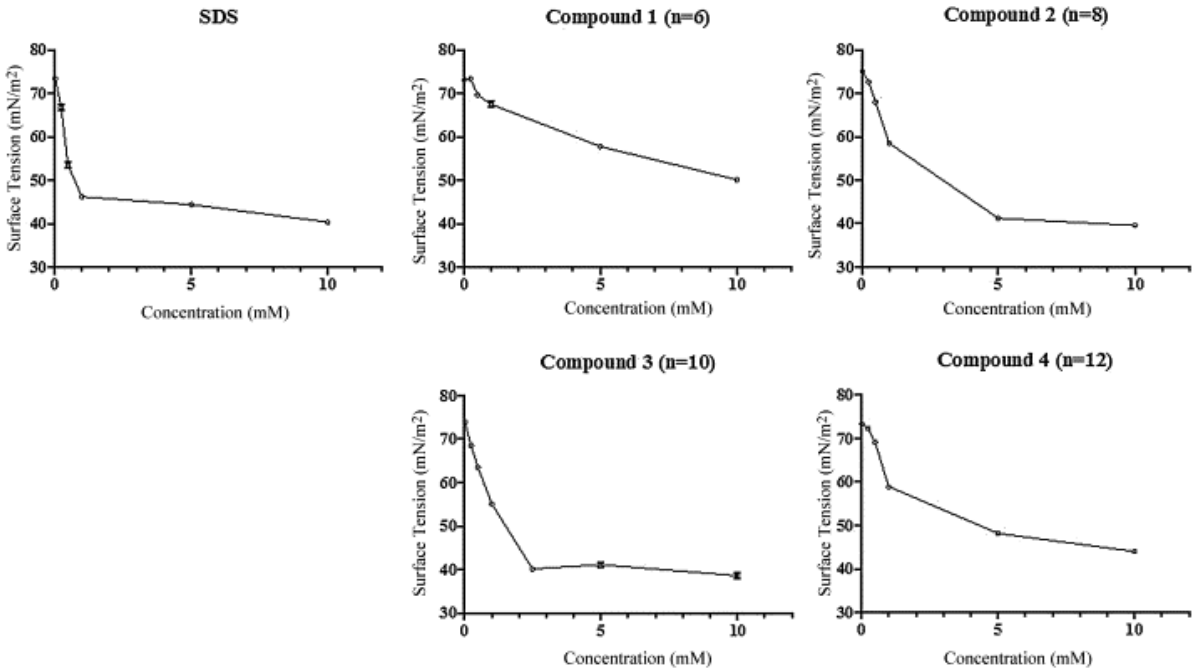

Fig 3. *Determination of surface activity and micellation behaviour of compounds* ***1***–***4*** *using SDS as positive control. CMC values are summarized in Table 1.*

Compound	n	Yield (%)	CMC (mM)	lysis (%) of RBCs at 100 µM	IC50 (µM) *S. cerevisiae*
SDS	-	-	**0.9**	**9.5 ±1.3**	**> 1000**
PSA	-	-	-	**2.83 ±1.4**	**> 1000**
1	**6**	**54**	-	**9.6 ±0.2**	**> 1000**
2	**8**	**55**	**2.0**	**33.9 ±2.8**	**147.9 ±7.6**
3	**10**	**53**	**1.2**	**74.5 ±2.2**	**281.8 ±8.4**
4	**12**	**56**	**1.1**	**86.8 ±3.3**	**295.1 ±6.2**
5	**14**	**57**	-	-	-

***Table 1**. Summary of the amphiphilic seleninic acids synthesized, their hydrophobic tail lengths n (see Fig. 1), synthetic yields, CMC, activity against RBCs and the model fungus S. cerevisiae. See text for more details*

After identifying compounds 2, 3 and 4 as the most promising candidates for further investigation, their ability to interact with cellular membranes was studied in a simple yet highly informative haemolysis assay based on RBCs. This assay is superior to simple liposome-based screens as it recruits real human cells with an adequately complex membrane, yet also avoids the pitfalls of using normal cells, which may show secondary membrane effects as a result of complex (intra-)cellular signaling [28], [29], [31], and [36-38]. In this assay, compounds 2, 3 and 4 are able to interact with and ultimately damage the RBCs membranes, resulting in significant haemolysis (Fig. 4a and b). The latter is concentration-dependent and also reflects the hydrocarbon chain length - and hence the CMC values. Compound 4, with the longest 'tail' and also the lowest CMC, is the most potent in this assay, haemolysing over 50% of RBCs at a concentration as low as 10 μM. As predictable by the CMC values, other compounds exhibit lower activity: Compound 2 only shows significant activity at concentrations of 100 μM or higher and 1, which was tested as a control, is virtually inactive. Similar to 1, phenyl seleninic acid, a compound without any hydrophobic tail, is also inactive. In contrast, SDS, used here as a benchmark anionic surfactant, only causes haemolysis when applied at a concentration of 1 mM. While SDS is therefore active at higher concentrations (above its CMC), it is considerably (*i.e.* around 100 times) less so than comparable seleninic acid compounds, such as 4.

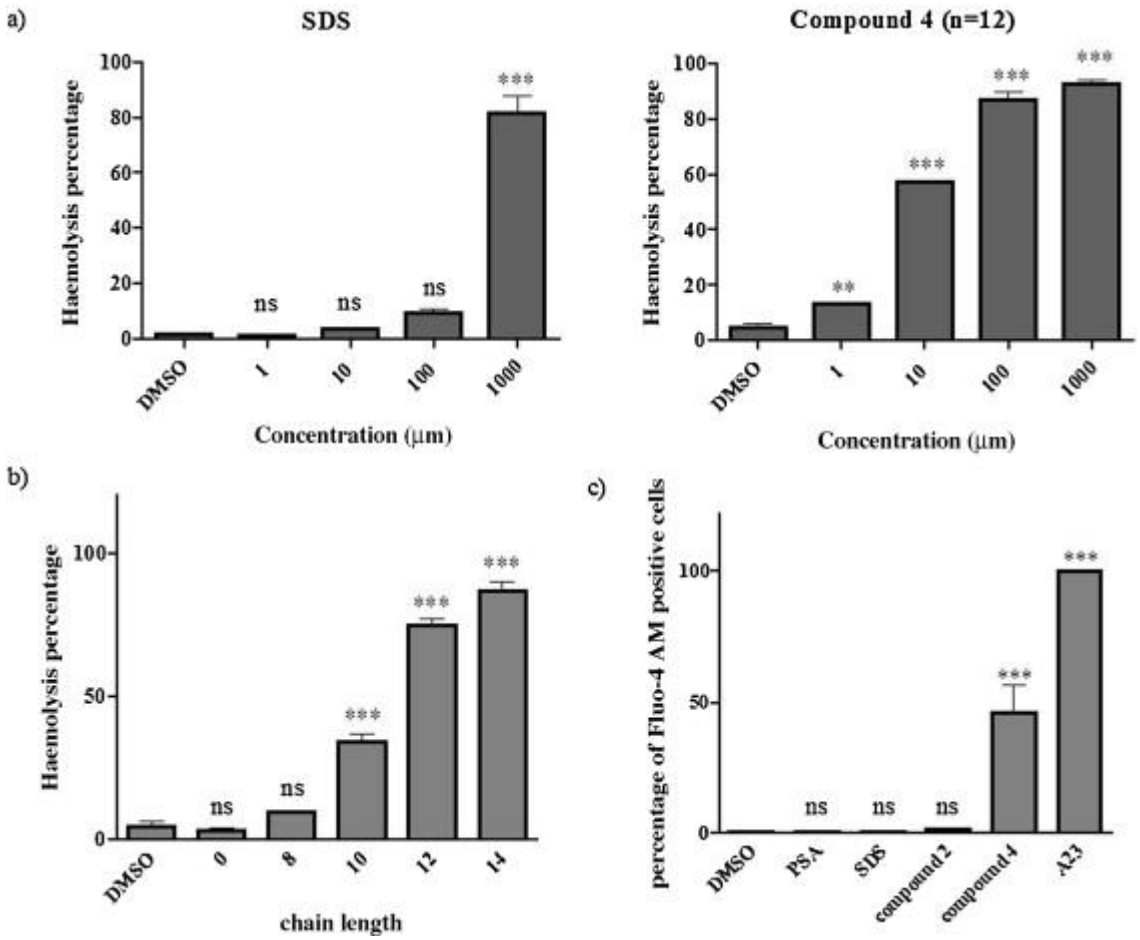

Fig 4*. Interactions of* ***2****,* ***3*** *and* ***4*** *with the cellular membrane of RBCs. At higher concentrations, these compounds behave like detergents and cause concentration-dependent haemolysis of RBCs, as illustrated for* ***4*** *(Part a). Haemolysis also depends on the structure of the molecule and seems to increase with increasing tail length (and decreasing CMC), as shown for the different compounds and their reference molecules at 100 µM (Part b, please note that chain length refers to total number of carbon atoms in the 'tail' and hence equals n + 2; n stated in Fig. 1). At lower concentrations, membrane effects are more subtle and include an increase of* Ca^{2+} *influx into the cells, as measured with Fluo-4 AM as* Ca^{2+} *specific fluorescent stain. A23187 (A23) was used as positive control. (Part c) Data are depicted as mean ± SD (n = 3).*

One way ANOVA (Dunnett) is used for statistical analysis. $^{*}p < 0.05$, $^{**}p < 0.01$ *or* $^{***}p < 0.001$.

To investigate this effect on cell membranes further, we have employed an assay which monitors changes to the RBCs membrane permeability by measuring the flux of Ca^{2+} ions. As expected, compounds able to seriously disrupt the RBCs membranes at higher concentrations are also able to interfere more subtly with membrane processes when used in lower concentrations. At a concentration of just 3 μM, 4 causes a significant influx of Ca^{2+} ions into the cell, whilst phenyl seleninic acid, 2 and SDS are virtually inactive under those conditions (Fig. 4c).

2.3.4.3. *Activity against S. cervisiae*

After a brief investigation of the interactions of such compounds with the cell membrane of RBCs, a whole cell system has been used to study effects on a more complex cellular organism. These results obtained with the model organism *S. cerevisiae*, albeit clearly of a preliminary nature and limited to just one strain, indicate that compounds 2, 3 and 4 are rather active against this fungus at concentrations from 100 μM onwards, *i.e.* at similar concentrations compared to the RBCs assay (Fig. 5). As shown in Fig. 5 for compounds at a concentration of 300 μM, the activity of 2 under those conditions is comparable to the one of miconazole, a well-known fungicide used here at a concentration of 100 μM as benchmark control. In fact, the most active compounds show a concentration dependent activity and an IC_{50} value of around 150 μM for 2 and 300 μM for 3 and 4, respectively (Table 1). As before, these findings are quite instructive, as neither phenyl seleninic acid nor SDS were active at these concentrations. In fact, those benchmark compounds, which either lack amphiphilicity or a redox centre, were inactive up to a concentration of 1 mM, highlighting once more the importance of a synergy between the redox active

seleninic acid and the amphiphilic character of the molecule. As far as practical applications of such selenium compounds are concerned, it should be mentioned that the compounds discussed here were not particularly hazardous against proliferating human cells, such as RAW 264.7 cells, where no notable cytotoxicity was found at these concentrations (Jacob group, unpublished data).

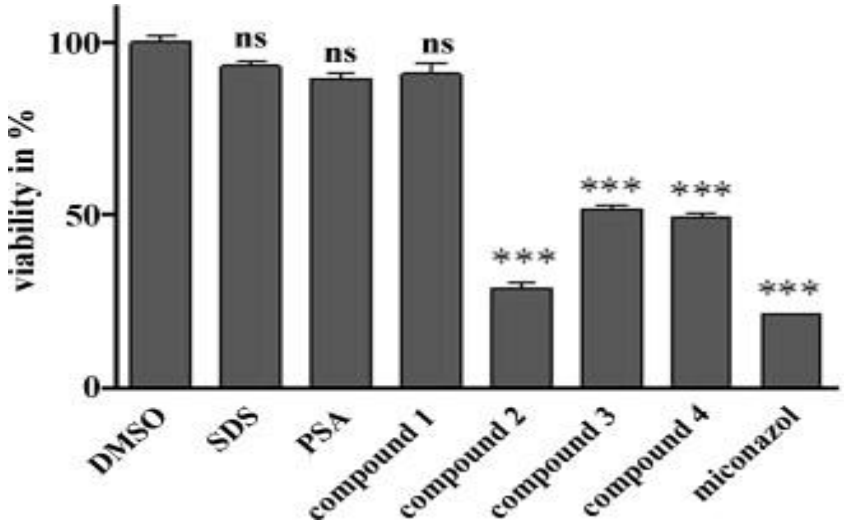

Fig 5*. Compounds* ***2****,* ***3*** *and* ***4*** *inhibit viability of S. cerevisiae after 10 h incubation at 300 μM. While phenyl seleninic acid (PSA),* ***1*** *and SDS are not active at a concentration of 300 μM,* ***2****,* ***3*** *and* ***4*** *are fairly active at this concentration. Compound* ***2*** *appears to be the most active compound in this assay with pronounced activity, killing almost 70% of fungal cells when employed at this concentration. The well-known antifungal agent miconazole (100 μM) is used as reference. Data are depicted as mean ± SD. One way ANOVA (Dunnett) is used for statistical analysis.* $^{*}p < 0.05$, $^{**}p < 0.01$ *or* $^{***}p < 0.001$.

2.3.5. Discussion

Taken together, our results confirm that it is fairly straight forward to synthesize amphiphilic seleninic acids with biological activities superior to the ones observed for simple seleninic acids or redox inactive surfactants. Here, the sequence of different synthetic steps needs to be planned and executed carefully in order to avoid the reaction of the seleninic acid with other functional groups in the molecule or reagents used (*e.g.* thiols). This potential problem is addressed by generating the seleninic acid in the final step of the synthesis. At the same time, structural diversity is achieved by introducing an acid chloride/amine coupling step which provides considerable flexibility as far as the structure and properties of the hydrophobic tail are concerned. Ultimately, the synthetic avenue we have mapped out means that the chemical synthesis of such seleninic acids is now comparably simple (with good yields of around 55%), yet also sufficiently flexible to construct a range of different seleninic acid-containing (amphiphilic) compounds. It is now possible, for instance, to synthesize different derivatives of our lead structures, and also to consider other coupling methods, *e.g.* involving hydroxyl instead of amine groups, as the resulting esters may possess pro-drug properties.

As the hydrophilicity of seleninic acids is comparable to the one of sulfinic acids, we have anticipated that some of the compounds synthesized are fairly soluble in aqueous media and also self-assemble. Indeed, we have found that seleninic acids with sufficiently long hydrocarbon tails are surface active, and compounds 2, 3 and 4 with hydrocarbon-chains of 10, 12 and 14 carbon atoms ($n + 2$ according to Fig. 1) possess amphiphilic properties comparable to the one of SDS. Not surprisingly, compounds with shorter ‘tails’ are fairly soluble in water and hence do not self-assemble under these conditions (*e.g.* compound 1), whilst compounds with longer ‘tails’ (*e.g.* compound 5) are not soluble enough. Whilst 2, 3 and 4 form micelles in clean

aqueous solutions, micellation itself is probably of minor importance in a more complex biological fluid, where micellation will be disrupted by the presence of salts, small molecules and larger biomolecules. Here, other interactions, such as the ones with the lipids and proteins of cellular membranes and (hydrophobic parts of) proteins, will probably dominate.

The results of the haemolysis assay support our idea of synergy, *i.e.* that seleninic acids are highly active biologically yet their simple chemical reactivity is not sufficient (as seen in the case of phenyl seleninic acid) and activity can be enhanced significantly by combining this reactivity with amphiphilicity (which on its own is also not sufficient, see SDS). In any case, the amphiphilic character of these compounds represents a considerable advantage, also in the context of pharmacokinetics (hydrophilic–lipophilic balance) and as far as interactions with cell membranes are concerned.

Indeed, 2, 3 and 4 interact strongly with the membrane of RCBs, where they seem to interfere with specific membrane processes, such as Ca^{2+} influx, when used at lower concentrations, and cause a severe disruption of membrane integrity resulting in haemolysis when used at higher concentrations. The influx of Ca^{2+} ions into RBCs, and its role(s) in subsequent intracellular processes, is clearly an important aspect, as many cellular processes are Ca^{2+} dependent (including the phospholipid scramblase, a key enzyme in RBCs). These processes need to be studied in more detail as part of future studies, for instance by analyzing – changes to – the distribution of phosphatidylserine within the cell membrane. Compound 4, the most active among the new compounds synthesized, shows such subtle effects at a concentration of just 3 μM, while haemolysis sets in at around 10 μM. Nonetheless, these interactions with the cell membrane are not solely due to the amphiphilic character of such molecules.

Compared to 4, the benchmark surfactant SDS was considerably less active, with haemolysis only pronounced at a concentration of 1 mM.

Similarly, selenium- and tellurium-containing surfactants bearing a sulfate head group are considerably less active, with haemolysis only becoming pronounced at concentrations of around 100 μM [18]. Here, one should note that such aryl-alkyl-selenides and tellurides are redox active, for instance as catalytic peroxidase mimics or radical generating sites, but cannot attach covalently to proteins and enzymes. The ability to form covalent selenium-sulfur or selenium-selenium bonds with cysteine and selenocysteine residues, respectively, is exclusive to the compounds reported here. This special reactivity may also contribute to the biological activity observed in this study.

Indeed, the presence of the seleninic acid warhead obviously contributes significantly to the activity of compounds such as 4. In fact, there seems to be a clear synergy between the seleninic acid-based redox centre and the overall amphiphilic nature of such compounds. Indeed, phenyl seleninic acid and SDS both are dramatically less active compared to 4 in the assays used as part of this study. Furthermore, many selenium-containing compounds have been tested by us and others in the past in similar assays, and the biological activities observed, such as antimicrobial activity, were usually only found when such compounds were used in the higher micromolar or low millimolar range [39-42].

Ultimately, it will be necessary to study the reasons behind the pronounced activity of such amphiphilic seleninic acids in more detail by employing a vast array of ‘intracellular diagnostics’ tools and cell-based assays. As an educated guess, it is possible that such molecules readily penetrate the cell membrane and hence enter the cell more efficiently compared to a simple seleninic acid or other selenium

compounds, even amphiphilic ones. It is also feasible that such agents become enriched in certain parts of the cell (*e.g.* at membranes, certain organelles), cluster together there and hence exhibit a concerted, cooperative chemical reactivity. Indeed, it is highly likely that such molecules become integrated into membranes and also attach to proteins. Then again, redox activity may also be important. It is known that seleninic acids react fast and effectively, yet also highly selectively with thiol groups present in most proteins. Ultimately, proteins particularly rich in (redox sensitive) cysteine residues may therefore form a prime target for such molecules. Such proteins would be particularly badly affected, though, as they would not only undergo widespread cysteine modifications but also structural damage caused by hydrophobic interactions and partial unfolding. The latter may even enhance covalent attacks further by laying bare some of the cysteine residues hidden within the normal structure. In comparison, small molecules, such as a simple phenyl seleninic acid, initially may have less dramatic effects on the protein structure and enzyme activity.

2.3.6. Conclusions

Our studies have confirmed that amphiphilic compounds based on a seleninic acid can be devised and synthesized with comparable ease. Such structures not only exhibit interesting physico-chemical properties but also show biological activities which exceed the ones associated with simple selenium compounds and surfactants. Such seleninic acids form a new class of interesting biologically active selenium agents which may hit their target cells in several ways, including a pronounced chemical reactivity against thiol groups, redox catalysis and specific, disruptive and unfolding interactions with selected proteins and membranes. A seleninic acid also compares favourably with its two other chalcogen-analogues: whilst sulfinic acids are usually unreactive, ‘tellurinic acids’ are chemically extraordinarily unstable.

In the future, the spectrum of possible applications for such amphiphilic redox modulators needs to be studied in more detail, with a focus on certain mammalian cells (*e.g.* cancer cells, macrophages), bacteria (*e.g.* biofilms), pathogenic fungi and also agricultural pests [36]. Simultaneously, pharmacological and pharmacokinetic properties of such compounds need to be considered, whereby the latter should be generally favourable due to their specific design. Ultimately, amphiphilic compounds such as 2, 3 and 4 represent interesting new lead structures for the design and development of potential anticancer and antimicrobial agents.

2.3.7. Acknowledgements

The authors acknowledge financial support from the Saarland University and the Landesforschungsfoerderungsprogramm Saarland (T/1-14.2.1.1.-LFFP 12/23). The authors would like to thank Dr. Josef Zapp from the Saarland University and Ms. Veronique Poddig from the University Lorraine for NMR measurements.

2.3.8. References

[1] C. Scherer, C. Jacob, M. Dicato, M. Diederich, Potential role of organic sulfur compounds from Allium species in cancer prevention and therapy, Phytochemistry Reviews, 8 (2009) 349-368.

[2] C. Jacob, P. Winyard, Redox Signaling and Regulation in Biology and Medicine, Wiley-VCH Verlag GmbH & Co. KGaA, Weinheim, 2009.

[3] L.A. Ba, M. Doring, V. Jamier, C. Jacob, Tellurium: an element with great biological potency and potential, Org Biomol Chem, 8 (2011) 4203-4216.

[4] V. Jamier, L.A. Ba, C. Jacob, Selenium- and Tellurium-Containing Multifunctional Redox Agents as Biochemical Redox Modulators with Selective Cytotoxicity, Chem-Eur J, 16 (2010) 10920-10928.

[5] M. Doering, L.A. Ba, N. Lilienthal, C. Nicco, C. Scherer, M. Abbas, A.A.P. Zada, R. Coriat, T. Burkholz, L. Wessjohann, M. Diederich, F. Batteux, M. Herling, C. Jacob, Synthesis and Selective Anticancer Activity of Organochalcogen Based Redox Catalysts, Journal of Medicinal Chemistry, 53 (2010) 6954-6963.

[6] P. Du, U.M. Viswanathan, Z. Xu, H. Ebrahimnejad, B. Hanf, T. Burkholz, M. Schneider, I. Bernhardt, G. Kirsch, M. Montenarh, C. Jacob, Emerging Biological Applications of Chalcogens: Amphiphilic Selenic Acids with Multiple Impact on Living Cells, in: E.R. Rene, P. Kijjanapanich, P.N. Lens (Eds.) G16 conference - Proceedings of the 3rd International Conference on Research Frontiers in Chalcogen Cycle Science & Technology, Unesco-IHE, Delft, 2013, pp. 59-68.

[7] M. Doering, B. Diesel, M.C.H. Gruhlke, U.M. Viswanathan, D. Manikova, M. Chovanec, T. Burkholz, A.J. Slusarenko, A.K. Kiemer, C. Jacob, Selenium- and tellurium-containing redox modulators with distinct activity against macrophages: possible implications for the treatment of inflammatory diseases, Tetrahedron, 68 (2012) 10577-10585.

[8] N. Lilienthal, C. Prinz, A.A. Peer-Zada, M. Doering, L.A. Ba, M. Hallek, C. Jacob, M. Herling, Targeting the disturbed redox equilibrium in chronic lymphocytic leukemia by novel reactive oxygen species-catalytic 'sensor/effector' compounds, Leukemia & Lymphoma, 52 (2011) 1407-1411.

[9] N. Lilienthal, A.A. Peer-Zada, L.A. Ba, H. Liu, C. Jacob, M. Hallek, M. Herling, Selective anti-leukemia activity of catalytic redox 'sensor/effector' agents, Onkologie, 33 (2010) 240-240.

[10] C. Jacob, L.A. Ba, Open Season for Hunting and Trapping Post-translational Cysteine Modifications in Proteins and Enzymes, Chembiochem, 12 (2011) 841-844.

[11] C. Jacob, Redox signaling via the cellular thiolstat, Biochemical Society Transactions, 39 (2011) 1247-1253.

[12] C. Jacob, G.L. Giles, N.M. Giles, H. Sies, Sulfur and selenium: The role of oxidation state in protein structure and function, Angew Chem Int Ed Engl, 42 (2003) 4742-4758.

[13] C. Jacob, E. Battaglia, T. Burkholz, D. Peng, D. Bagrel, M. Montenarh, Control of Oxidative Posttranslational Cysteine Modifications: From Intricate Chemistry to

Widespread Biological and Medical Applications, Chemical Research in Toxicology, 25 (2012) 588-604.

[14] R.F. Feissner, J. Skalska, W.E. Gaum, S.S. Sheu, Crosstalk signaling between mitochondrial Ca2+ and ROS, Frontiers in bioscience, 14 (2009) 1197-1218.

[15] T. Schneider, A. Baldauf, L.A. Ba, V. Jamier, K. Khairan, M.B. Sarakbi, N. Reum, M. Schneider, A. Roseler, K. Becker, T. Burkholz, P.G. Winyard, M. Kelkel, M. Diederich, C. Jacob, Selective antimicrobial activity associated with sulfur nanoparticles, Journal of Biomedical Nanotechnology, 7 (2011) 395-405.

[16] T. Schneider, Y. Muthukumar, B. Hinkelmann, R. Franke, M. Doring, C. Jacob, F. Sasse, Deciphering intracellular targets of organochalcogen based redox catalysts, Medchemcomm, 3 (2012) 784-787.

[17] P. Han, N. Ma, H. Ren, H. Xu, Z. Li, Z. Wang, X. Zhang, Oxidation-responsive micelles based on a selenium-containing polymeric superamphiphile, Langmuir : the ACS journal of surfaces and colloids, 26 (2010) 14414-14418.

[18] P. Du, U.M. Viswanathan, N.E.B. Saidu, Z. Xu, B. Hanf, I. Bazukyan, A. Trchounian, F. Hannemann, I. Bernhardt, T. Burkholz, K.-H. Schaefer, M. Montenarh, G. Kirsch, C. Jacob, Synthesis of amphiphilic, chalcogen-based redox modulators with pronounced biological activity, Medchemcomm, (2013).

[19] C. Jacob, H.T. Yang, H.A.O. Hill, Electrochemical investigations of a novel ferrocene surfactant, J Electroanal Chem, 416 (1996) 83-88.

[20] C. Jacob, A.Y. Safronov, S. Wilson, H.A.O. Hill, T.F. Booth, Investigations of a novel ferrocene-containing lipid by cyclic voltammetry and cryogenic transmission electron microscopy, J Electroanal Chem, 431 (1997) 7-10.

[21] C. Jacob, A.Y. Safronov, S. Wilson, H.A.O. Hill, T.F. Booth, Synthesis, characterization and electrochemistry of a novel ruthenocene surfactant, J Electroanal Chem, 427 (1997) 161-167.

[22] C. Jacob, A.Y. Safronov, S. Wilson, H.A.O. Hill, T.F. Booth, S.K. Chapman, Redox-active lipid-incorporating proteins as a novel immobilisation technique, J Electroanal Chem, 430 (1997) 119-125.

[23] C. Jacob, W. Maret, B.L. Vallee, Ebselen, a selenium-containing redox drug, releases zinc from metallothionein, Biochemical and Biophysical Research Communications, 248 (1998) 569-573.

[24] B.K. Sarma, G. Mugesh, Antioxidant activity of the anti-inflammatory compound ebselen: a reversible cyclization pathway via selenenic and seleninic acid intermediates, Chemistry, 14 (2008) 10603-10614.

[25] B.K. Sarma, G. Mugesh, Thiol cofactors for selenoenzymes and their synthetic mimics, Org Biomol Chem, 6 (2008) 965-974.

[26] A.V. Kachanov, O.Y. Slabko, O.V. Baranova, E.V. Shilova, V.A. Kaminskii, Triselenium dicyanide from malononitrile and selenium dioxide. One-pot synthesis of selenocyanates, Tetrahedron Lett, 45 (2004) 4461-4463.

[27] D. Plano, Y. Baquedano, D. Moreno-Mateos, M. Font, A. Jimenez-Ruiz, J.A. Palop, C. Sanmartin, Selenocyanates and diselenides: A new class of potent antileishmanial agents, Eur J Med Chem, 46 (2011) 3315-3323.

[28] P. Steffen, A. Jung, D.B. Nguyen, T. Muller, I. Bernhardt, L. Kaestner, C. Wagner, Stimulation of human red blood cells leads to Ca2+-mediated intercellular adhesion, Cell calcium, 50 (2011) 54-61.

[29] T. Schneider, L.A. Ba, K. Khairan, C. Zwergel, N.D. Bach, I. Bernhardt, W. Brandt, L. Wessjohann, M. Diederich, C. Jacob, Interactions of polysulfanes with components of red blood cells, Med Chem Comm, 2 (2011) 196-200.

[30] Y.V. Kucherenko, I. Bernhardt, The study of Ca2+ influx in human erythrocytes in isotonic polyethylene (glycol) 1500 (PEG-1500) and sucrose media, Ukrainskii biokhimicheskii zhurnal, 78 (2006) 46-52.

[31] E. Weiss, H.J. Lang, I. Bernhardt, Inhibitors of the K^+ /H^+ exchanger of human red blood cells, Bioelectrochemistry, 62 (2004) 135-140.

[32] L. Kaestner, W. Tabellion, E. Weiss, I. Bernhardt, P. Lipp, Calcium imaging of individual erythrocytes: problems and approaches, Cell calcium, 39 (2006) 13-19.

[33] NCCLS, M27-A2, in, NCCLS, Wayne, Pennsylvania, 2002.

[34] C.K. Banks, C.S. Hamilton, Organoselenium Compounds. II. Derivatives of Phenylseleninic Acid and Phenylseleninamide, J. Am. Chem. Soc., 62 (1940) 1859-1860.

[35] P.D.I. Fletcher, R.J. Nicholls, Alkylbenzenes in diiodomethane. A novel, "primitive" micelle-forming surfactant system, Langmuir : the ACS journal of surfaces and colloids, 16 (2000) 1050-1056.

[36] N.E.B. Saidu, I. Abu Asali, B. Czepukojc, B. Seitz, C. Jacob, M. Montenarh, Comparison between the effects of diallyl tetrasulfide on human retina pigment epithelial cells (ARPE-19) and HCT116 cells, Bba-Gen Subjects, 1830 (2013) 5267-5276.

[37] M. Montenarh, N.E.B. Saidu, The Effect of Diallyl Polysulfanes on Cellular Signaling Cascades, Natural Product Communications, 7 (2012) 401-408.

[38] N.E.B. Saidu, R. Touma, I. Abu Asali, C. Jacob, M. Montenarh, Diallyl tetrasulfane activates both the eIF2 alpha and Nrf2/HO-1 pathways, Bba-Gen Subjects, 1830 (2013) 2214-2225.

[39] S. Shaaban, R. Diestel, B. Hinkelmann, Y. Muthukumar, R.P. Verma, F. Sasse, C. Jacob, Novel peptidomimetic compounds containing redox active chalcogens and quinones as potential anticancer agents, Eur J Med Chem, 58 (2012) 192-205.

[40] S. Mecklenburg, S. Shaaban, L.A. Ba, T. Burkholz, T. Schneider, B. Diesel, A.K. Kiemer, A. Roseler, K. Becker, J. Reichrath, A. Stark, W. Tilgen, M. Abbas, L.A. Wessjohann, F. Sasse, C. Jacob, Exploring synthetic avenues for the effective synthesis of selenium- and tellurium-containing multifunctional redox agents, Organic & Biomolecular Chemistry, 7 (2009) 4753-4762.

[41] S. Mecklenburg, C.A. Collins, M. Doring, T. Burkholz, M. Abbas, F.H. Fry, C. Pourzand, C. Jacob, The design of multifunctional antioxidants against the damaging

ingredients of oxidative stress, Phosphorus Sulfur and Silicon and the Related Elements, 183 (2008) 863-888.

[42] C.A. Collins, F.H. Fry, A.L. Holme, A. Yiakouvaki, A. Al-Qenaei, C. Pourzand, C. Jacob, Towards multifunctional antioxidants: synthesis, electrochemistry, in vitro and cell culture evaluation of compounds with ligand/catalytic properties, Organic & Biomolecular Chemistry, 3 (2005) 1541-1546.

3. Conclusion and outlook

The present work has focused on the development of new amphiphilic selenium or tellurium containing compounds as potential anti-cancer drug candidates. The specific design of these compounds allowed them to kill cells by amphiphilic interactions (with membranes) and by breaking the redox haemostasis in cancer cells. The amphiphilic derivatives of sulfuric acid were successfully synthesized and purified. Then the membrane interactions of these compounds were analyzed with RBCs, nematodes and *S. cerevisiae*. The preliminary results proved that these selenium and tellurium-containing compounds can penetrate the cell membrane without destroying the structure of the cell membrane. Ultimately, the activities of these compounds as redox modulators were analyzed in HCT 116 cancer cells. The experimental results demonstrated that these compounds assert their anti-cancer effects by inducing cell apoptosis as a result of modulating the redox balance, for instance, by inducing ROS generation.

Based on the chemical considerations, as motioned above (see chapter 1.6 for chemical considerations), the new amphiphilic selenium or tellurium containing sulphuric acid derivatives DP31-DP35 and DP41-DP45 (chemical structure as shown in chapter 2.1 in Publication 1) were synthesized successfully via fairly straightforward synthesis procedures, and good yields (up to 63%) were achieved even without further optimization.

All the compounds present excellent solubility in aqueous medium due to their amphiphilic properties. Subsequently, these selenium and tellurium containing sulfuric acids show excellent interactions with RBCs cell membrane and reduce the viability of *Steinernema feltiae*, RAW 264.7 macrophage cells as well as HCT116 cancer cells in a dose dependent manner. The tellurium containing sulphuric acids are

more potent than their selenium containing analogous. Although these compounds cause the haemolysis of RBCs in very high concentrations (several hundred micromolar), these compounds at their respective IC_{50} concentrations did not cause significant haemolysis, but strongly reduced the viability of RAW 264.7 macrophage cells and HCT116 cancer cells. These results indicate that the tellurium compounds can penetrate the cell membrane and perform their biological activity in the cytosol instead of simply interacting with the cell membrane. This conclusion is further confirmed with the EDX analysis.

The tellurium compound DP41 can induce rapid ROS production (usually within two hours) on HCT116 cancer cells, while the selenium analogue DP31 has no effect on the ROS production. The ROS induced by DP41 triggers further ER stress as is confirmed by the phosphorylation of eIF2α and the expression of ATF4 and CHOP. The DP41-induced ER-stress subsequently induces an intrinsic apoptosis pathway, which is confirmed by the loss of the mitochondrial membrane potential, the release of cytochrome *c*, decreased expression of Bcl-2, the cleavage of PARP and the activation of caspase3. Interestingly, the tellurium compound DP41 does not induce the ROS production in a normal epithelial cell line (ARPE-19). Furthermore, DP41 can disrupt the tubulin network in HCT116 cancer cells that leads to cell cycle arrest. Future research has to explore the various effects of the ROS production on the tubulin network and cell cycle arrest.

As the other part of this thesis, several amphiphilic seleninic acid derivatives were designed based on the same rationale. Five amphiphilic seleninic acid derivatives were synthesized successfully (chemical structure as shown in chapter 2.3 in Publication 3). In these compounds, the seleninic acid moiety provides two functions: the hydrophilicity to increase the solubility and the catalytic redox activity regards for activity in and against cells. These amphiphilic seleninic acid derivatives were

investigated with RBCs and *S. cervisiae*. Interestingly, the amphiphilic compounds 2 to 4 (chemical structure as shown in publication 3) demonstrated significant biological effects on RBCs and *S. cervisiae* in contrast to the nonamphiphilic compound 1, which implies that the amphiphilicity is a necessary requirement for the biological activity of this kind of compounds. At the same time, these seleninic acids (compounds 2 to 4) should also cause an even stronger ROS production in cancer cells, which may induce apoptosis at even lower concentrations of compounds used. Therefore, future studies should be focused on the biological behaviour of compounds such as 2 to 4 and on their possible applications in intracellular redox modulation of cells associated with diseases like scleroderma, certain types of cancer and serious infections and inflammatory diseases.

4. Summary

The present PhD thesis describes the development of new organic selenium and tellurium containing compounds as synthetic redox-modulating surfactants and their biological activities.

Ten organic selenide and telluride compounds (in publication 1) were designed, successfully synthesized and chemically characterized. These compounds are amphiphilic. The tellurides, in contrast to their selenide analogous, are more effective against not only RAW 264.7 macrophages, *S. feltiae* and *E. coli* but also against HCT116 cancer cells. The tellurides can modulate the intracellular redox balance by generating the superoxide anion radicals, which trigger the intrinsic apoptotic pathway.

Further tests (in publication 2) show that the selenide compound DP31 has no effect on either HCT116 cancer cells or ARPE-19 cells, while the telluride analog DP41 induces the activation of the PERK/eIF2α/ATF4 signaling pathway by modulating ROS, which triggers the intrinsic apoptotic pathway in HCT116 cancer cells, but not in ARPE-19 cells.

Based on the success of tellurium compounds such as DP41, a series of surfactants containing seleninic acid head groups has been designed, synthesized, purified and characterized chemically (in publication 3). These compounds form micelles and interact strongly with the cell membrane of RBCs. Hence they promote Ca^{2+} influx, which induces eryptosis. Furthermore, the series of these surfactants with CMC properties also shows anti-funginal activity against *S. cerevisiae*.

5. Zusammenfassung

Diese Dissertation beschreibt die Entwicklung der neuen organischen Selen- und Tellur-Verbindungen als Redox modulierende Tensiden und ihre biologischen Aktivitäten.

Zehn organische Selenid- und Tellurid-Verbindungen (in der Veröffentlichung 1) wurden erfolgreich synthetisiert und chemisch charakterisiert. Sie sind amphiphil. Die Telluriden, im Gegensatz zu den analogen Seleniden, sind nicht nur wirksamer gegen RAW 264.7 Makrophagen, *S. feltiae* und *E. coli* sondern auch gegen HCT116 Krebszellen. Diese Telluriden können das Redoxgleichgewicht durch die Erzeugung von Superoxid Radikalen so modulieren, dass der intrinsische apoptose ausgelöst wird.

Weitere Experimente sind in der Veröffentlichung 2 zusammengefasst. Die Selenid DP31 zeigt keinen Effekt auf HCT116 Krebszellen oder ARPE-19 Zellen. Hingegen aktiviert das analoge Tellurid, DP41, die Signalweg von PERK/eIF2α/ATF4 durch Generierung von ROS, wodurch die intrinsische Apoptose in HCT116 Krebszellen ausgelöst wird. Dies geschieht aber nicht in ARPE-19 Zellen.

Basierend auf dem Erfolg der Telluriden, wie beispielsweise DP41, wurde eine Reihe von Selensäure-enthaltender Tenside synthetisiert und chemisch charakterisiert (in der Veröffentlichung 3). Sie formen Mizellen, interagieren stark mit der Zellmembran von Erythrozyten und fördern den Ca^{2+} Einstrom. Dies induziert wiederum Eryptose. Interessanterweise zeigen diese Selensäure-enthaltenden Tenside mit amphiphiler Eigenschaft auch fungizide Aktivität gegen *S. cerevisiae*.

6. Abbreviation list

ATF4	activating transcription factor 4
ATF6	transcription factor 6
ATP	adenosine triphosphate
Bax	Bcl-2-associated X protein
Bcl-2	B-cell lymphoma 2 protein
BiP	immunoglobulin protein
CAT	Catalase
CD	circular dichroism measurement
CHOP	C/EBP homologous protein
CMC	critical micelle concentration
DAPI	4,6-diamidino-2-phenylindole
DHE	dihydroethidium
DNA	desoxyribonuclein acid
EDX	energy-dispersive X-ray spectroscopy
eIF2α	eukaryotic initiation factor 2α

eq.	equivalent
ER	endoplasmic reticulum
et al.	et alii
FACS	fluorescence-activated cell sorting
5-FU	5-fluorouracil
G0	quiescent
G1	Gap 1
G2	Gap 2
GPx	glutathione peroxidase
GR	glutathione reductase
GSH	glutathione
GSSG	glutathione disulfide
H_2O_2	hydrogen peroxide
Hb	hemoglobin
HO-1	heme oxygenase 1
IC_{50}	half maximal inhibitory concentration

IRE1α	inositol-requiring enzyme 1α
Keap1	kelch like-ECH-associated protein 1
MS	mass spectrometry
MTT	3-(4,5-dimethylthiazol-2-yl)-2,5-diphenyl-tetrazolium bromide
NADPH	nicotinamide adenine dinucleotide phosphate
NMR	nuclear magnetic resonance
Nrf2	nuclear factor (erythroid-derived 2)-like 2
OS	oxidative stress
PARP	poly-ADP-ribose polymerase
PC,	phosphatidylcholine
PE	phosphatidylethanolamine
PERK	protein kinase RNA-like endoplasmic reticulum kinase
P-SH	protein-SH
P-S-S-P	protein-S-S-protein
Prx	peroxiredoxin
PS	phosphatidylserine

RBC	red blood cell
REM	Reflection electron microscope
R_f	retention factor
RNOS	reactive nitrogen oxygen species
RNS	reactive nitrogen species
ROS	reactive oxygen species
S phase	synthesis period (in cell cycle)
SD	standard deviation
SDS	sodium dodecylsulfate
Se	selenium
SOD	superoxide dismutase
Sph	sphingomyeline
Te	tellurium
UPR	unfolded protein response
UV/VIS	ultraviolet/ visible
δ	chemical shift